The Effects of Ketamine on the Brain's Spontaneous Activity as Measured by Temporal Variability and Scale-Free Properties. A Resting-State fMRI Study in Healthy Adults.

Omar Ayad

Thesis submitted to the

Faculty of Graduate and Postdoctoral Studies

in partial fulfillment of the requirements

for the Master of Science degree in Neuroscience

Department of Neuroscience

Faculty of Medicine

University of Ottawa

Abstract

Converging evidence from a variety of fields, including psychiatry, suggests that the temporal correlates of the brain's resting state could serve as essential markers of a healthy and efficient brain. We use ketamine to induce schizophrenia-like states in 32 healthy individuals to examine the brain's resting states using fMRI. We found a global reduction in temporal variability quantified by the time series' standard deviation and an increase in scale-free properties quantified by the Hurst exponent representing the signal self-affinity over time. We also found network-specific and frequency-specific effects of ketamine on these temporal measures. Our results confirm prior studies in aging, sleep, anesthesia, and psychiatry suggesting that increased self-affinity and decreased temporal variability of the brain resting state could indicate a compromised and inefficient brain state. Our results expand our systemic view of the temporal structure of the brain and shed light on promising biomarkers in psychiatry.

To *Mama El-Kabira,*

Madiha Abdulwahab Jassim

(July 1925 - October 2013)

الفاتحة

List of contents:

6. Appendices

List of figures and tables:

List of abbreviations:

AC: Anterior Commissure

ADHD: Attention Deficit Hyperactivity Disorder

BD: Bipolar Disorder

BET: Brain Extraction Tool

BOLD: Blood-Oxygenation-Level-Dependent

CEN: Control Executive Network

CSF: Cerebrospinal Fluid

DFA: Detrended Fluctuation Analysis

DLPFC: Dorsolateral Prefrontal Cortex

DMN: Default Mode Network

ECoG: Electrocorticography

EEG: Electroencephalography

FA: Flip Angle

FC: Functional Connectivity

fMRI: Functional Magnetic Resonance Imaging

FSL: FMRIB Software Library

FWHM: Full Width at Half Maximum

GLM: General Linear Model

GM: Gray Matter

H: Hurst exponent

ISF: Infraslow Fluctuation

LFP: Local Field Potential

LRTC: Long Range Temporal Correlation

MDD: Major Depressive Disorder

MEG: Magnetoencephalography

MNI: Montreal Neurological Institute

MRS: Magnetic Resonance Spectroscopy

MSE: Multi Scale Entropy

NEX: Number of Excitations

NMDAR: N-methyl-D-aspartate receptor

NMR: Nuclear Magnetic Resonance

NREM: Non-Rapid Eye Movement

PACC: Perigenual Anterior Cingulate Cortex

PANSS: Positive and Negative Syndrome Scale

PC: Posterior Commissure

PCA: Principle Component Analysis

PCC: Posterior Cingulate Cortex

PCP: Phencyclidine

PET: Positron Emission Tomography

PFC: Prefrontal Cortex

RF: Radiofrequency

ROI: Region of Interest

sgACC: Supragenual Anterior Cingulate Cortex

SN: Salience Network

SNR: Signal to Noise

TE: Echo Time

TR: Repetition Time

VS: Vegetative State

Statement of Contribution and Acknowledgements

All the raw data in this ketamine resting state experiment were originally collected and shared with us by Dr. Naomi Driesen at the Yale University's School of Medicine (Connecticut, USA), after we proposed our investigation to her. The original data are part of Dr. Driesen's project exploring the effects of ketamine on resting state's global connectivity and working memory tasks, which will be reported somewhere else independent of this study. Otherwise, I have conducted all the work presented here including proposing the study, processing raw data, designing and conducting the analysis, and the writing of this thesis under the supervision of Dr. Georg Northoff. I have collaborated with my laboratory colleagues in several other projects in fMRI and EEG and now have first-hand experience with ethics proposals, data collection, data management, subject recruiting, etc.

I would like to thank Dr. Georg Northoff for his supervision and guidance, and for letting me be part of his dynamic research group. Special thanks go to Dr. Niall Duncan for guiding me throughout the learning stages with the analysis methods and for always being there to answer questions. Many thanks go to my mentor Dr. Zirui Huang for his supervision and valuable advice that he provided along the way. I would also like to thank Dr. Nils Wagner for being a pleasant company and an excellent supporter both in and outside the lab. Finally, I wouldn't have achieved anything without the support of my wonderful parents and siblings, who were supporting me in every stage of my life; I couldn't ask for better people in my life and I've always felt truly lucky.

1. Background and Introduction

1.1. Current research themes, and emerging views of the brain.

Brain imaging has recently expanded its scope to include many phenomena that have been otherwise attributed to non-brain concepts, i.e. the soul or the mind. We now see scholars speaking of phenomena such as the self, consciousness, intention, decision making and free will as functions associated with the brain (Churchland, 2002; Frith, 2007; Gallagher, 2005; Koch, 2004; Northoff, 2004; Searle, 2004). While trying to make sense of such phenomena helped hundreds of philosophers keep their underpaying jobs, neuroscientists now want to take a piece of the pie. This contributed to the birth of what is now dubbed "neurophilosophy". However, neuroscientists face particular difficulties because, in the majority of approaches, they are yet to present more satisfying explanations other than simply mapping certain phenomena to brain regions. Indeed, magnificent results have emerged from such approaches, and keep doing so with no signs of slowing down. However, we still lack the knowledge of the fundamental underpinnings that enable the brain to render such phenomena possible. How can a brain made of neurons construct "mind-like" or "soul-like" phenomena? Surely, we are still far away from an answer to this romantic question. The question, however, is still of particular relevance because interestingly, perturbations in these phenomena and associated concepts continuously appear to be the hallmarks of many psychiatric disorders. And biomarkers for these disorders remain largely missing. Thus, exploring mental disorders with new experimental approaches may lead to a whole new understanding of such disorders and their treatment methods. This current study, its experimental approach, analysis, and results attempt to support emerging views of the

brain and hints towards new avenues in the journey of understanding the very fundamental brain architecture that gives rise to those things that make us feel human.

There has been a suggested shift in views of our conceptual understanding of the brain (Raichle, 2009). This shift is primarily between two views; the first, more widely used, sees the brain as a mirror of the environment. Thus its neural responses are merely reflections of the stimuli it receives. The second sees the brain as an active organ which dictates the nature of the brain-environment interaction. Marcus Raichle contrasts these two views by labelling them the "reactive" vs "proactive" brains respectively. The "reactive" or reflective view has been implemented in the larger body of Neuroscience. Dr. Raichle mentions that this is not surprising as the focus of neuroscience on many levels of research has been on the event-related activity, which is by its nature implying the reflective view of the brain driven by the demands of the environment (Raichle, 2009). Furthermore, one can argue that the main reason for such focus is that event-related activity can be studied by designing rigorously controlled experiments, presenting specific tasks, controlling exact variables and thus yielding highly precise results. All of which, of course, are characters of a sound fruitful scientific method, highly sought after by any researcher hence the popularity of the reflective view. By the same token, the second "proactive" view imposes fundamental difficulties in brain research that are yet to be dealt with; in the most basic sense, in the absence of a specific stimulus, what do we really look for and what type of activity to measure? Specifically, what are those brain's own characteristics that render the brain-environment interaction possible in the first place? And in reality, how do we investigate them in our study designs? A good place to start is by investigating the intrinsic features of the brain that could be captured using the

privileges that current imaging techniques have given to us, such as functional magnetic resonance imaging fMRI. Hence we start by focusing on the brain's intrinsic activity.

Why is the brain intrinsic activity important? One of the most striking features of the brain is that it accounts for 20% of the energy available to the human body at rest (Clarke and Sokoloff, 1999), despite representing only 2% of the total body mass. Why does the brain use so much energy considering its relatively low mass? And is that energy devoted to functional purposes or is it mainly the self-upkeep cost of the brain? Using magnetic resonance spectroscopy "MRS" technique, (Sibson et al., 1998; Shulman et al., 2004) together reported an estimated 80% of the entire energy consumption of the brain is utilized for glutamate-cycling and thus concluding it as a functional cost of neuronal signaling. This is supported by several studies covering anatomic, physiologic and metabolic data (Ames, 2000; Attwell and Laughlin, 2001; Lennie, 2003). These studies examined the cost of excitatory signalling in the gray matter. While this leaves open the demand of functional inhibitory neurons, the evidence remains that the majority of energy consumed by the brain is devoted to functional processes. Strikingly, additional energy consumption associated with task related activity accounts for only 5% of baseline levels of consumption, an overlooked observation made 50 years ago (Sokoloff et al., 1955). Concluding, the majority of the energy consumed by the brain pertains to *intrinsic* functional processes, highlighting the importance of such processes in brain functioning and calling for more attention from researchers compared to task-induced activity.

Another argument supporting the importance of the brain intrinsic activity comes from studying sensory information processing. Specifically, looking at the visual cortex, sensory information coming from the retina and reaching the visual cortex are highly

compressed (Anderson et al, 2005). To put this into perspective, it is argued that only 10^{10} bits s^{-1} of the environment visual input is picked up by the retina (Norretranders, 1998). Furthermore, due to the limited number of axons in the optic nerves, 10^6 bits s^{-1} leave the retina and eventually only 10^4 make it to layer 4 of the V1 of the visual cortex. As a result, a highly compressed version of the environment is actually reaching the brain. Norretranders discusses in his book, *The User Illusion*, that the bandwidth of conscious awareness is in the range of 100 bits s^{-1} while the bandwidth of phenomenal experience is much wider than this figurative estimate. Despite all of these proposed limitations and impoverishment of sensory information, the brain still has to integrate, interpret, respond and even, in some cases, predict environmental demands creating extremely rich experiences, arguably much richer than the information reaching it. And its success in doing so must lie largely in its intrinsic features and processes that link representations and experiences of the environment to the limited sensory inputs that actually reach the brain (Fiser et al., 2004).

1.2. The brain's resting state activity:

Increased attention has been given to the concept of the "brain's resting state" or "brain's spontaneous activity" as operational labels to the brain "intrinsic activity" (Northoff el al., 2010). In both animals and humans, research has repeatedly shown high brain resting state activity in specific set of regions dubbed the Default Mode Network (DMN) (Humans: Raichle et al., 2001; Fransson, 2005; Northoff et al., 2006; Buckner et al., 2008) (Animals: Rilling et al., 2007; Vincent et al., 2007; Shulman et al., 2009). Before discussing specific networks in the resting state, one has to attempt to define what the brain resting state is as this concept can be problematic. In reality, the brain is never at rest as it continuously receives input, for example sensory, even when specific stimuli are absent. Despite that, we still need to set an operational method to describe, as close as experimentally possible, the brain intrinsic activity. For example, Barry et al. (2007) attempted to set a strictly experimental definition for the resting state by comparing two conditions of the resting state, eyes opened and eyes closed. Showing different levels of activations in the two conditions, Barry and colleagues considered "eye closed", with subjects being instructed not to think of any particular thoughts, to be the baseline for the resting state. Since then, "eyes closed" condition without any specific stimuli has been used as a fruitful condition in many subsequent studies to examine the brain's resting state (Logothetis et al., 2009; Raichle, 2010). However, there is still no agreed upon method to measure the resting state as other studies of the resting state used eyes opened techniques to arrive at similar results (Patriat et al., 2013). As a result, generally in the literature, three methods have shown similar reliability and consistent findings: eyes open, eyes closed, and eyes open and fixated on a target which we used in the current

study (Patriat et al., 2013). Thus, the operational definition of the brain's resting state is now repeatedly described by the state of the brain prior in time to any stimuli specifically applied extrinsically by the experimenters (Shulman et al., 2009), represented in one of three ways, eyes opened, eyes closed, or eyes open with fixations (Patriat et al., 2013).

To understand the relevance of the brain's resting state, one of the first questions researchers tried to answer is how this activity affects, if at all, the rigorously studied stimulus induced activity. Decreased activity in the DMN upon stimulation, described earlier to have high resting state activity, was shown to impact subsequent activity in the visual and auditory cortices during relevant tasks (Greicius and Menon, 2004). This group showed that the lower the resting state activity in the regions of the DMN that usually show task negative responses (decreased activity following task stimulus), the higher the stimulus induced activity in both the auditory and visual cortices. Thus, this suggests that the brain's resting state not only affects local regional activity, but also affects global functioning of other regions that are not necessarily described to be functionally connected to the DMN.

Furthermore with the rest-stimulus interaction theme, Maandag et al. (2007) anesthetically induced both high and low resting state activity in rats and studied the neural response to forepaw stimulation. They found that high resting state activity correlated with activity throughout the cortex but not with the sensorimotor cortex, while low resting state activity showed the opposite. That is, low resting state activity correlated with high activity in the sensorimotor cortex but not with any other specific regions through the cortex. Thus they provide evidence of a differential modulation of the

brain's resting state that is regional specific and not pertaining to the effect of anaesthesia itself.

A central question is: what neuronal measures can also be studied in the resting state that may play a role in the rest-stimulus interaction? Fox et al. (2006) showed that neural oscillations in the resting state in behaviourally relevant regions also impact subsequent behaviour in humans. In more detail, they showed that the ongoing resting state activity illustrated by neural oscillations, which also persist during stimulus induced activity, predicts trial-to-trial variability in the somatomotor cortical activity and reaction time in button press tasks. Hence, the neural oscillations of the resting state not only correlate with subsequent neural activity but also modulate behaviour outputs, illustrated in this study by "reaction times" (See also Fox et al., 2007). Michael Fox and his colleagues investigated the oscillations of the brain using the spontaneous fluctuations in the fMRI signal, a feature that has been closely linked with local field potentials LFPs (Khader et al., 2008). Interestingly, a remarkable characteristic of fMRI is the noisy signal it yields: the blood-oxygen-level dependant BOLD signal. This has led researchers to mainly depend on averaging their signals over time to report findings (Garrett et al., 2011). However, earlier noted by Biswal et al., (1995), *variance* in the BOLD signal shows interesting tendency of coherence between specific brain systems, especially in the slow frequency range (<0.1 Hz). Moreover, Greicius et al. (2003) showed similar coherence patterns in the entire DMN. This led researchers to confirm similar patterns in the resting state across several cortical and subcortical systems (Zhang et al., 2009; Smith et al., 2009). Thus, *variance* of slow fluctuations in BOLD signal provides us with valuable measure to investigate in our studies that can tap directly into the brain intrinsic

activity. This will be discussed in more detail in later sections concerning neuronal variability.

In current research, what are the best imaging tools that we can use to tap into the brain's interesting activity? First, metabolic techniques such as positron emission tomography (PET) can be used to quantitatively measure the brain's energetic metabolism of glucose during the resting state (Shulman et al., 2014). PET scans provide spatial measures of the metabolic demands of the resting state with virtually no temporal resolution because PET scans take up to 60 minutes for the radiotracer agent to travel through blood and be absorbed into body organs. Resting state fMRI targets the momentary signal change in the neurovascular activity (rather than metabolic, which needs PET technique that has a low temporal resolution) and provides, in the case of functional connectivity, the statistical correlations between different regions thus introducing temporality into the picture while maintaining a fairly good spatial component. EEG on the other hand provides excellent temporal resolution but low spatial resolution because of the limited brain regions that can be grouped into scalp electrodes. Consequently, measuring and segregating both spatial and temporal features of the resting state using the same imaging technique is very difficult. However, the resting state is by nature spatiotemporal and any perturbations thought to be correlated with any disorders can be assumed to be spatiotemporal as well (Northoff, 2015). This point will be discussed in more detail in the psychiatric disorders section later on.

What about the main networks of the resting state? Spatially, different networks of the resting state include the default-mode network DMN, the control executive network (CEN), the salience network (SN), and the sensorimotor network (Cabral et al.,

2014; Deco et al., 2013; Raichle, 2009). The DMN includes cortical midline regions in the bilateral posterior parietal cortex (Buckner et al., 2008). These regions, as described earlier, exhibit high activity, high functional connectivity in between the regions and strong low frequency fluctuations (evident in fMRI, <0.5 Hz) during the resting state; it is important to note that sometimes the DMN activity is inaccurately equated with the brain resting state activity which instead is evident in the whole brain. The executive network includes the lateral prefrontal cortex, the supragenual anterior cingulate cortex, and the posterior lateral cortical regions. These regions are documented to be involved in higher-order cognitive and executive functions (Ganzetti and Mantini, 2013). This network is further divided into fronto-parietal network and dorsal attention network (Northoff, 2014). The salience network includes regions such as the insula, the ventral striatum, and the dorsal anterior cingulate cortex. These regions are linked to reward processing, empathy, introception, extroception, and salient processes (Fan et al, 2011; Menon, 2011; Wiebking et al., 2011). Finally, the sensorimotor network comprises the auditory, somatomotor, and visual networks (Ganzetti and Mantini, 2013; Northoff, 2014).

These resting state networks exhibit strong both within network and inter-network functional connectivity. Most interestingly, the DMN and CEN networks are often documented to be "anti-correlated" meaning high activity in one network results in low activity in the other (Ganzetti and Mantini, 2013). This anti-correlating relation to each other has been recently linked clinically to the distinction between internal processing (e.g. internal thoughts) and external processing (e.g. perceptions of environmental stimuli) (Carhart-Harris et al., 2013; Northoff, 2014; Vanhaudenhuuyse et al., 2010; Wiebking et al., 2014). This anti-correlation can be of particular concerning the link

between the resting state and some of the most basic symptoms of psychopathology in a variety of psychiatric disorders, which will be discussed later in the psychiatry section.

Temporally, evidence in the literature leads towards an elaborate structure to the brain's intrinsic activity illustrated by frequency-specific fluctuations in a variety of ranges (Buszaki, 2006). The DMN in particular predominantly exhibits low-frequency spontaneous fluctuations in the resting state (<0.1 Hz). In fact, both low and high frequency fluctuations are evident in regions other than the DMN such as sensory and motor cortices, insula, subcortical regions like the basal ganglia and thalamus (Freeman, 2003; Hunter et al., 2006; Shulman et al., 2009; Zuo et al., 2010). Thus fluctuations in different frequency bands are hallmarks of intrinsic neural activity in general and not limited to the paradigmatic resting state network, the DMN. Specifically, fMRI studies illustrate BOLD fluctuations in the lower frequency ranges including the delta range (1-4 Hz), up and down state (0.8 Hz) and infra-slow fluctuations (ISF's) (0.01-0.1 Hz). Furthermore, recent studies illustrated that within the infra-slow fluctuations captured by fMRI, two more frequency bands emerge as distinct entities with suggested distinct neuronal mechanisms, namely slow-5 (0.01-0.027 Hz) and slow-4 (0.027-0.073 Hz) (Baria et al., 2011; Han et al., 2010; Zuo et al., 2010). Finally, these slow frequency fluctuations captured in fMRI are thought to be associated with slow cortical potentials SCP's in EEG (He and Raichle, 2009; Khader et al., 2008l; Northoff, 2014). However, SCP obtained in EEG are problematic because they are often affected by artefacts arising from sweating, head movements and electrode drifts favouring fMRI in studying these fluctuations (He and Raichle, 2009; Northoff 2014).

Higher frequency fluctuations are also heavily studied in EEG in the brain's resting state theta (4-0 Hz), alpha (8-12 Hz), beta (12-30 Hz), and gamma (>30 Hz) (Sadaghiani et al., 2010). Interestingly, Vanhatalo and colleagues (2004) investigated the relationship between low frequencies (0.02-0.2 Hz) and faster frequencies (1-10Hz) in EEG. They observed phase-synchrony of the phase of the slow frequencies with the amplitude of the high frequency oscillations. This phase-locking of the high frequency power with the phases of lower frequency is described in the literature as phase-power coupling (Canolty and Knight, 2010; Sauseng and Klimesch, 2008). It is generally observed that the direction of such coupling is from low to high frequency fluctuations in a phase-to-amplitude manner (Buzsaki, 2006), i.e. the phase of the lower frequency entrains the amplitude of the higher frequency. This makes studying lower as well as higher frequency bands important in our understanding of the resting state.

Classifying the resting state both spatially and temporally is of particular importance and relevance especially in understanding the relationship between the resting state and psychiatric disorders. Recently, evidence leads towards the suggestion that psychopathology is a spatiotemporal abnormality of the brain's resting state (Northoff, 2015). It has been suggested that disturbances in both the spatial and the temporal structures of the resting state have been linked to affective, cognitive and social symptoms of psychiatric disorders such as depression, schizophrenia and bipolar disorders (Northoff and Qin, 2010; Northoff, 2014). This point will be discussed in more detail, especially the temporal aspect, in the section discussing the resting state and psychopathology.

In terms of the neuronal measures that can be studied in the resting state without the need to specific stimuli, and as briefly discussed earlier, temporal variance is evident to play an important role in the brain resting state despite being generally considered "noise". Moreover, the resting state literature up to this point is mostly concerned with the functional connectivity between the different spatially distributed resting state networks as discussed in the earlier paragraphs. Functional connectivity in principle describes the degree of coordination of brain activity both within and between regions (Zang et al., 2004; Zuo et al., 2010, 2013; Biswal et al., 1995; Cordes et al., 2000; Greicius et al., 2003, 2004). However, these signal synchronization measures scale away temporal variability by default in their calculations. And there is strong evidence suggesting that temporal variability is a central measure of large-scale brain activities (Faisal et al., 2008; Garrett et al., 2010, 2011, 2013; McIntosh et al., 2010; Vakorin et al., 2011). In fact, higher temporal variability has been observed in the resting state in regions which constituted the DMN as well as in the thalamocortical networks (Zang et al., 2007). All of this make temporal variability a valuable experimental measure to target in our exploration of the brain's resting state.

In addition to temporal variability, another temporal structure measure has been increasingly investigated in the resting state literature, which is *scale-free brain activity*. Scale-free brain dynamics concern self-similarity in brain activity patterns across time, i.e. long-range temporal correlations (LRTC), which is increasingly being established as a basis to the brain's temporal structure (Bullmore et al., 2001; He et al., 2010), adding yet another temporal dimension to the way we observe brain signals over time. Recently, scale free dynamics have been illustrated in resting state brain activity using fMRI data

(He, 2011; He et al., 2010). Moreover, recent sleep studies illustrated that scale free properties in the resting state are relevant in maintaining certain levels of consciousness (Lei et al., 2015; Tagliazucchi et al., 2013). And most recently, an intriguing close relationship has been illustrated between temporal variability and long term temporal dynamics (Scale-free) activity by Biju He (2011). She found that the more variable the brain activity the higher index of long term correlations in the brain. This makes *temporal variability* and *scale free dynamics* attractive targets to investigate in our experiment as the functional and behavioral significance of both measures remain to be investigated in addition to the relationship between them.

1.3. Temporal variability.

Researchers mainly collect mean values of recorded signals and consider it the most representative value of the variable in question. This is motivated by the traditions of statistical methods, in which the mean represents the central value for the signal of interest falling within a "distributional" noise. This led researchers, as described earlier, to average signals over time to get mean activation patterns pertaining to the specific task the subjects are presented with, positively reinforced by the reflective view of the brain. However, this practice, while being fruitful and beneficial for many reasons, may blind us from potentially meaningful insights about the brain signal, namely *variability*. While much work was dedicated to explore brain variability (Biswal et al., 1995; Stein et al., 2005; Faisal et al., 2008), we rarely consider it a meaningful and target measure for brain functioning. Moreover, Researchers in fMRI field often attribute BOLD's variance to scanning-related confounds and other nuisance effects, thus attempt to remove noise signals to retain the signal of the neuronal process of interest (Huettel et al., 2009; Jones et al., 2008; Birn, 2012). Despite the continuously fruitful focus on mean BOLD signal (Bandettini 2012), the brain remains naturally variable (Faisal et al., 2008; Garrett et al., 2010) and we still need to investigate that side of it.

Recently, brain's variability has been highlighted as a measure of intrinsic meaning within the context of aging (Garrett et al., 2010, 2011, 2013). Examining the old assumption that cognitive deterioration associated with aging can be caused by noisy and inefficient neuronal functioning (Cremer and Zeef 1987; Salthouse and Lichty, 1981), Garrett and his colleagues found that individual differences in BOLD variability are more powerful indicators of age than averaged signals (Garrett et al., 2010). They used fMRI

data of 19 young adults (mean age=25) and 28 older adults (mean age=67) to obtain patterns of both brain variability (standard deviation of signal of each brain voxel during a resting state period) and mean brain activity. They found a strong relation between BOLD SD during rest and age (R^2= 0.81). Interestingly, they observed that the majority of brain regions show decreased variability with older age. The correlation of mean-based activity with age were weaker (R^2=0.59) and the spatial patterns of brain activity were largely distinct from that of SD spatial patterns. Then the researchers tested which measure better predicted age and found out that SD-based measures of the brain were five times larger than that of mean-based measures. The study's significance lies in the findings that SD measures during "rest" have distinct spatial patterns from that of mean based activity and those variability patterns are better predictors of age suggesting a valuable measure of brain activity and not merely noise that should be controlled for.

The next question was how variability predicts cognitive performance, a hallmark behavioral test in age-related studies. In a follow-up study by the same group, the influence of variability on behavior was tested (Garrett et al., 2011) by examining BOLD variability and reaction times (RT) variability in the same population of older and younger adults in three cognitive tasks covering perception, attention and delayed matching. Based on the previous study (Garrett et al., 2010), the group predicted that younger brains would show more variability and this variability would be positively correlated with increased cognitive performance. This prediction was supported by their findings as younger and faster brains exhibited significantly higher BOLD variability in a distributed set of regions regardless of the task they were presented with, compared to older poorer performer adults. Furthermore, supporting the previous study, variability

versus mean-based spatial patterns were non-overlapping and SD patterns predicted cognitive performance more strongly than mean BOLD patterns. Thus we now see that higher variability resting state is associated with younger brains and more variability during task performances predicts better cognitive capacity of the adult brains. Remaining is the question whether the transition between resting state and task state, a process vital to normal brain functioning, is modulated by variability as well.

Notably, neuronal variability has been proposed to be the basis of the alleged probabilistic nature of the brain (Knill and Pouget 2004; Ma et al., 2006), which refers to the brain employing Bayesian processes that generate an optimal response state to incoming stimuli of variable reliabilities. In this context, neuronal variability makes possible adaptability to uncertain stimuli (eg., when stimuli degrade or change in frequency) and thus higher signal variability would take place when presented with greater stimulus uncertainty. Additionally, neuronal variability was shown to be important for state to state transitions, despite still being labelled and considered "noise" (Ghosh et al., 2008; Deco et al., 2009, 2011; McIntosh et al., 2010). Given that particular evidence and the findings highlighted earlier that older adults exhibited less signal variability both during rest and task periods, Garrett and colleagues also predicted that variability-based transitions from rest to task would be compromised in older adults. Thus in a third study (Garrett et al., 2013), they investigated the transition from the resting state to the same three cognitive tasks in their previous study. They found that SD measures increased on task periods compared to rest across a distributed set of regions in both old and young adults. And this increase was significantly larger in young high performing adults. Interestingly, this increase was global in terms of the regions it

covered in the brain, i.e. no regions showed decrease in variability during all tasks whether that region was a task positive or task negative region (e.g. executive network vs DMN). They concluded that increased variability represents a complex brain neuronal system with an increased dynamical range within and between brain states leading to enhanced capability to process variable and unexpected stimuli. Remaining to explore, however, is the functional consequence of possessing either high or low variability for the different brain networks.

All of these studies highlight temporal variability as a measure of unique importance in cognitive processing despite being mainly considered noise in the main body of literature. This calls for investigating temporal variability in other brain research areas such as developmental, psychiatric and cognitive disorders. Exploring this avenue, Huang and colleagues (2014a) examined the resting state activity and self-referential processing in vegetative state (VS) patients. These two neuronal activities were shown in previous studies to be highly overlapped in a specific areas called cortical midline regions (D'Argembeau et al., 2005; Qin and Northoff, 2011; Whitfield-Gabrieli et al., 2011), which include the default mode network (DMN) discussed in the resting state section. They found abnormal temporal variability in these patients, calculated in the style of Garrett et al. (2010). Controlling for age, they revealed reduced SD in the cortical midline regions in VS patients compared to healthy individuals. Furthermore they illustrated that resting state temporal variability correlated positively with task-induced activity during self-referential processing (activity of brain during presentation of own name) in the precuneus, showing yet another evidence of the resting state's variability modulating task processing. In their standard fMRI analysis, activity during self-referential processing

was captured by subtracting signal changes during presentation of own name from signal changes during presentation of a control name. This suggests that increased variability in the resting state may be linked with greater ability in humans to differentiate between self and non-self stimuli, thus variability could serve as a predictor for self-referential neuronal processing efficacy. Future studies however need to investigate this question.

The next step was to test whether the altered brain variability was specific to VS patients or rather due to altered consciousness/self-processing in general. Thus in a follow-up study, Huang and colleagues compared temporal variance in the resting state during awake state and drug induced unconscious state (Huang et al., 2014b). They showed a decrease in temporal variance in the same cortical areas reported in the previous study during the resting state under anesthesia. To verify the independence of the drug choice, the experiment was repeated with two different anesthetic agents that have distinct molecular targets (propofol and sevoflurane). However, this time, they also observed increased temporal variability in the lateral regions of the brain. This suggests a deeper relevance of variability as it hints towards an existence of a medial-lateral balance of variability. This is consistent with previous findings showing increased SD in the sensory (lateral) areas (Fukunaga, 2006; Horovits, 2008). Furthermore, to look deeper into temporal variance, they illustrated frequency-specific effects in the thalamus similar to those of lateral regions, where SD increased only in the 0.01-0.027 Hz band of the anesthetic resting state activity (called slow-5). As mentioned before, the target spectrum of neuronal activity is usually filtered between 0.01-0.1 Hz (termed common) frequencies. This emphasizes the needs to look deeper into the different frequency bands that construct signals captured in the variety of brain imaging techniques. In conclusion,

as we go from the global level in investigating temporal variance, we start from observing general tendencies that are experimentally shown to be relevant for cognitive processing (as in aging and cognition). Then as we group the regions we observe balanced patterns between the midline and lateral areas. Moreover, in individual regions/networks, we observe frequency specific effects of variability (as in the thalamus). All of this extends the recently highlighted significance of temporal variability in neuronal activity in multiple layers. This calls for investigating temporal variability in such global, network specific and behavioral levels in our studies.

Much of the attention to the resting state and its measures also has come from the psychiatry literature. Recently, fMRI studies revealed resting state's neuronal alterations in bipolar disorder (Vargas et al., 2013). Bipolar Disorder (BD) is a mood disorder characterized by cycling between episodes of mania, hypomania, and depression (Smith et al., 2012). These studies mainly discuss the resting states in terms of functional connectivity (FC) and their results vary from one study to another. However, the majority suggests alterations in patients in several stages of the illness in connectivity patterns of the prefrontal cortex (PFC) and the anterior cingulate cortex (ACC) with other cortical and subcortical regions (Vargas et al., 2013). This revealed a prefrontal theme of dysfunction of affective networks (Strakowski et al., 2005). Interestingly, among the networks of the resting state, the DMN and the salience network (SN) and their interactions with the central executive network (CEN) may play an essential role in the psychopathology of BD. The DMN mainly contain cortical midline structures such as the ACC and posterior cingulate cortex (PCC) and association cortices (Buckner et al., 2008). Although most of the time the DMN is discussed as a single functional system, its

posterior and anterior parts seem to facilitate different interactions with other networks (Uddin et al., 2009). The anterior regions are reported to be involved in affective regulations, representations of emotions in the absence of an immediate incentive, and anticipation of affective consequences (Davidson, 2000). On the other hand the posterior regions seem to be involved in internal ideas and thoughts and mind wandering (Christoff et al., 2009). The CEN, which includes the dorsolateral prefrontal cortex (DLPFC) and the posterior parietal cortex, are reported to be associated with higher cognitive and executive functions (Goulden et al., 2014). Interestingly, the DMN, mostly responsible for internal processing, and CEN, associated with rather external contents, are observed to be anti-correlated (Uddin et al., 2009). It is hypothesized that the SN mediates the switching between DMN and CEN, leading to the reduction of DMN activity and increase of CEN activity when attention is required for the outside world (stimuli) (Goulden et al., 2014; Seeley et al., 2007). Here the significance of the cortical midline regions is highlighted in mediating different functions of the DMN and SN which appear to be affected in BD and other psychiatric disorders (Paola Magioncalda et al., 2015).

To explore the DMN in a rather regional specific manner and in the context of BD, Paola Magioncalda and Matteo Martino and their colleagues examined the PACC and the PCC. These two regions are shown to be highly connected during resting state period. Moreover, the PACC and the PCC represent the main anterior and posterior parts of the DMN, respectively (Qin and Northoff, 2011). Furthermore, they also investigated the SACC (supragenual anterior cingulate cortex), which is a pivotal in the SN, another part of resting state networks. Based on previous finding, they hypothesized that bipolar patients would have impaired connectivity in the DMN especially in the PACC.

Interestingly, they also investigated neuronal variability due to its increasing relevance in ageing, consciousness disorders and even brain injury research (Raja Beharelle et al., 2012). They predicted that neuronal variability would mirror functional connectivity findings in BD in the DMN. The group found decreased FC (especially in the slow-5) from the PACC to the posterior parts of the DMN (PCC), while variability measures remained unaltered. However, they found that variability and FC were correlated in control group but not in patient group. While the physiological mechanisms underlying the relationship between FC and variability remain unclear, FC is thought to reflect synchronization between neuronal systems and activities in different regions (Fingelkurts et al., 2004). Speculatively, that implies that the decoupling in BD patients between FC and variability affects normal connectivity patterns in which higher variability may make synchronization between neuronal systems more likely.

In summary these studies show deficits in the PACC in BD, being part of the anterior DMN, which could cause deficits in information transfer from this area to other cingulate gyrus regions (e.g. PCC). These deficits may cause abnormal shifting towards the DMN explaining the abnormal increase of internal content focus in BD patients. This is important as it highlights the dynamic nature of the brain. Thus this study is first to report specific PACC-based alterations in midline regions in specific frequencies (slow-5), and the decoupling with variability in BD. The case remains to be investigated in other psychiatric disorders and psychotic states, because those findings suggest neuronal variability as a biomarker in clinical diagnosis and therapy of BD and other psychiatric disorders.

Finally, using resting state imaging and biologically informed computational modelling (Deco et al., 2013; Wong and Wang, 2006), Yang and colleagues (2014) demonstrated how alterations in local (recurrent self-coupling) and distant (long-range coupling) signal synchronization impact temporal variability in the context of schizophrenia, which is an extreme example of a conscious state representing perturbations in sense of self, self-awareness, external world awareness. Their modeling results revealed that variability increased as a function of increasing local and distant signal synchronizations (the basis of functional connectivity which as discussed earlier abundant in the resting state research). Consequently it was suggested that the observed alterations in neuronal variability in schizophrenia may arise from alterations in neural coupling at both local and long-range scales, leading to a cortical network that functions closer to the edge of instability than in normal awake humans (Yang et al., 2014). This highlights the temporal dynamics of the brain neuronal systems as important aspect of brain functioning and perturbations in brain's temporal structures may contribute to the typical phenomenal attributes of psychiatric disorders, especially in schizophrenia.

Lastly, variability in principle is the measure of deviation of a series of time points from their mean. Hypothetically, if we rearrange the time points in the time series, the variability numerical value remain unchanged even though the whole integrity and temporal structure of the signal is altered. This illustrates that the picture is still incomplete as we still don't capture how the signal behaves over time by only measuring temporal variability. This is where scale free dynamics of brain activity come into the picture (also termed long term autocorrelation, complexity, and signal redundancy, depending on context they are used). And this highlights our need for additional measures

of the brain resting state to understand its temporal structure with more depth. As mentioned earlier, He (2010) illustrated a close relationship between temporal variability and scale free dynamics (long term correlations) of the brain and we emphasize in the next section the significance of such measures in investigating the temporal structure of the brain's intrinsic activity and the following section explores why.

1.4. Scale free activity.

Neuronal activity generally follow two modalities; the first is a Poisson-like firing activity that, for example, comes from cortical single or multiunit measurements of pyramidal neurons' spiking and the other is oscillatory activity that is evident the majority of EEG, MEG and local field potentials "LFP" measurements (He, 2014). Although less studied, the majority of signal power captured in LFP, EEG and MEG experiments show irregular patterns in contrast to the less common, yet more explored, rhythmic neuronal firing patterns (He, 2014). Brain oscillations are mostly studied in specific frequency domains, for example the early discovered occipital alpha waves which oscillate at 10 cycles per second, first illustrated by Hans Berger in 1929 (Hermann et al., 2015). These frequency- specific oscillations have their power peaking at that very frequency. In fact, many frequencies have been studied in neuroscience and each corresponds to different neuronal mechanisms, such as alpha, beta, omega and theta oscillations (Buzsaki et al., 2013). The power spectrum of brain activity, however, exhibits a dominant arrhythmic "frequency-free" activity.

This frequency free activity is illustrated by a so called "1/*f*" component which means that the power falls off as frequency decreases based on a power-law function: ($P \alpha 1/f^{\beta}$) where P is power, f is frequency, and β is a parameter usually falling between 0~3 (He et al.,2010), named the "power-law" exponent. Thus this activity is free of periodicity, as opposed to brain oscillations and studies of variability, and for that reason it has been recently dubbed "Scale-free" brain activity highlighting its scale-independent nature. It is worth noting that "white noise", which includes Poisson firing patterns, is an arrhythmic activity in which β equals 0 and thus power is constant as frequency changes

(He et al., 2010). Remarkably, this power-law distribution is evident in the temporal dynamics of the brain at several levels including neurotransmitter release statistics (Lowen et al., 1997), fluctuations in membrane potentials (Destexhe et al., 2003), local field potentials (LFP) (Milstein et al., 2009), EEG (He et al., 2010; Freeman and Zhai, 2009), fMRI signals (He, 2011; Bullmore et al., 2001; Ciuciu et al., 2012), and even fluctuations of behavior outputs such as reaction times, hit rates and forces (Kello et al, 2010; Smit et al., 2013; Palva et al., 2013).

The brain activity exhibiting this $1/f$ slope has been long considered irrelevant noise and often removed in analyses to obtain brain oscillations (He, 2013). To understand this long held practice, one must consider the universality of the "$1/f$ " behavior, which is strikingly widely evident in nature, such as in earthquakes, solar flares, economics, evolution, epidemics, electronics, and music (Bak, 2013; Hsu and Hsu, 1991). This universality encouraged researchers to distrust the connotation of the power law exponent in neuronal functioning and thus is almost always removed, in similar fashion to neuronal variability, from imaging signals in the processing steps. However, it is important to consider that power spectra are merely second-order statistics and similarities in power spectrum across several natural phenomena does not mean resemblances in higher-order statistics beyond that power spectrum. This indicates that the variety of mechanisms in nature responsible for generating scale free dynamics leading to power spectral shape, may not necessarily share the same structures that underlie such dynamics (He et al., 2010).

He and colleagues (2010) considered this issue by comparing higher-order statistics of the human ECoG signals during the resting state (19-83 mins of resting state),

with continuous earth seismic waves (4 months) and stock market daily price of the Dow-Jones index (80 years). They found that all three signals displayed "1/*f*" power spectra. To establish an index that can work for all three statistics in terms of scale-free dynamics, they borrowed an approach from the field of oscillatory neuronal activities, namely *nested frequencies*. Nested frequencies refer to the relationship of a low-frequency phase with the amplitude of a high frequency component in a signal (Canolty et al., 2006). To illustrate, most of such relationships were described between the phase of theta and the amplitude of gamma oscillations (Bragin et al., 1995; Tort et al., 2008) and between the phase of delta and amplitude of high frequencies (Lakatos et al., 2008). However, He et al., (2010) presented evidence of nested frequencies in a broader fashion than previously thought, extending beyond brain oscillations to within brain arrhythmic activity.

The results of this study revealed that nested-frequency tendencies were evident in all three types of signals (brain, seismic and stock activities) compared to a control signal which didn't exhibit evidence of such patterns (simulated random walk that shared an identical power spectrum with the other three signals). Moreover, nested-frequency patterns were largely distinct between the three types of signals; the preferred phase of the brain's ECoG signals were around 0 and +/- π, earth seismic fluctuations around +/- $\pi/2$, and interestingly no preferred phase in stock market fluctuations. These results demonstrate that, despite having similar power spectra between the different signals of different sources, each signal contains unique higher order structures. More importantly, these results emphasize that the "1/*f*" scale free brain activity contains rich temporal structures as opposed to the negative connotations associated with these signals and that they should be investigated more closely in research, rather than be considered noise.

Despite being relatively young, research on the functional meaning of scale free brain activity is beginning to show evidence that this activity is closely related to brain functioning. To begin, the arrhythmic broadband activity (5-200Hz) power of LFPs has been found to be in close correlation with neuronal firing rates in humans (Mannings et al., 2009). This finding was also replicated in a study on macaques by Ray and Maunsell (2011), who furthermore showed a strong dissociation between scale-free brain activity and brain oscillations in the same frequency range in the visual cortex (V1) of awake macaques using visual stimulation; as the stimulation increased, the population firing rates and broadband power in the gamma frequency decreased, while the power of narrow-band gamma oscillations increased. In other words, the broadband arrhythmic activity, rather than gamma oscillations, is associated with firing rates. Broadband activity in the gamma frequency range (30-200 Hz) is less obscured by prominent oscillations in the theta, alpha, and beta ranges (He, 2013). In fact, the power spectrum of this broadband activity shows strong task specificity evident in a wide range of tasks such as finger movement in humans (Miller et al., 2009), speech articulation (Bouchard et al., 2013), movie viewing (Honey et al., 2012), and default-mode functions, for example self-referential tasks and the resting state (Dastjerdi et al., 2011), two activities mentioned earlier to be notably overlapped.

More evidence emerged in several studies showing that the slope of the 1/f activity, which is estimated by the power-law exponent β, is modulated by sensory stimuli and task performances. El Boustani et al., (2009) recorded intercellular membrane potentials, in vivo, in the cat V1 to show that the power-law exponent in the high-frequency range is correlated with spatio-temporal statistics of the visual stimuli.

Interestingly, He et al. (2010) observed, using ECoG recordings in human, that the power law exponent in the low-frequency range (<4 Hz) decreased significantly across the brain when subjects were given a visual detection task. What could a reduction in power law exponent mean neuronally?

The Wiener-Khinchin theorem states "the autocorrelation function of a wide-sense-stationary random process has a spectral decomposition given by the power spectrum of that process" (Darabi, 2015). In other words, the power spectrum equals the Fourier transform of the autocorrelation function. This indicates that reduced power law exponent may showcase shorter and weaker autocorrelation of brain activity in time (He et al., 2014). This is important as the autocorrelation of brain activity may provide great insights into the temporal structure of brain activity and highlight the scale free activity as an essential measure in neuronal functioning referring to how similar brain activity is maintained in the time domain (i.e., redundancy).

ECoG signals measure the slow cortical potentials SCP in the brain and SCPs are found to be tightly correlated with fMRI signals (Pan et al., 2013; Kahn et al., 2013). Consequently similar findings are observed in the fMRI studies, i.e. the power-law exponent decreased during visual detection task as opposed to rest (He, 2011). These findings are evident in both activated and deactivated regions covering both visual task and rest regions in the brain. Given the advantage of the whole brain coverage of fMRI, further research illustrated the variations of power-law exponents across different brain networks. Fransson et al. (2013) showed that the power law exponent is largest in DMN, saliency network, and visual cortices and smallest in subcortical, sensory and motor regions, suggestion a network specific spatial patterns of scale free brain activity.

Moreover, He (2010) illustrated that the regions with higher power law exponent also have higher glucose metabolism. These findings suggest that the degree of autocorrelation in the fMRI signals varies across the resting state and task networks and tend to increase with increasing resting metabolisms.

More evidence for the significance of scale free property in neuronal functioning comes from the human development literature. The first two decades of human life undergo remarkable developmental change in sensory, motor, and cognitive capabilities arising from the continuous, some say lifelong, functional reorganization of neuronal circuits (Fair et al., 2009). White and gray matter changes are well documented to continue developing even in the third decade of the human life (Thatcher et al., 2008). Investigating 1433 subjects (aged 5 to 71 years), using EEG, Dirk Smit and his colleagues (2011) observed distinct developmental profiles for long term autocorrelations (estimated by power law spectra exponent) with significant changes from childhood to adolescence and even into young adulthood (~25 years of age) with the brain scale free property of the brain generally stabilizing after age of 25. More specifically, they show a moderate increase in autocorrelations from childhood into adolescence. Given that normal brain developments follow a clear path from temporally unstructured to high structured EEG, these findings suggest that autocorrelations/scale free properties of the brain may provide useful devices for studying a variety developmental disorders such as ADHD and schizophrenia. Furthermore, speculatively, the increases in scale free property exponents observed during adolescence and early adulthood may relate to cognitive functions such as sustaining attention, maintain information in working memory that represent the development of the general human cognitive abilities. Finally,

this study showed increased uniformity of brain distribution of autocorrelations/scale free components suggesting that, with age, brain areas become more connected and functionally integrated. This is supported by combined findings in fMRI illustrating three main modules of functional connectivity in the brain (Frontal, central, and posterior) show higher degree of intermodular connectivity with increasing age suggesting increased functional integration of distrain brain areas with age (Meunier et al., 2009; Fair et al., 2009).

The integration of segregated brain functional modules is reported to be a prerequisite for conscious awareness during wakeful rest (Boly et al., 2012). And as described earlier, power law exponents represent long term temporal memory of signals (hence repeatedly referred to as long-range temporal correlations LRTC in the literature). In fact, temporal integration is arguably measured by the long term memory in history of neural activity highlighting another important quantity scale free properties can serve (Tagliazucchi et al., 2013). Taking all of this into consideration, it is generally hypothesized in emerging literature that these temporal correlations play an important role in consciousness. To investigate this, Enzo Tagliazucchi and his colleagues (2013) explored the temporal memory of the fMRI signals across the human brain during non-rapid eye movement sleep cycle (NREM). They showed that the scale free properties quantified by power law exponents in fMRI gradually decrease as subjects go from wakefulness to deep non-rapid eye movement sleep. Interestingly, they also show that these decreases are especially evident in areas associated with default mode and attention networks suggesting both global and network specific alterations in scale free activity in diminished conscious awareness.

As discussed earlier, task-induced deactivations, especially in visual tasks, result in reduced long-term correlations across the brain as well (He, 2011). Taken together with the findings in the NREM sleep study, long range temporal memory appears to be an essential characteristic of a temporally dynamic range that support a conscious, wakeful resting state that can be suppressed by either loss of consciousness (NREM) or shifting focus on a demanding task. Thus, alongside the findings in development of integrated brain modules and scale free activity discussed earlier, temporal autocorrelations may serve an important biomarker of wakeful, aware consciousness and abnormal alterations of such property may indicate brain temporal deficits that need to be studied in a variety of developmental, consciousness and psychiatric disorders.

Illustrating such potential of scale free dynamics as "biomarkers", Wei et al. (2013), estimated the long term memory of resting state networks in both healthy and patients diagnosed with major depressive disorder (MDD). Resting state networks were identified using principal component analysis in 20 patients as well as 20 control subjects. They used "Hurst" exponents to describe the scale-free properties of the spontaneous brain activity in each network identified in the PCA, a method also used widely in the literature and is considered equivalent to the power law exponent β (Maxim et al., 2005; Park et al., 2010) (details can be found in the methods section). Generally, values of Hurst exponents "H" falling between 0.5 and 1.0 indicate the presence of a persisting long term autocorrelation in the signal. A larger H indicated a stronger long-term autocorrelation in the time-series. First, the study showed that BOLD signals of the resting state networks displaced long-term temporal memory replicating the several other studies showing long term autocorrelations/scale free dynamics in the resting state

networks. Second, they illustrated that the values of *H* could predict and discriminate MDD patients with impressive 95% accuracy providing a direct evidence of scale-free properties as biomarkers and provide insights into the pathophysiological mechanisms of depression. Moreover, they identified two classification patterns in a similar fashion to a previous Autism study (Ecker et al., 2010): Excess networks displacing an increase in H in MDD and deficit networks displaying decrease H in the MDD group. They found that right pronto-parietal and the DMN showing deficit networks while the left fronto-parietal, ventromedial prefrontal and salience networks showing excess networks. This provides clear evidence encouraging studying these temporal properties both globally and in a network-wise manner to identify and understand the neural substrates of MDD. Also, whether such strategies can be extended to other psychiatric disorders remain largely unexplored, such as in schizophrenia and bipolar disorders.

1.5. Psychiatry and the resting state.

As discussed earlier, the brain's resting state activity has gained increased attention in the field of psychiatry. Spatially, the brain resting state can be categorized into multiple neuronal networks exhibiting high functional connectivity or coherence. These networks include the paradigmatic DMN, showing elevated low frequency fluctuations (Raichle et al., 2001), sensorimotor networks, salience network and the executive network. All of these networks are dynamically integrated in the resting human brain (de Pasquale et al., 2012). Consequently, looking into the temporal component of the resting state, one can characterize activity in these networks by fluctuations in different frequency bands as shown in EEG studies such as delta (1-4 Hz), theta (5-8 Hz) alpha (8-12 Hz) etc., and infraslow frequencies captured in fMRI (0.01-0.1 Hz). Notably, emerging evidence suggests that even the infraslow frequencies captured in fMRI have now distinct frequency bands with distinct functional properties such as slow-5 and slow-4 (Baria et al., 2011; Han et al., 2010; Zuo et al., 2010). These distinct frequencies are inter-correlated with each other's (Buszaki et al., 2013) contributing to a highly complex temporal structure in the resting brain (Cabral et al., 2014). Thus, it is necessary to understand the brain's resting state as an integrated spatio-temporal structure that is explored in a physiological and functional manner in addition to the classic anatomical and structural one in imaging studies (Northoff, 2014a, Northoff 2014b).

Studies of functional connectivity (or neuronal coherence) have constituted the main body of the resting state literature within the context of psychiatry. In schizophrenia, functional connectivity within the cortical midline structures/DMN increase while functional connectivity of the executive network, including the lateral

prefrontal cortex, is decreased (Karbasforoushan and Woodward. 2012). Moreover, elevated low frequency fluctuations are observed in schizophrenia particularly in anterior midline regions, which include the DMN (Hoptman et al., 2010). These alterations in the spatial correlates of the resting state can be linked to symptoms of schizophrenia which represent alterations in the balance between internal vs external mental contents in patients (Vanhaudenhuyse et al., 2011). Specifically, the documented anti-correlation between the DMN and control executive network CEN has been associated with maintaining balance between internal self-related and external environment-related mental contents in consciousness (Northoff et al., 2004; Vanhaudenhuyse et al., 2011; Wiebking et al., 2014). When resting state activity/coherence in the medial regions and DMN is stronger, mental focus seems to be shifted to internal mental contexts related to own self, thoughts and body (Vanhaudenhuyse et al., 2011). In contrast, stronger coherence in the lateral regions/CEN leads to increased external mental contents in consciousness. Interestingly, the predominance of one activity, internal vs. external, takes place at the expense of the other making a reciprocal balance between them (Northoff et al., 2004). And such reciprocal balance is evident to be maintained by the anti-correlation between DMN and CEN.

Recently, this anti-correlation was also investigated in the psychedelic experience using psilocybin, which the substance found in few types of mushrooms, colloquially known as “magic mushrooms”, to mimic early psychosis in healthy subjects (Carhart-Harris et al., 2013). Carhart-Harris and his colleagues observed a significant decrease in the anti-correlation between the DMN and CEN following psilocybin injection and during the psychedelic experience. Interestingly, this decrease in the anti-correlation has

also been observed in schizophrenia (Salvador et al., 2010; Woodward et al., 2011; Chai et al., 2011; Whitefield-Gabrieliet al., 2009). Moreover, decreased DMN-CEN anti-correlation has been found in humans at high risk of psychosis (Shim et al., 2010). The inability or the confusion in distinguishing between internal world and external environment is a prominent shared feature between early psychosis (Bowers and Freedman, 1966) and the psychedelic experience in general (Klee, 1963) regardless of how positive or negative it is experienced by subjects (e.g. spiritual experiences vs bad trips). And temporal activity in the DMN and its relation to the CEN and potentially other resting brain systems appear to provide the possibility of the brain to distinguish between internal and external thoughts and perturbations in such activity is evident to be linked to such ego disturbance found in the psychedelic experience in healthy adults and schizophrenic patients. While this point is discussed within the context of the functional connectivity, it is unclear how the temporal correlates such as variability and scale free activity of the DMN are affected during psychotic states.

The blurring effect between internal and external contents has been proposed to underlie auditory hallucinations evident in schizophrenia (Northoff, 2014). Studies have shown abnormally high resting state activity and coherence in the auditory cortex in patients with chronic auditory hallucinations (Sommer et al., 2012). The voices are mainly perceived as external speculatively as a result of the alterations of the DMN in relation to the CEN and other functionally connected areas to it. The DMN itself is weakly connected to the auditory cortex in the resting state, and the latter is strongly associated with the CEN. This may be responsible for assigning hallucinations to external sources rather than keeping them to internal origins (Northoff and Qin, 2011). In

addition, temporal features of the resting state appear to play a significant role in generating auditory hallucinations. As shown in EEG, phase synchrony in the alpha band in the auditory cortex increases just before and during auditory hallucinations. Also, different frequency bands, such as gamma and theta, exhibit increased phase-phase coupling in fronto-temporal brain regions and temporal electrode T7 in EEG, which includes the auditory cortex during auditory hallucinations (Koutsoukos et al., 2013). Even though psychiatric studies shed light on the resting brain resting state activity and its abnormalities in psychiatric disorders, such as the case in schizophrenia, the exact nature of such abnormalities in the resting state itself still remain largely unclear. Which leaves open the questions about the measures that can be captured in the temporal structure of the brain's resting states and their relationship with psychopathological symptoms of psychiatric disorders beyond investigating functional connectivity and fluctuations phase couplings.

As discussed in earlier sections functional connectivity in principle describes the degree of coordination of brain activity within and between regions (Biswal et al., 1995; Cordes et al., 2000; Grecius et al., 2004). These calculations by their nature scale away most of the temporal properties and characters of brain signal such as variability and the brain signal behavior over time, such as illustrated in scale free dynamics for instance. In other words, functional connectivity measures the temporal correlation between two timeseries rather than exploring the individual timeseries per se. Also we discussed evidence showing that both temporal variability and scale free dynamics are central and potentially complimentary measures of large-scale brain activities in a variety of contexts from aging, consciousness, sleep, and psychiatric studies. Thus, beyond functional

connectivity, the temporal dynamics of brain functioning can provide valuable insights into normal and diseased brain states. However, the concept of the brain signal's behavior across time has been investigated under several labels that nonetheless share the same underlying concepts such as timeseries auto-correlations, redundancy, complexity, entropy, predictability, long term memory and scale free power spectra.

Recently, these times varying dynamics of brain signal has been highlighted in psychiatric disorders within the context of complexity science. The origins of such views were established early by Henri Poincare in 1881 (Barrow-Green, 1997) and have been applied to different fields in biology in the past decades (Yang and Tsai 2013). In fact, the core concepts of complexity science represented by fractals and chaos measurements have been applied to cardiac activities (Glass and Mackey 1988). Generally, early studies of human physiology in the context of complexity revealed that more complex physiological outputs are generally obtained from healthy individuals compared to individuals in a pathological state or when aging (Goldberger et al., 2002; Lipsitz and Goldberger, 1992; Vaillancourt and Newell, 2002). Intriguingly, quantifying methods derived from complexity science have drawn attention in classifying behavioral issues and pathological states in various psychiatric disorders (Paulus and Braff, 2003). Notably, schizophrenic patients exhibit more predictable or redundant behavior measured by binary choice tasks compared to healthy individuals (Paulus et al., 1996). This is also found in bipolar patients as they report daily record of mood with more organized manner compared to healthy subjects (Gottschalk et al., 1995). Analysis of EEG neurophysiological data in recent years illustrated abnormalities in the dynamics of these signals in a variety of mental disorders (Fernandez et al., 2010). In schizophrenia,

abnormal EEG complexity, measured by multiscale entropy analysis, was found in patients and could be reversed using antipsychotics (Takahashi et al., 2010). In addition similar reversing effects in complexity measurements using antidepressants were observed in patients with depression (Mendez et al., 2012). All of this evidence has led to the development of a recent hypothesis proposing that mental illness is a loss of brain complexity (Yang and Tsai, 2013).

What is a complex system in the human physiological sense? In human physiology, complexity can be viewed as a system of numerus parts varying from molecules, cells to organs complicatedly intertwined together. A classic approach to analyze any system is to reduce and disassemble such system into the building blocks and examine each component and then reassemble them to recreate the original system. In most cases however such approach is not optimal as it is only possible to observe and measure the macroscopic physiological outputs such as EEG, heart rate, respirations and brain functions (Yang and Tsai, 2013). In the case of functional magnetic resonance imaging fMRI, a single voxel (three dimensional unit of size in fMRI) represents extremely complex and intertwined responses from a large number of neurons. Thus, to characterize and measure brain complexity in neuroimaging, a reasonable place to start at is to measure the system's behavior across time. For example, a system may be either ordered or random. To note however, that physical meaning of randomness does not necessarily correspond to how complex a system is (Goldberger et al., 2002). This means that a good measure of complexity should include how much information is evident in the system, as both random and complex systems don't necessarily convey meaningful information or structure but rather a system with rich information content can be

considered complex. Therefore, one has to be careful when applying the science of complexity to physiological outputs. A good example to illustrate this point comes from studies of heart rates where randomness of heart rate was assessed using entropy-based methods to quantify regularity of a heart time series (Richman and Moorman, 2000). A conventional entropy increases in close relation with irregularity. In the heart of healthy person, higher entropy was observed compared to the pathological state myocardial infarction (Makikallio et al., 1997) and heart failure (Ho et al., 1997). However, higher degree of entropy was observed in other pathological states such as atrial fibrillation (Costa et al., 2004). This makes generalization harder in the context of complexity which mainly arises from the different mathematical frameworks and methods that measure complexity in physiological timeseries. Thus, measurements of scale free brain activity and temporal variability, based on the substantial neuronal evidence discussed earlier, provide valuable systemic insights into brain functioning rather than mere randomness vs orderliness that can be obtained in some of the mathematical methods used to measure complexity, which don't necessarily measure information about the brain temporal structure.

Many approaches have been proposed to be meaningful measures of complexity such as multiscale entropy MSE (Costa et al., 2005), which was successfully used in differentiating the complexity of heart rates in a variety of pathological conditions (Cheng et al., 2009) in addition to several physiological outputs such as the human gait (Costa et al., 2004), postural sway (Costa et al., 2007), EEG signals (Catarino et al., 2011). In studies of mental disorders, several complexity measures have been proposed such as approximate entropy (Caldirola et al., 2004), correlation dimension (Gottschalk et

al., 1995), Hurst exponent (Lai et al., 2011) and others. Notably, essential differences in the physical meanings can be found in these measures as for example the Hurst exponent is a chaos-based estimation of complexity while Lempel-Ziv statistics are based on algorithmic complexity. Substantial work is needed to review comprehensively and differentiate the several mathematical methods that are used in studying complexity of physiological brain signals.

In psychiatric disorders and especially in schizophrenia, the unpredictable nature of behavioral patterns in psychosis has motivated the use of complexity measures to study the behavioral patterns of patients in the pathological state (Ehlers, 1995; Paulus and Braff, 2003; Breakspear, 2006). In this context, complexity is discussed as a systemic measure of the brain's capability to interact with constantly changing environment. And this ability appears to be altered in schizophrenia and several other mental disorders which may lead to abnormal behavioral patterns, cognitive attributes and social functions (Bassett and Gazzaniga, 2011). Therefore, studying complexity and signal behavior over time may provide a direct link and measurement between behavioral patterns of schizophrenia with physiological brain functions. In addition, complexity measurements may provide valuable clinical tool for psychiatric evaluations of the severity of symptoms and help measure treatment effectiveness.

Indeed, altered brain complexity have been showed in schizophrenia using several imaging techniques such as EEG (Koukkou et al., 1993; Raghavendra et al., 2009; Takahashi et al., 2010), MEG (Gernandez et al., 2011) and structural imaging of gyri folding (Narr et al., 2004). Recently, the analysis of fMRI resting state complexity over time has attracted significant attention. As briefly discussed before, the nonlinear

attributes of the brains resting state activity served as marker for aging and mental illness (Meunier et al., 2009), such as in Alzheimer's disease (Liu et al., 2013), attention-deficit hyperactivity disorder ADHD (Anderson et al., 2006; Sokunbi et al., 2013), autism (Lai et al., 2011) and aging (Smith et al., 2014). All of these studies provide considerable evidence that altered temporal properties of BOLD signals in the resting state due to the disease state and strongly suggest novel neuroimaging approaches to investigate brain dysfunction associated with mental disorders.

1.6. Ketamine as a model for schizophrenia.

Schizophrenia is characterized by a set of psychotic symptoms described as either positive or negative symptoms in addition to social and occupational abnormalities. Mainly, two neurotransmitter systems are used to explain the biochemical basis of schizophrenia: the dopamine and glutamate systems. Initially, dopamine D_2 receptor antagonists such as chlorpromazine were found to attenuate psychosis which encouraged the development of the *dopamine hypothesis of schizophrenia* early in 1970s (Howes and Kapur, 2009). In general, abnormally high dopamine levels (hyperdopaminergia) were proposed to be responsible for the positive symptoms of schizophrenia (Lau et al., 2013). However, later findings and refinements to the dopamine hypothesis postulated that striatal regions exhibit hyperdopaminergia while prefrontal cortical regions show hypodopaminergia (Howes and Kapur, 2009; Lau et al., 2013). The first criticisms of the dopamine hypothesis highlighted its failure of explaining this differential subcortical and cortical dopamine dysfunction (Abi Dargham and Guillin, 2007). Moreover, another weakness of the dopamine hypothesis is the poor efficacy of D_2 receptor antagonists in reducing the negative and cognitive symptoms of schizophrenia (Javitt et al., 2012). On the other hand, the *glutamate hypothesis of schizophrenia* proved to be a stronger candidate.

Developed in the mid-1990s, the glutamate hypothesis of schizophrenia proposes glutamatergic dysfunction as a mechanism responsible for both the positive and negative symptoms, in addition to the cognitive impairments of schizophrenia (Olney and Farber, 1995). Such hypothesis was based on the widely replicated observation that N-methyl-D-aspartate glutamate receptor (NMDAR) antagonists, which include phencyclidine (PCP)

and ketamine, temporarily induce psychotic states resembling those positive, negative and cognitive symptoms of schizophrenia (Thornberg and Saklad, 1996; Newcomer et al., 1999; Olney et al., 1999; Morris et al., 2005). Moreover, the interaction of D_1 receptors and NMDAR suggests that dopaminergic dysfunction is a later step in a pathway that begins with NMDAR dysfunction (Roberts et al., 2010) emphasizing the important of the glutamate hypothesis of schizophrenia as the root cause. Moreover, support for the glutamate hypothesis comes from similarities between schizophrenia's age of onset in early adulthood and the age of persons in whom ketamine induce hallucinations most commonly (16 years of age and older) (Reich and Silvay, 1989; Kehrer et al., 2008). Notably, the proportion of ketamine's psychomimetic effects that can be attributed to receptors other than NMDAR still represents a challenge in the ketamine model of schizophrenia. However, extensive evidence shows that NMDAR dysfunction is responsible for the ketamine effects on the brain.

Ketamine effects on the NMDAR are themselves complex and can be considered counterintuitive in few cases. For example, ketamine as NMDAR antagonists has been shown to induce a net effect of increased glutamate release (Rowland et al., 2005; Kim et al., 2011). Moreover, ketamine has also been found to increase release of glutamate in the anterior cingulate cortex (ACC), which is a paradigmatic region of the DMN, which in turn correlated with positive psychotic scores in healthy humans (Stone et al., 2012). Indeed, molecular evidence strongly points to NDMAR dysfunction in schizophrenic brains as they have reduced levels of proteins linked to NMDAR function in working memory (Karlsgodt et al., 2011), dystrobrevin-binding-protien-1 (dysbindin) (Talbot et al., 2004), and dysbindin mRNA (Weickert et al., 2004). Also, direct *in vivo* evidence

using intra-channel NMDAR radiotracer found reduced binding in the left hippocampus in schizophrenia patients (Pilowsky et al., 2006). Finally, adrenochrome (metabolite of epinephrine) and -9-tethadyrocannabinol (-9-THC) (main psychoactive ingredient in cannabis) can also induce schizophrenia like symptoms (Smythies, 2002; D'Souza et al., 2004) but neither of these models have shown repeated and substantial evidence as much as the ketamine model. Thus evidence supports NMDAR as the principal site of ketamine's psychomimetic effects and favors the ketamine model of schizophrenia over competing models.

How about ketamine and the resting state? As discussed earlier, much of the knowledge concerning psychiatry and the resting state comes from functional connectivity studies. The concept of disturbed network connectivity in schizophrenia matches the common notion that schizophrenia is a disconnection syndrome (Sporns, 2011). In fact, this hypothesis dates back to Wernicke (1906), who linked psychosis with disruptions of association fibers. The choice of the term schizophrenia itself by Bleuer in 1908 (Ashok et al., 2012), describes the "splitting" of the mind. Both increased and decreased network connectivity have been observed in schizophrenia (Pettersson-Yeo et al., 2011). And ketamine alters functional connectivity with same patterns as schizophrenia in both humans and animals (Voss et al, 2012; Dawson et al., 2013). In the resting state specifically, ketamine increases overall global based connectivity (the functional connection of each brain voxel with all other voxels in the brain) (Driesen et al., 2013). Ketamine also was shown to reduce the anti-correlated relationship between task positive networks and the DMN during a memory task (Anticevic et al., 2012) which is consistent with reduced DMN suppression during memory tasks observed in

schizophrenia (Whitfield-Gabrieli et al., 2009). Moreover, in the resting state, ketamine reduces connectivity between the DMN and the affective network with the dorsal medial PFC (Scheidegger et al., 2012), between the auditory and somatosensory network and pain processing areas. Ketamine also increases connectivity between both cerebellum and visual cortex with the medial visual network (Niesters et al., 2012). Thus it remains for investigation how ketamine affects temporal variability and scale free properties in the resting state. Since ketamine is proven to be a good model for schizophrenia, it makes an ideal candidate to induce psychotic state and study the temporal structure of the brain in healthy individuals and then relate them to schizophrenia studies.

1.7. The current study.

Based on the discussion in earlier sections, imaging results have highlighted abnormalities in the temporal structure of the resting state in psychiatric disorders, such as schizophrenia. The exact meaning of such abnormalities for psychotic states remains largely unclear. Perturbations in the spatio-temporal structure of the resting state have been recently suggested as basis to key psychopathological symptoms such as auditory hallucinations and ego disturbances especially in schizophrenia (Northoff, 2014). Thus our study aims to investigate directly the temporal structure of the resting state in the psychotic state as induced by ketamine, which is known to induce schizophrenia-like symptoms. Based on accumulated evidence, temporal variability and scale-free dynamics are suggested to be key markers for an efficient and healthy brain from converging lines of research such as aging, sleep, anesthesia, psychiatry. Such measures of the resting state have been especially linked to inefficiencies and abnormal balances in neuronal functioning. Specifically, increased temporal variability has been associated with younger and more cognitively efficient brains. Furthermore, complexity studies also suggested that loss of brain activity complexity (which is a label for scale-free brain activity) across time provides a basis for a variety of mental disorders, especially schizophrenia. Thus, we hypothesize that increased activity autocorrelation (can be expressed as a loss of complexity, or increased redundancy in the time series) and decreased variability are associated with a compromised brain state that leads to inefficiencies in the brain's ability to interact with incoming stimuli and that may explain a variety of symptoms characterizing schizophrenia.

With the above in mind, the general aim of our study is to examine the effects of ketamine on the temporal variability and scale free brain activity. Our specific aims are to illustrate effects of ketamine on 1) global brain temporal variability and scale free dynamics and the relationship between them, 2) on the different key networks of the brain, and 3) the relationship of temporal variability/ scale free dynamics with psychological changes induced by ketamine. To achieve that, we investigated 4 minutes of resting state in fMRI scanner in 32 healthy individuals under the effects of both placebo and ketamine. We conducted a region-of-interest (ROI) analysis, using two established templates, to cover the brain in global (264 ROIs covering the whole brain) and network-wise (41 ROIs divided into key networks) approaches. We calculated temporal variability as the standard deviation (SD) of time series and estimated the scale free activity (Hurst exponent) for each of the regions of interests and compared between two conditions: placebo (saline) and ketamine injections. The linkage between SD and Hurst were investigated by correlating the two via an ROI-based correlation (or node based correlation) in both saline and ketamine, respectively. We then studied correlations of the differences of these measures (Saline vs ketamine) with the positive and negative syndrome scale (PANSS) obtained before and after the ketamine experience.

2. Methods

2.1. Magnetic resonance imaging: principles and background.

The essence of magnetic resonance imaging (MRI) is based on nuclear magnetic resonance (NMR) spectroscopy. MRI utilizes the absorption and emission of radiofrequency electromagnetic radiation (RF) by nuclei that behave like magnets and can be made susceptible to such absorption and emission by placement in a large static magnetic field (Huettel et al., 2004). In the human body, hydrogen is the most abundant atom consisting of an unpaired proton. These protons spin around themselves creating a magnetic momentum, and are usually labelled "spins" in the NMR literature. In addition, these individual protons are magnetic sources themselves and can interact with each other (termed in some contexts: spin-spin interactions) in addition to the applied external field. In normal conditions, these spins are randomly oriented (figure 1a). When placed under a static, strong magnetic field such as the one in MRI scanners, B_0, protons change their orientation. Instead of completely aligning themselves with the direction of the magnetic field B_0, theses spins undergo a gyroscopic motion known as "precession" rotating around the axis of the magnetic field. In other words the protons don't perfectly spin along the magnetic field axis; instead their spinning axis is tilted creating a circle around the strong magnetic field axis B_0 (figure 1b). Quantum physics tell us that precessing protons exist in two states: parallel and antiparallel to the magnetic field axis, with the latter existing in a higher-energy state than the first. Since parallel processing protons exist in a lower-energy state, it is more stable and they are slightly more abundant than the antiparallel spins. When protons transfer from the low energy state to the high energy state they need to absorb energy (photons) and vice versa. It is this emission of energy,

going from high-energy state to low-energy state, which can be detected in MRI scanners and form the basis of this imaging technique. It is important to note that as spins exist in a large numbers, only net magnetization can be taken into consideration in the context of understanding the basics behind MRI imaging.

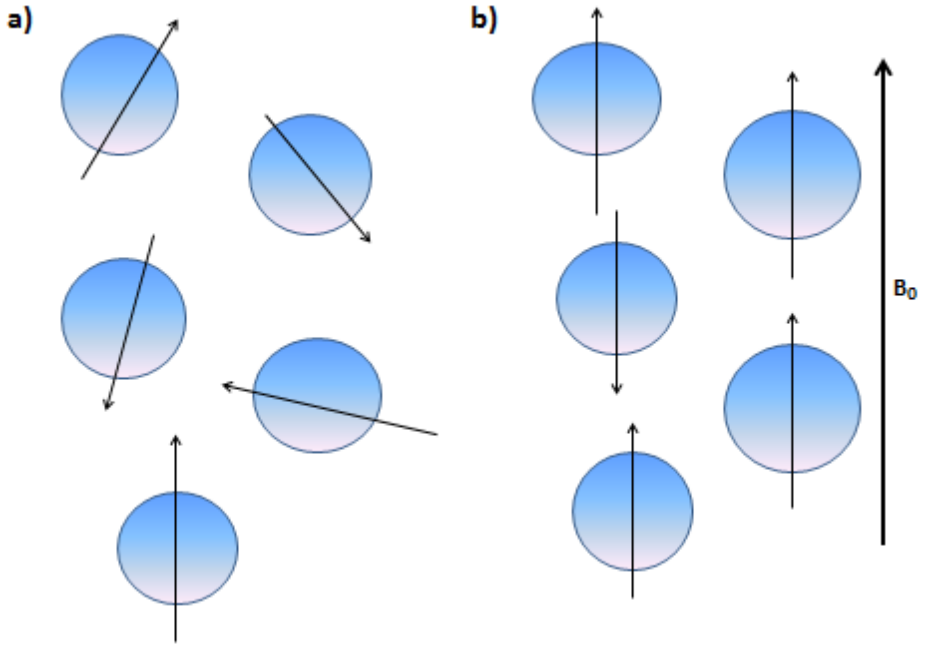

Figure 1. Orientation of protons (spins). Under (a) normal conditions and (b) strong magnetic field as can be found in the MRI scanner. Arrows show the axis of precessing.

To initiate the transition of the spins from low-energy states to high-energy states, a radiofrequency coil (RF coil), placed usually perpendicular to the scanner's magnetic field in the transverse plane, blast the spins in the magnetic field B_0 with photons that act as electromagnetic fields resonating at the same frequency of the target spins. The angle to which the net magnetization of all the spins is tipped is termed as "flip angle". As a result, some spins transfer from the low energy parallel state to the high energy antiparallel spins (Figure 2b). This leads to the net magnetization of the frequency to spin

in the transverse plane instead of the initial longitudinal plane (parallel spins). Immediately after this energy source is removed, these spins return to the low-energy state by emitting the energy they absorbed. Measurements pertaining to this emitted energy provide the data that construct MRI images (figure 2c).

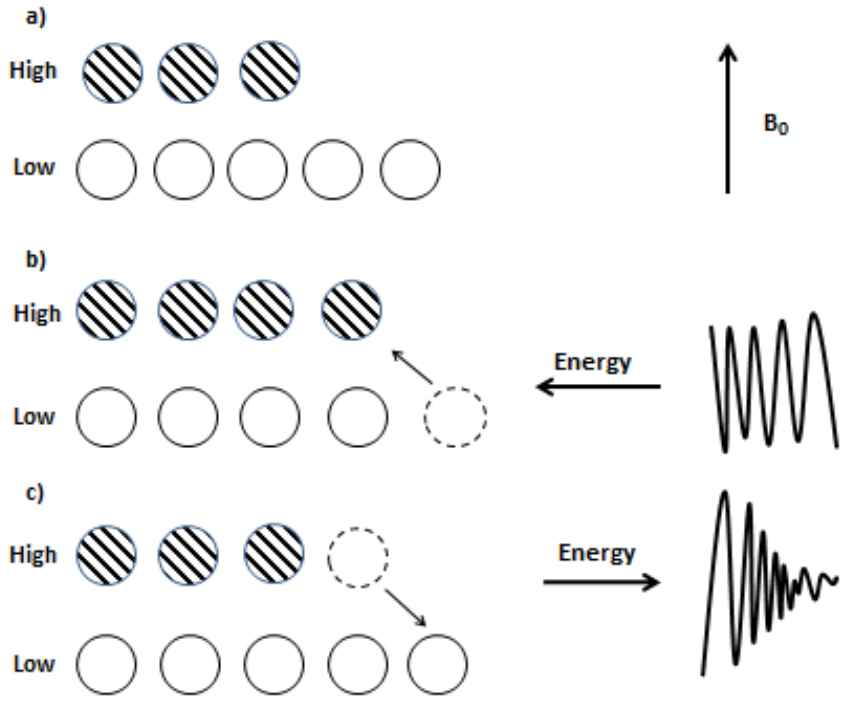

Figure 2. The behavior of spins in the scanner's magnetic field (B_0) and transfer of spins from low energy to high energy state when the RF coils are activated. a) Before RF coils are activated. b) After RF coils bombards the spins with energy with certain flip angles. c) RF coils stops introducing energy into the scanner; spins start to emit the absorbed energy.

In more detail, the magnetic resonance signal emitted after this excitation by the RF coil decay within seconds representing a phenomenon termed "relaxation". There are two primary sources underlying this loss of signal, one is longitudinal relaxation and one is transverse relaxation (figure 3a). After the initial tip by the RF coil pulse, the spins that transferred from the parallel to the antiparallel states gradually return to the parallel longitudinal orientation of B_o. The time constant associated with this relaxation type is

termed “T1” relaxation. Moreover, after the spins are tipped by the initial pulse, they start their precession process at the same point (same phase) on the transverse plane. Then, due to spin-spin magnetic interactions, they start to lose coherence and precess out of phase in a phenomenon termed “transverse relaxation” (figure 3b). The time constant associated with the signal loss due to this phenomenon is termed as “T2”. Furthermore, an additional source for differential spins in the transverse plane is the external static magnetic field B_0 itself. Any magnetic field is inhomogeneous and variation in the strength of the field from one location to another causes spins at different locations to precess at different frequencies, adding another reason for the loss of coherence in the transverse plane. The combined effects of the spin-spin interaction and the inhomogeneity of the magnetic field lead to a signal loss known as T2* which is always faster than T2 due to the combined effects of the two magnetic interaction factors. These different relaxation times (T1, T2, T2*) determine how much MR signal can be detected during a single RF coil pulse and multiple pulses are used to acquire complete images. The success of MRI as an imaging technique comes from sensitivity to varying relaxation properties of the different body tissues (e.g.: fat, CSF, bone, white and grey matter...etc.).

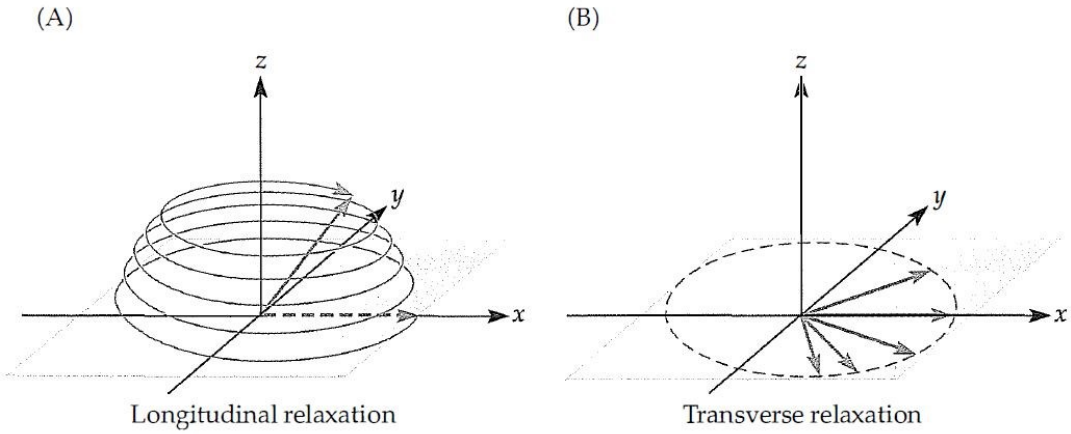

Figure 3 Relaxation types responsible for MRI signal detection. A) Longitudinal relaxation as spins return from anti parallel to parallel states. B) Transverse relaxations as spins lose coherence in the phase of precessing. (Huettel et al., 2004).

Another set of coils is present in the scanner called the "gradient coils" to localize the specific absorption and emission properties of the tissue being imaged to small volumes termed "Voxels". The term voxel is used to specify a three-dimensional unit of resolution in a similar fashion to the two-dimensional unit "pixel" used in a variety of applications. Depending on the settings chosen by the experimenter, these voxels can vary in size. The frequency of the spin precessing depends on the strength of the applied magnetic field $B_{0.}$ Thus, these gradient coils make slight modulation of the applied field creating a map of different frequencies and making possible the localization of spin relaxation times in voxels. Structural MRI makes use of the differences between the values for each voxels to differentiate neighboring types of tissues. For example, if a water-rich tissue and water-poor tissue are beside each other, voxel intensities differ between these two tissues as T1 relaxations are different due to intrinsic magnetic

differences of the tissues. And thus it is possible to differentiate in structural MRI between bones, white, grey matter, and CSF as they appear in different intensities due to their distinct intrinsic magnetic properties making possible the construction of MRI images.

2.2. Functional magnetic resonance imaging fMRI.

In theory there is no fundamental difference regarding the signal collected by fMRI imaging compared to structural MRI. However, functional imaging requires speed and sensitive acquisition to account for momentary activity changes in the brain. Thus the primary target in functional imaging is not anatomical discriminability but rather the change in tissue properties over time. The foundation of fMRI rests on the observation that activated neural tissue cause a significant vascular change in blood flow (Ogawa et al., 1990). Activated brain areas, following task stimulation for example, are accompanied by a dramatic increase of blood flow and volume to that same area due to increased oxygen consumption over a period of few seconds following stimulus and activation (Leniger-Follert and Lubbers, 1976). In fact, this phenomenon was investigated by means of electrophysiology and MRI imaging to reveal that such increase in blood flow was truly due to increase in neuronal activity; and evidence was indeed supporting such stand (Attwell and Iadecola, 2002; Logothetis, 2002; Logothetis and Wandell, 2004). These studies showed increase of fMRI signal and neuronal spiking during motion tasks (Rees et al., 2000) and the direct correlation of fMRI signals was linked to local field potentials LFP (Logothetis, 2002). This also might be an additional motivation and underlying cause behind the focus on task evoked activity. That is, the imaging technique itself was made popular based on the observations concerned with functionally localized tasks.

In principle, multiple low resolution images are obtained for the area of interest, or whole brain, and are recorded in rapid succession. Then the images are compiled in series to eventually produce a timeseries of intensities for each voxel. The nature of the

signal obtained depends on the contrast method the experimenter chooses, which will be discussed in the next paragraphs. This timeseries can then be used for experimental evaluation of the targeted response to the applied stimulus in stimulus-induced activity or analyzed as a resting state timeseries independent of any stimulus. In other words, in an event-related study, a single task is given to the subjects and usually is repeated several times with the corresponding responses aligned upon the onsets of the task. Then, the timeseries related to the task is averaged over the multiple trials in order to measure the time course of activation in a target brain area.

The amount of blood sent to the particular area increasing in activity contains a surplus of oxygen for such activity (Huettel et al., 2004) leading to a corresponding surplus of local blood oxygen. The signal measured in fMRI depends on this change in blood oxygenation level and thus is termed the blood oxygenation level dependent *BOLD* signal. The technique relies on the fact that deoxyhemoglobin is weakly paramagnetic. As local blood oxygenation decreases, its T2* relaxation time shortens. When an area in the brain becomes active, blood flow and blood volume increase leading to an eventual decrease in the level of deoxyhemoglobin. As deoxyhemoglobin decreases, the paramagnetic effects are no longer present and an increase in BOLD signal intensity is measured in the activated area of the brain.

The change in blood flow that follows a period of neuronal activity is known as the *hemodynamic response*. Two characteristics of this response shape the features of the BOLD signal and the way BOLD data are analyzed in general. First, the hemodynamic response is slow as compared to the neuronal activity which may last for milliseconds. The increases in blood flow take about 5 seconds to reach its maximum and then is

followed by a long undershoot that returns completely to its baseline in 10-20 seconds (figure 4a). Second, the hemodynamic response can be treated as a linear time-invariant system (Cohen, 1997; Dale, 1999). The meaning of linearity here is that if the neuronal response is scaled by a factor of x, the BOLD response is also scaled by the same factor. Looking at figure (4a), we can see when the neuronal response is doubled in magnitude; the expected BOLD response also doubles. Moreover, knowing what the response would be like for two separate events, if they occur close together in time the resulting signal would also be the sum of the independent events (figure 4b). The "time-invariant" here means that if the stimulus is shifted by *t* seconds, the BOLD response also shifts by the same *t* amount. Consequently, to find out whether a voxel's change in activity corresponds to a specific task, a model is constructed to predict the BOLD response of the voxel. A statistical match between the model and the actual BOLD curve is the measure that is reported in stimulus induced experiments. Thus the basis of fMRI statistical analysis for task-evoked activity depends on the complex convolution functions to match the BOLD's hemodynamic signal and its physiological properties with a modelled response. If a match is found between the hemodynamic response and a modelled response then a t-score can be obtained for a voxel and such t-scores infer to the amplitude of activation of the voxel in response to the task. Due to the current study's focus on resting state activity and its temporal properties, no convolution analysis is necessary because there is no stimulus to be traced in the time series. Therefore we will not go into the details of the convolution techniques used in fMRI.

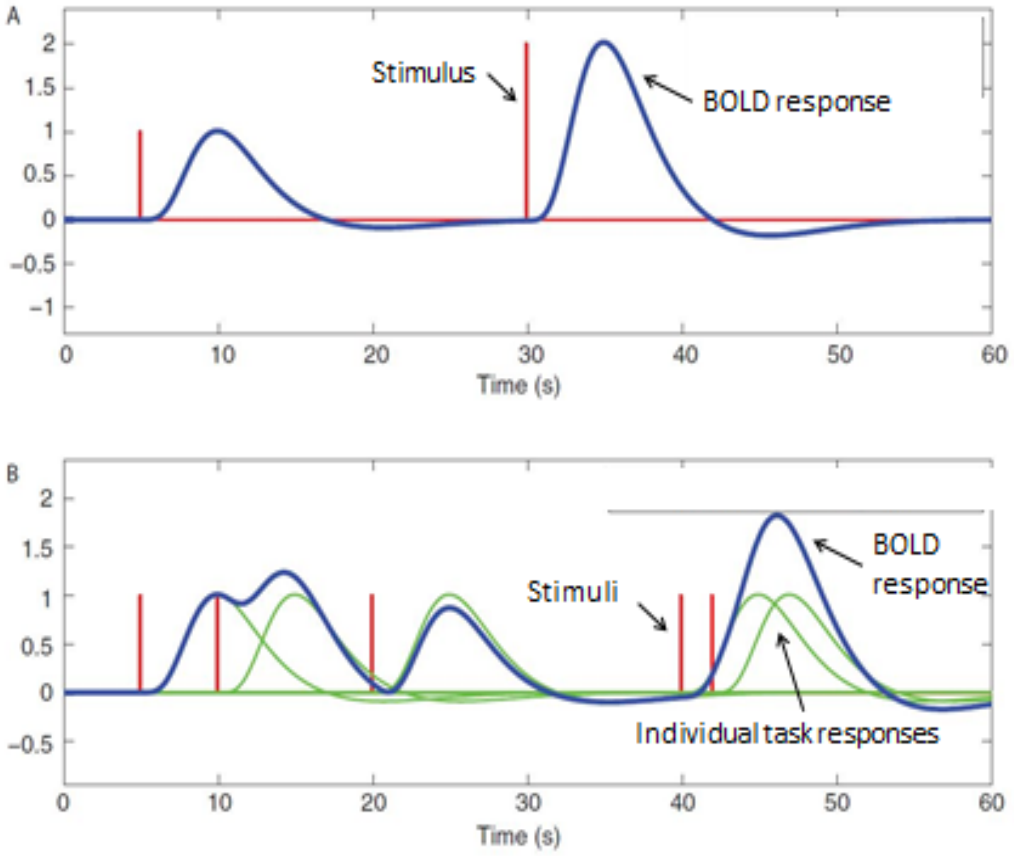

Figure 4. Illustration of the the hemodynamic response BOLD signal. In relation to (A) a single stimulus. (B) Multiple stimuli and the corresponding task responses. Adapted from Poldrack et al., (2011).

2.3. Participants and Procedures.

Data from 32 healthy volunteers are included (American residents, right handed, 22 males and 10 females aged 21-55 years with mean age=30.6 years and SD=9.2 years). Subjects were assessed using a structured interview for diagnosing psychiatric disorders, following the Diagnostic and Statistical Manual of Mental Disorders (DSM-III-R) (Non-Patient) (First et al., 2002). Psychotic-like symptoms were assessed with the Perceptual–Aberration-Magical Ideation and the Revised Social Anhedonia Scale (Chapman and Chapman, 1978; Eckblad and Chapman 1983). Subjects found to be affected, have a personal history, or have a first degree family member affected with Axis I psychiatric disorders were excluded. According to the DMS-III-R, Axis I disorders include anxiety disorders such as panic, social anxiety and post-traumatic stress disorders, mood disorders such as major depression and bipolar disorders, eating disorders such as anorexia nervosa and bulimia nervosa, psychotic disorders, dissociative disorders, and substance use disorders. Participants received a physical exam including a urine drug screen, breathalyzer test, full blood count and clinical chemistry. They were eliminated if found to be in unstable medical condition or in poor general physical health. The study protocol was approved by the Yale Human Investigators Committee and the Western Institutional Review Board. All subjects provided written informed consent. Female subjects who passed screening were scheduled for the experiments in the follicular phase if at all possible, as this phase has been suggested to affect working memory performance in females (Konishi et al., 2009).

On the day of scanning, participants were assessed with the positive and negative syndrome scale (PANSS) (Kaye et al., 1987). The PANSS is a clinical scaled used for

measuring symptom degree of patients with psychotic like syndromes (as in schizophrenia). Approximately 45 minutes is allocated to conduct the test and the subjects are rated from 1 to 7 on 30 different symptoms. The positive subscale consisted of: Delusions, conceptual disorganization, hallucinations, hyperactivity, grandiosity, suspiciousness, hostility. The negative subscale consisted of blunt effects, emotional withdrawal, social withdrawal, abstract thinking, lack of spontaneity and flow of conversation, and stereotyped thinking. Then two intravenous catheters were placed, one for infusing saline/ketamine and another for drawing blood samples. Participants were then placed in a 3 Tesla Trio scanner (Siemens Medical Solutions, Malvern, PA, USA). Each subject's pulse' respirations, oxygen saturation and heart rate were monitored throughout the scanning session.

Scanning began by obtaining high resolution three-dimensional T1-weighted anatomical images (1 slab of 160 1 slices, field of view 200 x 200, TI = 800, TR=1500ms, TE=2.83, NEX=1, Flip Angel=15, matrix 256 x 256 voxels. Then functional imaging started with a visual fixation scan during which participants looked at a project cross on a mirror. Seventy five seconds into the scan subjects received a saline bolus followed by constant saline infusion. Then subjects underwent 4 minute resting state under saline infusion used in this study, followed by 8 task runs not included in the current study (task runs last 40 minutes in total). Following these saline infusion scans, the visual fixation resting state scans and task runs were repeated with ketamine infusion. However, to insure stable ketamine blood levels, after their final task scans, an extra resting state scan with continued constant ketamine infusion was obtained and used in the current study. Thus we are using the constant saline and constant ketamine (after drug

effect stabilization) in our current study. Initial ketamine bolus was 0.23 mg kg $^{-1}$ followed by a constant infusion of 0.58 mg kg $^{-1}$. In the literature, subanesthetic doses of ketamine range from 0.1 to 0.5 mg kg $^{-1}$ (Krystal et al., 1994). Similar saline volumes were administered during the saline runs. Afterwards, participants were removed from the scanner and reassessed with the PANSS rating their entire ketamine experience.

Functional images were acquired with the same slice selection and a repetition time TR-1500ms, echo time = 30 ms, flip angle = 80 degrees, matrix size 64 x 64, field view 200 x 200 mm using a T2*-sensitive gradient-recalled single shot echo-planar pulse sequence. Each subject completed 18 scans in total of 166 images (166 1500 TRs = 4.15 minutes) covering the whole brain. The 6 first images are discarded in our analysis. Thus our resting states runs are 160 TRs = 4.00 minutes, within the limits for usual resting state experiments ranging from 4-10 minutes (Biswal et al., 2012).

2.4. Preprocessing of MRI data.

MRI raw data require extensive preprocessing operations to prepare the data for analysis. Such operations are mainly concerned with detecting potential artifacts in the data that come from either the scanner itself, or by the subject being scanned, all of which MRI signals are highly sensitive to. Automatic preprocessing and preparation of MRI data is not considered a correct practice even though it is practically possible. Thus the data analyst should manually check the raw data by either eye or software tools at each preprocessing step of the time series.

Preprocessing steps were implemented using FSL software package (FSL, Oxford, UK). First, the first 5 volumes were discarded in each functional run and then images were *head motion corrected* using FSL MCFLIRT (MCFLIRT, FSL, Oxford, UK; Jenkinson et al., 2012). Head motion results in a mismatch between the locations of subsequent images in the time series, known as "bulk motion". This is corrected by realigning the images in the time series to a single reference image, which in our case was selected to be the middle image. In the first step, motion is estimated between each image and the reference, and then the parameters obtained for each image were used to recreate a modified version of the image that matches the reference image. This process assumes that head motion can be described using rigid body transformation matrices. In other words, the position of the head changes by either displacement or rotation along the x,y,z axes while the head retains its shape. Then we constructed plots illustrating mean head displacement and rotation from time point to time point (figure 5 for illustration of head displacement graphs). By checking these plots of each subject's resting state runs, 5 subjects exceeding exclusion criteria were discarded from our analysis and the remaining

32 subjects were included. The exclusion criteria that are most common in the literature are ½ voxel size displacement in any direction (x,y,z) and (3 degrees) rotation around any axis (figure 5). Subjects' plots that appear to have excessive motion below these thresholds were also discarded as a safety measure. This is due to our interest in the temporal dynamics of the time series which can be highly affected by motion. Moreover, to account for artefacts and motion related variance in the time series, six nuisance motion regressors representing the translations and rotations the x,y,z axes were computed and then regressed out from the data using the general linear model.

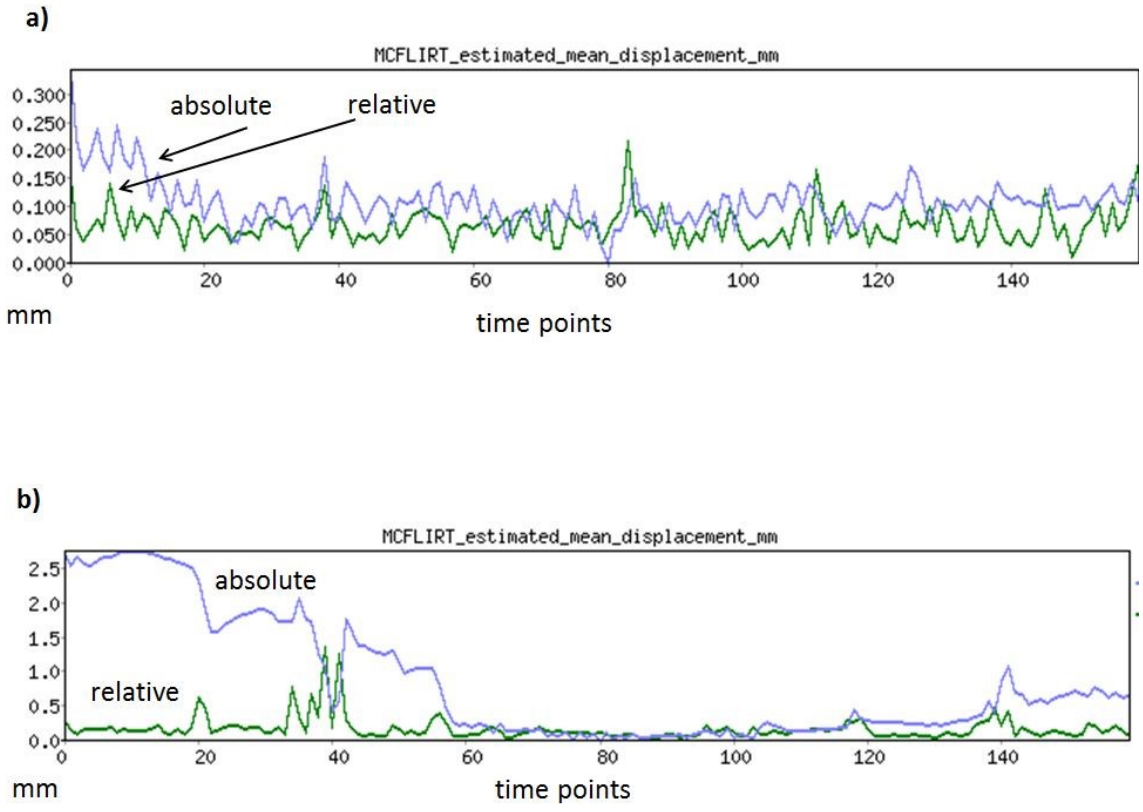

Figure 5. Example of a) included subject with mean displacement (x,y,z) not exceeding 1.5mm b) excluded subject. Relative movement is relative to the reference image.

After accounting for head motion, we performed *slice-timing correction* of the functional data. fMRI data are acquired using sequential two dimensional imaging technique (Stehling et al., 1991; Turner et al., 1998). Thus at each time point in the time series, whole brain coverage is achieved by sequentially repeated image acquisition to construct a whole brain volume. Our scanning protocol used interleaved acquisition meaning every slice was acquired such that half of the odd number slices were acquired followed by the other even-numbered slices (as in: 1, 3, 5 … 0, 2, 4 ...) (Figure 6). This results in slice acquisition delays between individual slices. Thus, slice timing correction aims to temporally realign each slice in the TR to a reference slice. This is achieved by using Hanning-windowed sinc interpolation (Sladky et al., 2011) to shift each time series by an appropriate fraction of the TR relative to the middle of the TR period.

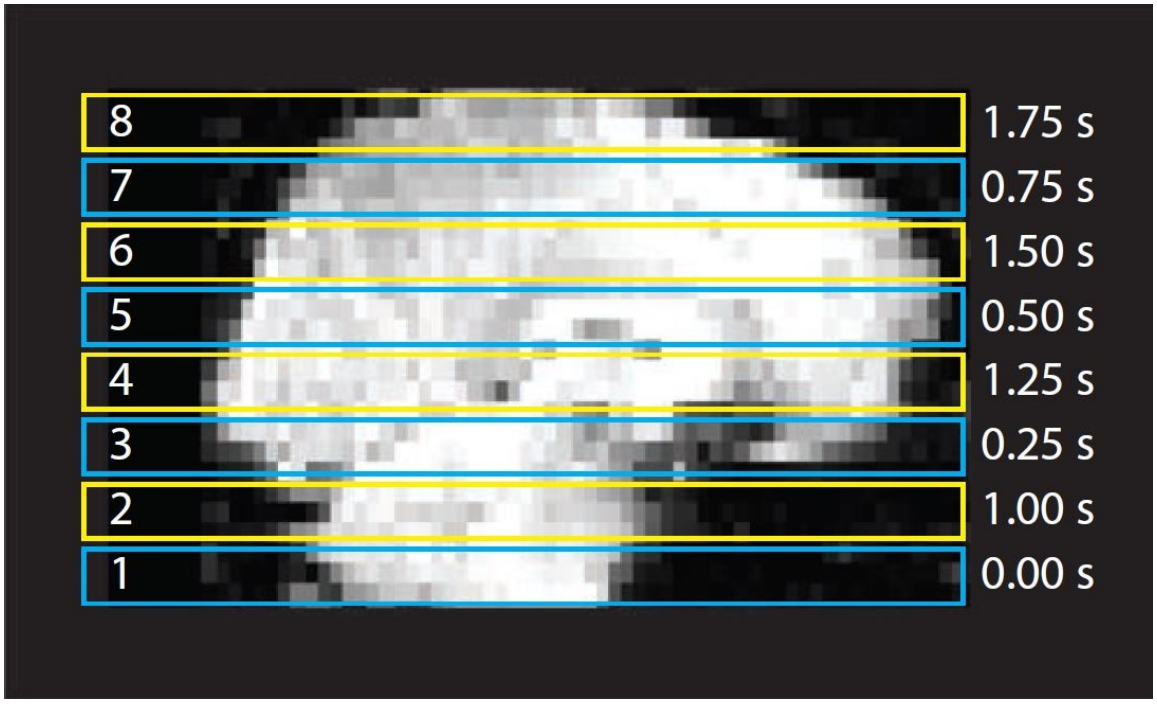

Figure 6 Illustration of slice timing interleaved acquisition sequence for an example TR of 2s. (Poldrack et al., 2011)

In the next step, functional data were *spatially smoothed* to improve their signal to noise ratio (SNR) (Rosenfeld and Kak, 1982). Spatial smoothing in essence is based on averaging voxel's data points with neighboring voxel resulting in a spatial blurring effect. The ultimate effect is removing high spatial frequencies from the signal and enhancing lower frequencies. Because most activation patterns in fMRI experiments extend well across several voxels, the benefits of spatial smoothing in terms of SNR outweigh the costs of losing higher frequency features of the signal. Second, when data are averaged across individuals (at the voxel level), there is variability that arises from the intersubjective differences in spatial location of functional regions that is not usually corrected by common spatial normalization techniques in fMRI (Yue et al., 2010). Thus by blurring signals across space, mismatch across individuals is reduced at a small expense of spatial resolution. Thus our data were smoothed by means of convolution of the three-dimensional functional images with a three-dimensional Gaussian filter (commonly termed kernel). This filter is described in imaging by the full width at half-maximum (FWHM). This measure the width of the Gaussian distribution where is it at half of its maximum. Thus to reduce SNR and partially reduce the effects of intersubjective variations of functional regions, we chose a 5mm FWHM Gaussian kernel to spatially smooth the data.

In terms of the structural preprocessing, T1 weighted high resolution anatomical images were *skull-stripped* or *brain extracted*. This process determines the boundary between brain and non-brain tissues using FSL's BET (brain extraction tool) function (Smith, 2002). Then we segmented brain tissues into images containing gray matter, white matter and CSF compartments. *Tissue segmentation* in anatomical images relies on

the large difference in the intensity of the different tissues in their T1 properties. Since we are interested in voxels containing gray matter, segmented images containing white matter voxels and CSF voxels will be used later on to filter out nuisance time series from functional data. Thus CSF and white matter images are segmented from the high resolution anatomical images for each subject. One issue that arises from this strategy comes from the fact that many voxels contain a mixture of different tissue types in varying proportions; this is known as *"partial volume effect"*. To minimize such effect white matter and CSF images resulting from the segmentation step were eroded by one voxel (Chai et al., 2012) to minimize partial voluming with gray matter. In other words, the whole surface of white and CSF regions were eroded by depth of one voxel. Mean timeseries from these eroded segmented tissues were then calculated then regressed out from the functional data using the GLM in a similar fashion to estimated motion repressors.

As discussed earlier, T1 anatomical images contain spatially rich information while T2* functional images contain temporal rich information at the expense of spatial discrimination. This is the reason why high resolution T1 weighted anatomical images are always obtained in fMRI studies to align the spatially poor functional images to spatially rich anatomical images to obtain spatially specific brain activation patterns. Moreover, as we saw in the previous paragraph, different brain tissues need to be accounted for to minimize nuisance signals coming from white matter and CSF. These tissues cannot be accurately mapped by the functional data accurately as they emphasize temporal resolution rather than anatomical segregation. And since we need to study the resting state across many individuals, the next step was *spatial normalization* of

functional data. In general, the human brain shows remarkable consistency in its structure across individuals despite being variable in its shape and size. Spatial normalization rests on the observation that almost every healthy brain contain major anatomical landmarks namely the central sulcus, sulvial fissure and the cingulate sulcus (Penhune et al., 1996; Rademacher et al., 2001). The goal of spatial normalization is thus to transform individual brains into a common standard space in order to make meaningful group analyzes.

To align individual brains, we need a reference frame to place the different individuals. Historically, Jean Talairach (1967) proposed a three-dimensional cartesian coordinate space as a common space based on anatomical landmarks: the anterior commissure (AC), and posterior commissure (PC), the midline sagittal plane and the exterior boundaries of the brain at each edge (Talairach, 1967). In brief, the zero point in this three dimensional space is defined as the point where the AC intersects with the midline sagittal plane (figure 7). Based on such dimensional space, the Talairach atlas and template were constructed for the localization of activations and interpretations of results. Using such template, Jean Talairach provided detailed procedures on how to transform any brain to his atlas using the landmarks described above (Talairach and Tournoux, 1988) in what remains one of the most popular atlases in MRI imaging. However, such template remains problematic and is being rejected in a number of studies (Devlin and Poldrack, 2007). A major problem in this method is that there is no MRI scan available for the individual on whom the template is based, which was a 60 year old female, thus not representative of the general population. Second, this atlas was based on

a single left hemisphere that was reflected to model the other hemisphere despite the well-known hemispheric asymmetries in normal individuals.

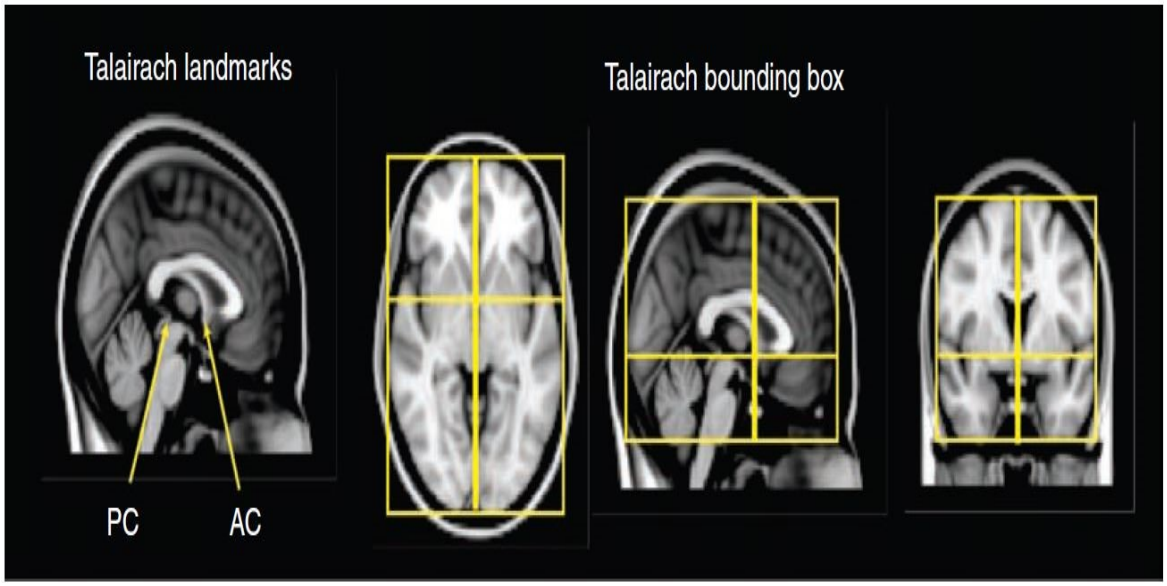

Figure 7 Illustration of the Talairach space, AC/PC and their intersections with the sagittal plane. Width has been adjusted to fit page.

In fMRI literature, there has been a shift towards using brain templates created by the Montreal Neurological Institute (MNI). These templates were developed based on actual MRI images to allow for automated registration rather than landmark-based registration and to create a template more representative of the population than the Talairach template. Thus they created a new template that was first aligned approximately to the Talairach brain in a two-stage fashion. First, they recorded 241 anatomical MRI scans from healthy individuals, and then manually mapped various landmarks similar to those used in Talairach system, in order to identify a line very

similar to the AC-PC line, and the edges of the brain. Then each brain was scaled to match the landmarks to equivalent positions on the Talairach atlas. The next step was to take 305 normal MRI scans, and used an automated 9 parameter linear algorithm to match the brains to the average of the 241 brains that had been matched to the Talairach atlas. Finally they obtained a population averaged and standardized brain template named the MNI305 (Evans et al., 1993). Later on, another template was created by registering another 152 subjects to the MNI305 template to create a template known as MNI152.

Subsequently, we opted in for the MNI152 standard space to register all the structural images to this space. To achieve accurate registration, a multistep method is used that make use of the high resolution anatomical images in order to register the functional images into standard space. Another set of images are obtained in the MRI scanner called the "coplanar images" which are high resolution T1 images that cover the same slices as the functional MRI acquisition. Thus in the multistep method, we first registered the subjects functional data to the coplanar image, and then we aligned the coplanar images to the high resolution anatomical images. Then we normalized the high resolution images to the MNI standard space. From each of these steps, we obtained transformation matrices of nine parameters (X/Y/Z translation, rotation and scaling) that dictate the transformation of images at each step (Functional A →Co-planar B , Co-planar B→ High resolution C, High-resolution C → MNI standard space D). These transformation matrices (AtoB, BtoC, and CtoD) where then concatenated to obtain resulting transformation matrices (AtoC) for each subject that could be used to directly transform the native functional data to the standard MNI space (Functional A→ MNI

Space D). Thus now we have all the subjects registered in the standard MNI space with same voxel size 2mm x 2mmx 2mm preparing for group averaging across subjects.

After spatial normalization, we *temporally filtered* the functional data between 0.015Hz-0.1 Hz representing the "common" frequency band thought to mainly reflect neuronal fluctuations (Fox and Raichle, 2007; Zhang et al., 2010). Temporal filtering was implemented in AFNI (Cox, 1996). Most resting state experiments and scans vary between 4 to 10 minutes (Biswal et al., 2012), limiting the fluctuations that can be captured in fMRI at frequencies between 0.01 and 0.25 Hz (Boubela et al., 2013). Furthermore, within such frequency range, the highest amplitudes of oscillations in the resting-state networks in these studies have been observed below 0.1 Hz. This led to the general notion of brain's resting state networks as networks of low-frequency fluctuations targeting signals between 0.01 and 0.1 Hz (Margulies et al., 2010; Yeo et al., 2011; Kalcher et al., 2012). Accordingly, *temporal filtering* aims to remove "unwanted" frequencies from the functional timeseries. The aim is to improve the SNR by maintaining only meaningful fMRI frequencies of interest. Frequencies pertaining to noise can be categorized into two classes: low frequency trends (< 0.01 Hz) resulting from scanner related drifts and coil interference and high frequency physiological fluctuations like breathing (0.3Hz) and heartbeat (1.0 Hz) (Boubela et al., 2013). The principles of temporal filtering rely on the Fourier transform (Fourier, 1878). In essence, any series of data can be expressed as a linear sum of sine waves of varying frequencies, amplitudes and phases and temporal transformations removes the hypothesized frequencies of noise and retain those thought to reflect neuronal functioning in fMRI signals. In addition to the common frequency band, we also included two sub-frequency

bands namely slow-5 (0.01-0.027 Hz) and slow-4 (0.027-0.073 Hz) for our analyses concerning temporal variability. Previous findings distinguished these two additional frequencies in analyses of resting state networks while still being unclear about their exact functional role (Buzsaki and Draguhn, 2004: Han et al., 2011; Hoptman et al., 2010: Zuo et al., 2010). Thus to examine any frequency specific effects of ketamine on temporal variability data were temporally filtered between these two ranges and a separate analysis was done for each frequency band. All linear trends were removed from functional data as well prior to temporal filtering.

2.5. Calculations of Scale-free activity, *detrended fluctuation analysis* and the Hurst exponent.

As discussed earlier, research has repeatedly shown that fMRI signal exhibits temporal autocorrelations and a power spectrum that shows "$1/f$ behavior (He, 2011) such that:

$$P\ (f) \propto 1/f^{\beta}$$

Where P is the power, f is the frequency, and β is the power-law exponent (Bullmore et al., 2001). The ratio of P measured at two distinct frequencies$f_1\ and\ f_2$, depends solely on the ratio $\frac{f1}{f2}$ and not on the absolute values of $f_1\ and\ f_2$:

$$\frac{P(f_1)}{P(f_2)} = (\frac{f_2}{f_1})^{\beta}$$

This indicates that a timeseries possessing temporal dynamics exhibiting power-law properties in its power spectrum contain no characteristic scale and thus is termed "Scale-free" (Mandelbrot, 1999).

A robust and established method to investigate scale-free activity in fMRI studies is the *detrended fluctuation analysis* (DFA) (Linkenkaer-Hansen et al., 2001; Eke et al., 2006; He, 2011). It is statistical methodology used to detect the presence of trends or autocorrelations in a timeseries by finding its Hurst exponent. This method was initially utilized in studying auto correlations in DNA sequences (Peng et al., 1994). First, the mean timeseries for each of the regions of interests was obtained from functional data. Then for each extracted timeseries, we obtained the sum and the mean was subtracted from it:

$$y_j = \sum_{i-1}^{j} x_i - \hat{\mu}$$

Thus, y_j is obtained as the cumulative sum of the fluctuations of x_i around its mean. The local trend $y_{j,l}$ is then estimated in non-overlapping time windows of equal size l. In each window of size, the fluctuation F_l is defined as the root mean square variance of its local trend via a least-squares fit.

$$\text{Ft}=\frac{1}{l}\sqrt{\sum_{\text{j=1}}^{\text{l}}(y_j - y_{j,l})^2}$$

The fluctuations are then averaged across windows. In scale-free timeseries, the fluctuation F_l can be related to the window size l by the following equation:

$$F_l = pl^{\alpha}$$

Using the laws of logarithms this can be expressed as

$$\log(F_l) = \log(p) + \propto \log(l)$$

If $0 < \alpha < 1$, then the timeseries is considered stationary and its Hurst exponent $H = \alpha$. On the other hand if $\alpha > 1$, then x in considered nonstationary and its Hurst exponent $H = \alpha - 1$ (Eke et al., 2002; He, 2011). The Hurst exponent describes self-affinity of the integral of the raw data as in:

$$y_{i,n} = {}_dS^{-H} y_{i,sn}$$

Where $y_{i,n}$ is a sample timeseries of length n, $y_{i,sn}$ is a longer timeseries of the same process of length sn, and $=_d$ indicates equality in distribution (Hurst, 1956; He, 2011).

Previous findings indicated that temporal filters can induce short range correlations. So to avoid such influence, window lengths were chosen to be n = 10, 16, 20, 32, 40, 80 time points (one time point = TR = 1.5s) so that the total number of time points in each run (160 time points according to our data) is an integer multiple of the window length n. The α in our resting state runs were always found to be between 0 to 1 and thus our signal could be considered stationary and the Hurst exponent H could be estimated by α in H=α. Thus in fMRI timeseries, Hurst exponents represent "long-term memory" of temporal dynamics and are reported in multiple studies to well describe the scale-free properties of spontaneous (resting state) brain activity (Maxim et al., 2005; Park et al., 2010). As a general rule, H between 0.5 and 1.0 indicates a persistent timeseries. In other words, a high value in the signals is more probable to be followed by another high value in the future. Thus a larger H indicates a stronger long term positive autocorrelation (memory) of the time series, i.e. more regular or persistent. By the same token, H between 0 and 0.5 indicates anti correlated timeseries or anti-persistent and values residing around 0.5 more or less indicate a random time series (Wei et al., 2013). The calculations of the detrended fluctuation analysis on the time series were done in MATLAB.

2.6. Calculations of temporal variability.

We followed the method of Garrett and colleagues in aging studies to calculated the temporal variability of time series for each of our regions of interest (Garrett et al., 2010, 2011, 2013). The standard deviation (SD) of blood oxygenation level-dependent (BOLD) signal describes the temporal variability of brain activity across time within a particular region The SD across time series was calculated for each subject's constructing maps of SD for each voxel. Then for each of the regions of interest, we extracted the mean SD score.

2.7 Definition of regions of interest.

All of the analysis in this study was based on a region of interest (ROI) analysis using established templates from fMRI literature. For the global/whole brain analysis, we adopted a well-established node template from a previous study (For detailed methodology: Power et al., 2010). This template contains 264 non-overlapping functional areas (5mm diameter spheres). This template was defined according to neurobiological principles with a combination of two methods; the first was a meta-analytic (Dosenbach et al., 2006) and explored large fMRI data sets to identify voxels that showed reliable and repeated modulation when a variety of certain behaviors were demanded (e.g. button-pressing) or certain signal types were found (e.g. error-related activity). The second method utilized resting state functional connectivity MRI (Barnes et al., 2011, Cohen et al., 2008). (A full list of regions with their MNI coordinates can be found in the Appendices).

For the network-wise analysis, we adopted an established template highlighting key brain functional regions based on extensive fMRI literature relating to resting state networks (For details: de Pasquale et al., 2010). These regions cover, ventral attention, dorsal attention, visual, language, default mode, motor (For complete list of regions within each network and coordinates, please see Appendices). We then added a salience network to this template from (Qin et al., 2015). This network was obtained from functional connectivity analysis from healthy individuals in combination with fMRI literature and various anatomical templates. We then constructed 6mm non overlapping anatomical spheres based on these MNI coordinates and used them for our network specific analysis.

3. Results.

3.1. Global results. Ketamine-induced changes in global brain distribution of SD and Hurst exponents:

Based on the 264 regions of interest template, we investigated the distribution of the Hurst exponent and the SD in a whole brain approach (Figure 8). Mean global SD for all 264 regions is 0.3775 (saline) and 0.3245 (ketamine). We found significant reduction in SD during ketamine runs ($p<0.001$, confidence interval: 0.049 to 0.057, with 1000 bootstraps performed) when compared to saline runs (Figure 8a). Mean global Hurst is 0.6039 (Saline) and 0.6261 (ketamine). The increase in global Hurst during ketamine runs is significant ($p<0.001$, confidence interval: -0.0256 to -0.0186, with 1000 bootstraps performed), when compared to saline runs (Figure 8b). During both placebo and ketamine resting state runs, correlations between SD and Hurst are significant, $r=0.446$ (saline) and $r=0.449$ (ketamine) with $p<0.001$ and 1000 bootstraps performed. All significance tests have been done on SPSS software package. This confirms a previous observation (He, 2011). There is no significant difference between the correlation coefficients of SD and Hurst between saline and ketamine conditions (Figure 8c).

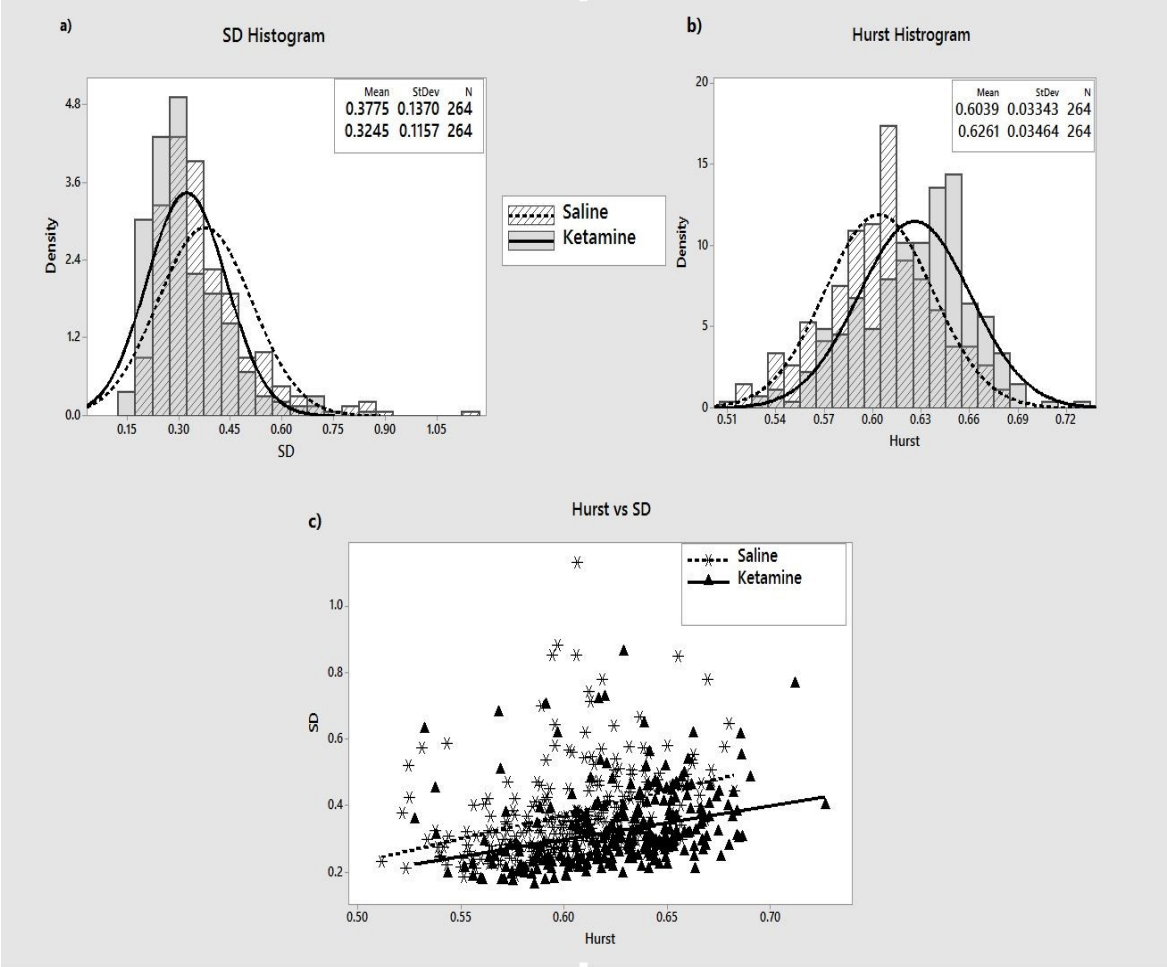

Figure 8 a) Density of SD for the 264 regions in both Saline and Ketamine resting states. Decreased mean in the ketamine is observed at corrected $p<0.001$. b) Density of Hurst exponent for the 264 regions in both Saline and Ketamine resting states. Increased mean in ketamine is observed at corrected $p<0.001$. c) Correlation between variability SD and Hurst exponent in both Saline and Ketamine. In both saline and ketamine, correlation is positively significant (r=0.446, r=0.449 respectively, Spearman's **with p <0.001**). No significant difference between the two correlation coefficients.

3.2. Network results. Ketamine-induced changes in neuronal networks' SD and Hurst exponents.

Based on the 41 ROIs network specific template we used, we investigated the differences between saline and ketamine resting state runs to study network differences in SD (common, slow-5 and slow-4 frequencies) and Hurst exponents (common frequency only). Furthermore, we illustrated frequency-specific differences in SD results. Results showed that ketamine induced significant decrease in SD in most networks in the brain (dATT*, vATT**, Visual*, Motor ***, Language*, Salience **) but not in the DMN. * denotes level of significance *p*, please see figure (9) for significance values. We also included a measure for the whole brain which is the average across all 41 ROIs in all networks defined as "whole" in figure (9). Whole brain value also showed significantly reduced SD during ketamine resting state runs. Furthermore, we show that these significant SD decreases are evident only in the slow-4 frequency band whereas no significant SD reductions were observer in slow-5 (Figure 9b).

The opposite pattern was observed for the Hurst exponent. Firstly, the Hurst exponent showed significant increase in ketamine when compared to saline (As opposed to significant decrease in SD during ketamine), thus confirming the global trend observed in the previous section. Secondly, the significant increase in Hurst exponent during Ketamine was observed only in the DMN ** (Figure 2c) while, unlike SD, it did not show significant changes in the other networks. All results were Bonferroni corrected for 16 comparisons (SD) and 8 comparisons for Hurst respectively.

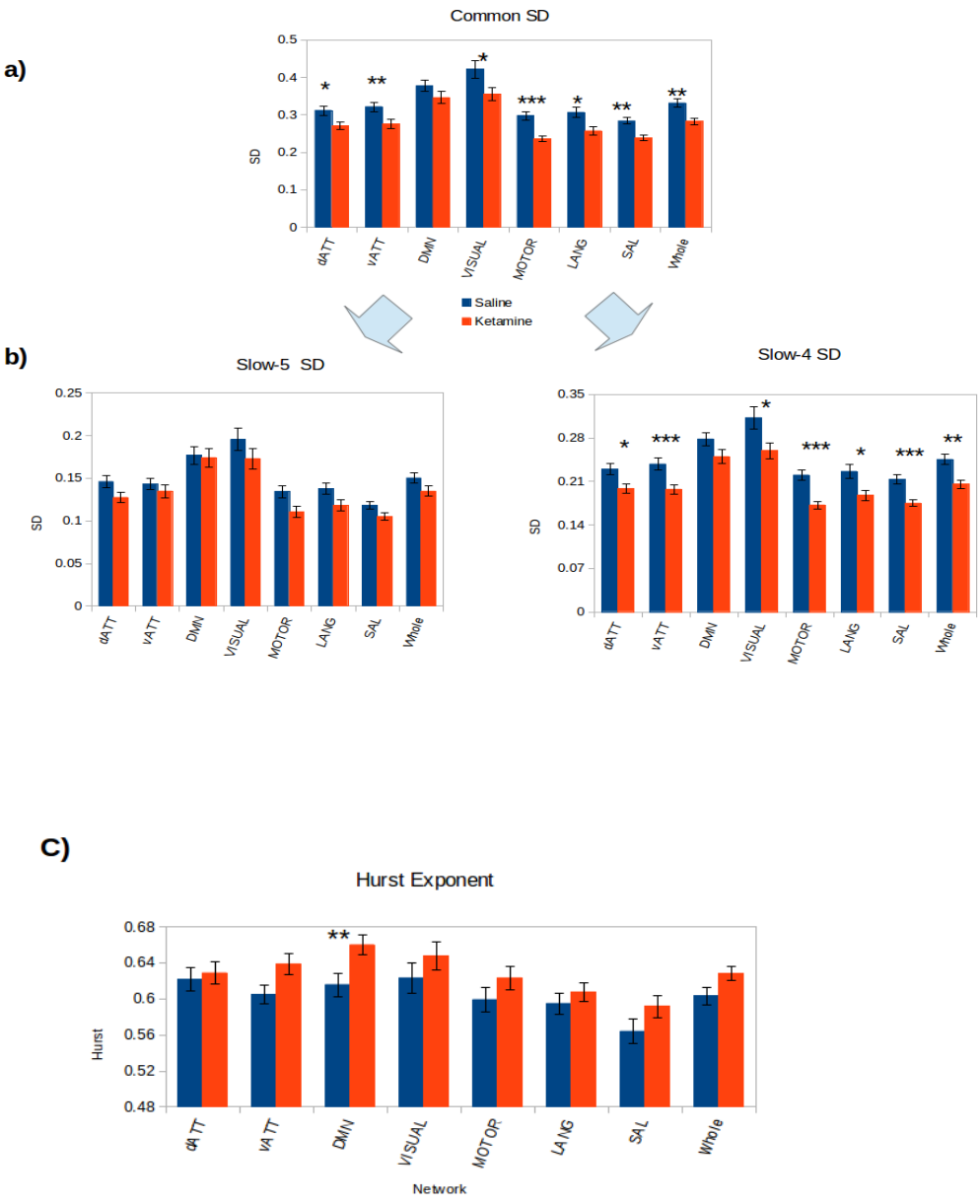

Figure 9 a) Network common frequency (0.015-0.1Hz) variability (SD) in both Saline and Ketamine. b) Slow-5 (0.015-00271Hz) and slow-4 (0.027-0.73Hz) variability (SD). All values are the average of all the voxels within each network. c) Network common frequency Hurst exponent in both Saline and Ketamine. . "*" denotes the significance of the difference between ketamine and saline SD of each network (*<0.05, **<0.01,***<0.001, Bonferroni corrected). "whole" network represents the average of all nodes. Error bars show Standard Error SE.

3.3. Psychopathology induced by Ketamine and its relation to the temporal correlates.

PANSS scores were obtained before and after the ketamine experience. We found that ketamine increased the total PANSS score total significantly, mean=22.09 (SD=1.42) (saline) and mean=27.80 (SD=4.7) (ketamine), (difference is significant at $p<0.0001$; 1000 bootstraps). In terms of the sub-scores, Saline mean values were: 6.44 (SD=0.84) (positive subscale), 8.16 (SD=0.80) (negative subscale), and 7.5 (SD=0.80) (cognitive subscale). Ketamine mean values were: 10.00 (SD=2.86) (positive subscale), 9.58 (SD=1.41) (negative subscale), and 8.22 (SD=1.58) (cognitive subscale). Before multiple comparison correction all three subscales were significant at $p<0.0001$ for the positive and negative subscales and $p<0.05$ for the cognitive subscale. After Bonferroni correction only the positive and negative subscales remained significant (Figure 10).

We then correlated the psychopathological changes in PANSS with the global changes in the SD and Hurst and found no significant correlations. In the network wise template, we however found positive correlation trends between whole brain SD (based on all 41 regions in the networks) and the total pre-ketamine PANSS score ($r=0.48$, $p<0.01$, 1000 bootstraps), which did not remain significant after Bonferroni correction. The higher the degree of whole brain SD reduction induced by ketamine, the higher the pre-ketamine total PANNS score (Figure 11a). Also, a weak correlation trend was found between the motor network SD reduction in ketamine and the positive PANSS ($r=-0.37$, $p<0.05$, 1000 bootstraps, which also doesn't remain significant after Bonferroni correction. The higher the reduction in the motor network SD in during ketamine, the lower the increase of the positive sub-score of the PANSS in subjects (Figure 11b). These

results don't survive multiple comparison corrections and therefore are reported here as non-significant trends rather than significant results.

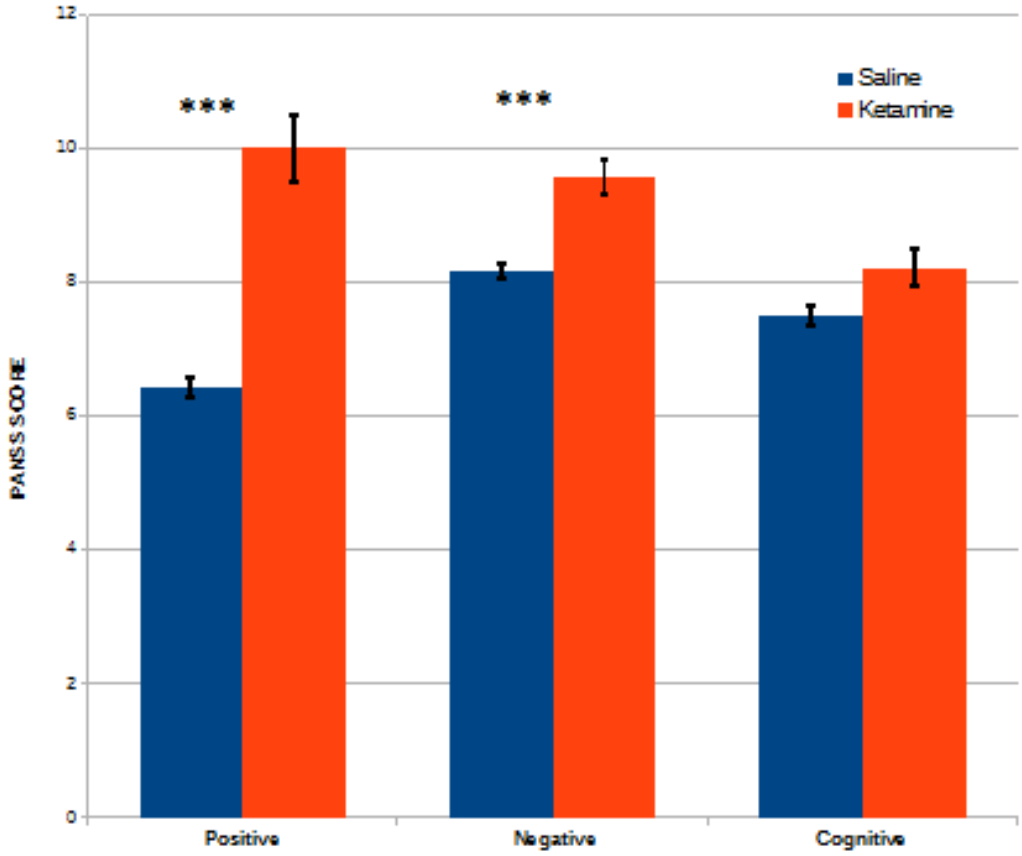

Figure 10. PANSS scores before and after the ketamine experience ($p<0.0001$ ***, Bonferroni corrected). Error bars show Standard Errors SE. Values are Bonferroni corrected.

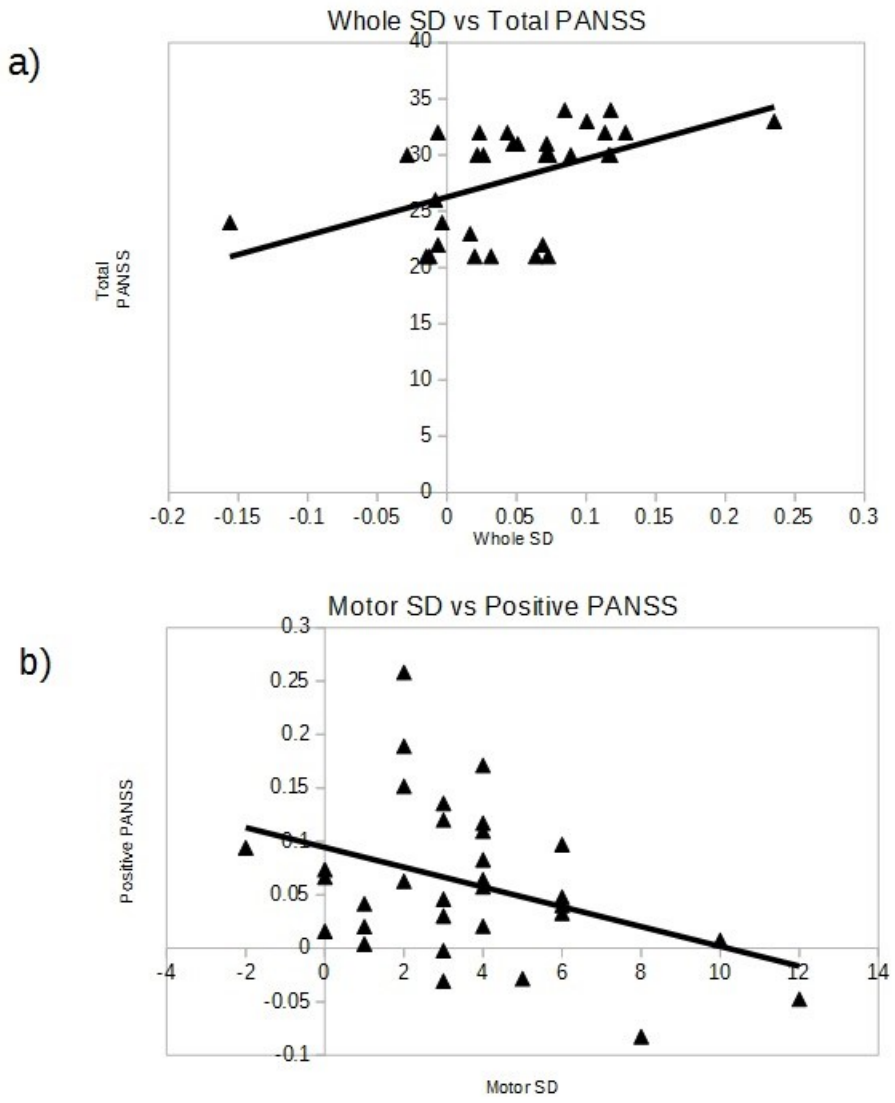

Figure 11 a) the relationship between the whole brain reduction in SD and pre-scan total PANSS score ($r=0.48$, $p<0.01$, Pearson, non-corrected).b) The relationship between the Motor network's reduction in SD with the increase in positive PANSS in the ketamine experience($r=-0.37$, $p<0.05$, Pearson, non-corrected).

4. Discussion:

Our current study reveals; 1) global reduction of temporal variability in the human brain under the influence of ketamine in the resting state; 2) network-wise effects of ketamine show such effects predominantly in the slow-4 frequency band; 3) we then show global increase of long-term autocorrelations illustrated by the scale free dynamics in the resting brain under the ketamine experience; 5) this increase of temporal long term correlations under the ketamine influence is most prevalent in the default mode network (DMN). And finally 6) we confirm earlier study by He (2010) of the link between temporal variability and scale free dynamics in the resting brain.

The decreased in global resting state's variability we reported here are in line with other studies suggesting decreased variability in other conditions that affect the level of consciousness like vegetative state (Huang et al., 2014a), anesthesia (Huang et al., 2014b) and sleep (Yang et al., 2013). This suggests a shrink of the dynamic range of brain activity which in turn may limit the possible neuronal response to stimulus. Thus the brain lacks efficiency. However it is important to consider in our ketamine study, we do not impair the level of consciousness per se. Rather, consciousness in our current study is altered in terms of its quality similar to early stages of schizophrenia, a state that represents an extreme case of consciousness. As discussed in the introduction concerning temporal variability, Huang et al., (2014a) examined the resting state and self-referential processing vegetative state patients. These two activities were repeatedly shown to be highly overlapping in the brain (D'Argembeau et al., 2005; Qin and Northoff, 2011; Whitfield-Gabrieli et al., 2011). Huang and colleagues found decreased signal variability in vegetative state patients and this decrease was correlated with self-stimuli processing.

Furthermore, in a separate study with anesthesia they revealed that this decrease wasn't specific to the vegetative state but rather to the loss of consciousness itself in general suggesting the importance of variability in maintaining a wakeful, self-aware state of consciousness. Our results support such stand as schizophrenic patients are known to have alterations in the sense of self and have difficulties differentiating between self and environment. This idea of increasing susceptibility to stimuli with increased variability is especially supported by findings in aging studies by Garrett and colleagues (2010, 2011, and 2013). Specifically, they suggest that temporal variability reflects a great dynamic range of possible responses to incoming stimuli, which is beneficial to adaptability and efficiency of neuronal systems as it permits a greater range of responses to a greater range of stimuli, evident in younger brains compared to older brains. In conclusion, abnormally decreased neuronal variability may lead to the inefficacy of processing stimuli that are self-specific, as evident in self-consciousness studies and also in cognitive functions in general found in schizophrenic populations. In this context, we can phenomenologically understand the basis of reported confusion between external and internal thoughts clinically evident in patients with schizophrenic symptoms. Moreover, negative symptoms of schizophrenia can also be related to such inefficiencies in neuronal variability which leads to the inability to normally interact with external stimuli, evident in the negative symptoms of schizophrenia pertaining to withdrawal from the environment.

As discussed before, most of the resting state findings are studied within the context of neuronal synchronization between different networks across the brain, i.e. functional connectivity. Notably the relationship between functional connectivity and

temporal variability was examined in a recent study (Yang et al., 2014) using a biophysically based computational model (Deco et al., 2013). Their modelling results revealed that the temporal variability increased as a function of increasing signal synchronization. The results then may serve as an initial proof-of-principle of the neural bases of temporal variability, as the model explicitly excludes non-neuronal signal sources (Yang et al., 2014). However, the exact relationship between functional connectivity and neuronal variability remains to be determined. Alterations in variability across the brain may form the basis for some of the resting state functional connectivity abnormalities often observed in schizophrenia (Garrity et al., 2007; Bluhm et al., 2007; Jafri et al., 2008). Moreover, schizophrenia is characterized for the false attribution of perceptual experience to an external source, perturbations in basic sensory processing and higher cognitive functions such as language (Yu et al., 2012). The networks (Attention, Visual, Motor, Salience and Language) that prominently showed the decreases in the current study are consistent with other studies showing deficits in cognitive, motor and low level sensory processing as well as deficits in reward sensitivity in patients with schizophrenia (Yu et al., 2012). Such decreases may provide neuronal bases to the excessive internally directed thought processing often observed in schizophrenia patients and the abnormal focus on internally generated stimuli as well as the confusion to their source. This is supported by our network results as the DMN doesn't show significant variability reductions in the same way as the other networks. Since this network has been associated with internal contents, this might explain the abnormal focus of the internal contents a. For this reasons it is postulated that this dysregulation is associated with hallucinations. And further work will be needed on the functional significance of

variability in the resting state in schizophrenic patients as well in relation to specific task activities.

The current study revealed reductions in variability prominently in the slow-4 frequency band, suggesting frequency specificity of NMDA receptor blockade on the brain's resting state. To date, most of the resting state fMRI studies have examined spontaneous activity in the common frequency band (0.01-0.1 Hz) which is the fMRI frequency band mainly thought to be linked to functional neuronal fluctuations (Biswal et al., 1995; Fox and Raichle, 2007). However, researchers have also observed earlier that neuronal oscillations are distributed linearly on the logarithmic scale. Most importantly, different independent frequency bands are generated by district oscillatory activities with distinct physiological underpinnings and functions (Buzsaki and Draguhnm, 2004; Penttonen and Buzsaki, 2003) and neighboring frequency bands within the same neuronal network may compete with each other (Engel et al., 2001). Few studies in fact have suggested that the two frequency bands slow-5 and slow-4 contribute differentially to the amplitude of slow frequency fluctuations of brain resting state (Baria et al., 2011; Han et al., 2010; Zuo et al., 2010). Moreover, slow-4 has greater test-retest reliability for the amplitude of slow fluctuations and more reliable BOLD fluctuations amplitude voxels than slow-5 (Zuo et al., 2010). However, we speculate this is due to generally higher amplitudes in low frequency fluctuations observed in the slow-4 band compared to slow-5 (Yu et al., 2012, Zuo et al., 2012), which might allow for more consistent findings and higher test-retest reliability in this particular band. This could serve as basis to our results showing stronger and more significant ketamine changes in the different brain networks in the slow-4 compared to slow-5. Also, slow-5 shows higher power and localizes more

within default-mode regions while slow-4 shows less power and is more robust in basal ganglia (Baria et al., 2011; Zuo et al., 2010). All of these discoveries suggest that the individual frequency bands within the common frequency bands (0.01-0.1Hz) may be associated with different specific neuronal properties (as suggested earlier by Buzsaki and Draguhn, 2004). This stand is indeed supported by the current study results as NMDA receptor antagonist, ketamine, is evident to have a frequency specific modulation of the temporal structure of the brain. The underlying mechanisms and functional roles of the slow4 and slow5 frequency bands remain largely unclear however. Finally, the neuronal basis of ketamine effects on the specific frequency bands and whether such frequency effects on brain variability can be extended to schizophrenic patients are central questions to future studies.

Next, the current study reveals global increase of the Hurst exponent in the brain following NMDA receptor blockade in the resting state. This finding implicates higher level of long-range temporal correlation LRTC, reduced complexity or increased redundancy in the resting state activity. Recently, mental illness has been proposed as a loss of brain complexity and that the complexity of mental illness can be studied under such framework by quantifying the order and randomness of the dynamic neuronal activity (Yang and Tsai, 2013). Furthermore, a reasonable method to understand and measure brain complexity is to obtain a system's behavior in time. While temporal variability contains valuable information about neuronal functioning and brain activity across time, it still lacks rich temporal structures that can be captured in other complexity measures such as scale free dynamics, quantified in our study by Hurst exponent. Our results support such stand as increased Hurst exponent indicates less complex and more

auto-correlated (redundant) brain activity across time. A resting state study measuring entropy of blood oxygen level dependent (BOLD) revealed that younger adults had increased complexity of their brain signals compared to older adults (Yang et al., 2012). Furthermore, in schizophrenia, most complexity studies have been done in the EEG domain and reported decreased signal complexity using several mathematical methods such as dimensional complexity (Hoffmann et al., 1996), mutual information analysis (Na et al., 2002), symbolic dynamic complexity (Mujica-Parodi et al., 2005), and approximate entropy (Bar et al., 2007). Intriguingly, a very recent study on schizophrenic patients have illustrated decreased resting state brain activity complexity in schizophrenia in fMRI in a large cohort of patients (Yang et al., 2015). Since ketamine has been reliably used to induce negative and positive symptoms similar to those of schizophrenia, as discussed earlier, our resting state fMRI Hurst findings are in line with those studies in schizophrenia from both EEG and most recently in fMRI (Yang et al., 2015), by showing decreased complexity of brain resting state activity under the effects of ketamine, ultimately supporting the loss of complexity hypothesis (Yang and Tsai, 2012). This loss of complexity expressed in our results as an increase redundancy or self-similarity of brain activity over time, may explain redundant and obsessive behaviors characteristic of schizophrenia (Yang and Tsai, 2012).

An interesting recent study showed reduced Hurst exponent in patients with schizophrenia and suggesting increased complexity in schizophrenia (Sokunbi et al., 2014). However, they studied brain signals during task states (social task) compared to the current study in continuous resting state. It has been shown that scale free properties are reduced during visual task periods compared to rest (He, 2010) due to yet unknown

mechanisms. The observation in schizophrenic patients that show speculatively even more reduction in scale free properties in brain signals constitutes a very interesting subject for future investigations.

Towards further understanding of the system dynamics of psychopathology, complexity measured by the temporal structure of brain activity may play significant role which can be practically applied in clinical practice as a biomarker, however still not fully understood. To support this stand, in general, psychopathological symptoms appear to follow contrasted patterns of order and randomness. Broadly, on one hand, patients appear to exhibit personality trains that illustrate impulsive behaviors that show randomness. On the other hand, patients who clinically show obsessive compulsive personalities tend to perform actions in an orderly and rigid manner, often redundant. Furthermore, similar categorizations can also be extended to observations in cognition, emotions, speech, thought and other specific mental functions such as stereotypy vs irrational behavior, echolalia (meaningless repetition of another person's words) vs word salad (connecting random words in sentences), fixed delusions vs flight of ideas (Yang and Tsai, 2013). The question remains whether such characterizations of order and randomness on the phenomenal level can be linked to parallel quantifications in the neuronal activity, such as scale free dynamics and other related complexity measurements. Looking at the brain in a systemic view, particularly a temporally dynamic one, a temporal structure of the brain's system can reflect its susceptibility to adapt to a continuously changing environment (Goldberger et al., 2002; Peng et al., 2009). And such adaptation is indeed impaired in the psychopathological population, which tends to exhibit random and/or ordered behavioral patterns. Thus increased

redundancy or self-similarity in brain activity may be linked with mirrored behavioral outputs. This stand is indeed supported by early findings of schizophrenic patients exhibiting more predictable or redundant behavior measured by binary choice tasks compared to healthy individuals (Paulus et al., 1996). This is also found in bipolar patients as they report daily record of mood with more organized manner compared to healthy subjects (Gottschalk et al., 1995). Thus, through scale free dynamics, a direct link may be now established between neuronal statistical measures and behavioral outputs. Future studies need to address this link between neuronal statistics and behavioral outputs.

In terms of brain networks, this global increase in Hurst is particularly observed in the DMN in comparison to other networks in the current study. To recall, internal content processing is abnormally high in schizophrenic patients and subjects in the psychedelic experience (Carhart-Harris et al, 2013). Since the DMN is largely implicated in internal content, the reduction in efficiency of processing stimuli in all other networks (as illustrated by reduced variability results), may explain the higher temporal structure observed in the DMN. As noted in the literature, abnormally high activity in the DMN is observed in the DMN in schizophrenic patients. In addition, the anti-correlation of the DMN with other networks is also reduced in schizophrenic patients. Regardless of the framework in which Hurst exponent is understood, i.e. complexity, autocorrelation, or redundancy etc., increased Hurst exponent implies that the activity re-occurs more often under the influence of ketamine than in normal conditions. This may lead individuals to be locked up in their internal content processing. In other words, such increase in the DMN may indicate that this network is no longer reactive to changes induced by external

stimuli and such stimuli is no longer capable of inducing deactivation in the DMN because of the reduced efficiency of other networks and increased self-similarity of activity in the DMN. Moreover, to recall the DMN is widely observed to be deactivated when the brain is presented with stimuli. Indeed, DMN is implicated in processes such as mind wandering, random thought, self-related processing; and such symptoms are notably often observed to be abnormal in schizophrenic patients. Thus our results provide a possible direct link between phenomenal perturbations of the psychopathological state and the temporal structure of resting state activity.

A previous study by He (2010) found that H and SD using a node-based correlation are positively correlated and this is indeed the case in our study. This indicates that Hurst and SD share similar topographical patterns across brain regions, which, to some extent, independent of the absolute values of Hurst and SD per se. Let's take the hypothetical example below in table (1):

Table 1. Hypothetical example of global Hurst and SD changes under a psychotic state.

ROI	Node 1	Node 2	Node 3	Node 4
Saline				
SD	10	11	12	13
Hurst	1	2	3	4
Ketamine				
SD	5	6	7	8
Hurst	3	4	8	6

We can see from this example that the SD in ketamine is globally reduced across nodes and Hurst is increased. However, the correlation between them is the same in both conditions. He's study (2010) and our results confirmed the positive correlation between them. But we here extend He's results by showing that these two measures are dissociable when examining ketamine induced altered state of spontaneous activity such that there is an opposite effect of the drug on these measures. This indicates there may exist an unclear neuronal mechanism that mediates the relationship of SD and Hurst. Further work is needed in that direction to show for example, how the relationship is affected in other altered states of minds also in different dosages of ketamine.

In terms of the psychological PANSS scores, ketamine induced a significant increase in the total, and positive, negative scales of the PANSS. However, no significant cognitive change was observed as ketamine is not sufficient to induce cognitive impairments in healthy subjects, which is more characteristic of advanced psychotic stages of mental illness. This confirms prior results that ketamine induces positive and negative symptoms of schizophrenia in addition and makes ketamine a better model for schizophrenia compared to competing models such as Dopamine, -9-THC and others. However, no correlations were observed between the ketamine induced psychological scores and the temporal correlates of the resting state. Effects of ketamine on the brain's psychotic state as measured in PANSS have been reported to be significantly milder than schizophrenia (Xu et al., 2015). Notably in healthy subjects, ketamine is known to have a remarkably steep dose response curve such that differences in few tenths of dosages may lead to differential psychotic responses observed, if at all (Honey et al., 2008; Krystal et al., 1994). Thus is it highly probable that higher sub-anesthetic ketamine would be

needed to induce significant correlations between the changes in PANSS scores and the temporal changes observed in our study. Thus, future research may address different sub-anesthetic ketamine doses and their effect on the psychological correlates of the psychotic experience and their relation to the neuronal correlates.

Several limitations arise in this study; first, these results provide no mathematical modelling support. And the relationship and mechanism between SD and Hurst remains to be investigated in future studies. Moreover, it is well known that higher dosages of ketamine could induce anesthetic effects on subjects. In fact, scale-free properties as measure by Hurst (or power law spectra) are illustrated to be reduced in anesthesia and sleep studies (Huang et al., in press; Lei et al., 2014). This indicates that there should be a turning point when increasing the dosage of ketamine where measurements of scale-free properties start being reduced rather than increased. This area needs to be investigated in future studies using several sub-anesthetic and anesthetic dosages of ketamine to study the proposed curve of scale-free properties and their relationship to consciousness. Third, while 4 minutes of resting state are within the established standard durations of resting state studies (Biswal et al., 2012), they may not provide sufficient time points to obtain reliable long term correlation properties of the time series. Future studies may investigate the scale-free dynamics with longer resting state periods. And lastly, given that we only have one resting state run for each condition, we are unable to perform test-retest reliability analysis of our results thus future replication is necessary.

In conclusion, we demonstrate reduced temporal variability in the resting brain during ketamine induced psychotic state and increased long-range temporal correlation. These results may provide basis to the characteristic clinical symptoms associated with

early psychosis in schizophrenia and provide potential for a direct link between the temporal statistics of the resting state with the statistics of behavioral outputs/phenomenology. As current psychopathology and philosophy still suffer from a dividing line between psyche and the brain (mind vs brain), i.e. between psychopathological symptoms and neuronal activity (Northoff, 2015), our approach here may solve this problem by providing measures that can transcends the different levels mental disorders are studied within. This motivates future studies with large sample sizes to confirm these temporal measures as useful biomarkers for healthy vs psychiatric disorders. If one can construct a temporal profile of the brain, new therapeutic interventions may come to life to modulate the temporal structure of the brain such as transcranial magnetic stimulation (TMS), deep brain stimulation, and music therapy.

5. References.

Abi-Dargham, A. (2007). *Integrating the neurobiology of schizophrenia*. Amsterdam: Elsevier/Academic Press.

Ames, A. (2000). CNS energy metabolism as related to function. *Brain Research. Brain Research Reviews*, *34*(1-2), 42–68.

Anderson, C. H., & Van Essen, D. C. (1987). Shifter circuits: a computational strategy for dynamic aspects of visual processing. *Proceedings of the National Academy of Sciences of the United States of America*, *84*(17), 6297–301.

Anderson, C. M., Lowen, S. B., & Renshaw, P. F. (2006). Emotional task-dependent low-frequency fluctuations and methylphenidate: Wavelet scaling analysis of 1/f-type fluctuations in fMRI of the cerebellar vermis. *Journal of Neuroscience Methods*, *151*(1), 52–61. http://doi.org/10.1016/j.jneumeth.2005.09.020

Anticevic, A., Gancsos, M., Murray, J. D., Repovs, G., Driesen, N. R., Ennis, D. J., … Corlett, P. R. (2012). NMDA receptor function in large-scale anticorrelated neural systems with implications for cognition and schizophrenia. *Proceedings of the National Academy of Sciences of the United States of America*, *109*(41), 16720–5. http://doi.org/10.1073/pnas.1208494109

Ashok, A. H., Baugh, J., & Yeragani, V. K. (2012). Paul Eugen Bleuler and the origin of the term schizophrenia (SCHIZOPRENIEGRUPPE). *Indian Journal of Psychiatry*, *54*(1), 95–6. http://doi.org/10.4103/0019-5545.94660

Attwell, D., & Iadecola, C. (2002). The neural basis of functional brain imaging signals. *Trends in Neurosciences*, *25*(12), 621–5.

Attwell, D., & Laughlin, S. B. (2001). An energy budget for signaling in the grey matter of the brain. *Journal of Cerebral Blood Flow and Metabolism : Official Journal of the International Society of Cerebral Blood Flow and Metabolism*, *21*(10), 1133–45. http://doi.org/10.1097/00004647-200110000-00001

Bak, P. (2013). *How Nature Works: the science of self-organized criticality* (Vol. 11). Springer Science & Business Media.

Bär, K.-J., Boettger, M. K., Koschke, M., Schulz, S., Chokka, P., Yeragani, V. K., & Voss, A. (2007). Non-linear complexity measures of heart rate variability in acute schizophrenia. *Clinical Neurophysiology*, *118*(9), 2009–2015. http://doi.org/10.1016/j.clinph.2007.06.012

Baria, A. T., Baliki, M. N., Parrish, T., & Apkarian, A. V. (2011). Anatomical and functional assemblies of brain BOLD oscillations. *The Journal of Neuroscience : The Official Journal of the Society for Neuroscience*, *31*(21), 7910–9. http://doi.org/10.1523/JNEUROSCI.1296-11.2011

Barnes, K. A., Nelson, S. M., Cohen, A. L., Power, J. D., Coalson, R. S., Miezin, F. M., … Schlaggar, B. L. (2012). Parcellation in left lateral parietal cortex is similar in adults and children. *Cerebral Cortex (New York, N.Y. : 1991)*, *22*(5), 1148–58. http://doi.org/10.1093/cercor/bhr189

Barrow-Green, J. (1997). *Poincaré and the Three Body Problem, Volume 2*. American Mathematical Soc.

Barry, R. J., Clarke, A. R., Johnstone, S. J., Magee, C. A., & Rushby, J. A. (2007). EEG differences between eyes-closed and eyes-open resting conditions. *Clinical Neurophysiology : Official Journal of the International Federation of Clinical Neurophysiology*, *118*(12), 2765–73. http://doi.org/10.1016/j.clinph.2007.07.028

Bassett, D. S., & Gazzaniga, M. S. (2011). Understanding complexity in the human brain. *Trends in Cognitive Sciences*, *15*(5), 200–9. http://doi.org/10.1016/j.tics.2011.03.006

Birn, R. M. (2012). The role of physiological noise in resting-state functional connectivity. *NeuroImage*, *62*(2), 864–70. http://doi.org/10.1016/j.neuroimage.2012.01.016

Biswal, B. B. (2012). Resting state fMRI: a personal history. *NeuroImage*, *62*(2), 938–44. http://doi.org/10.1016/j.neuroimage.2012.01.090

Biswal, B., Yetkin, F. Z., Haughton, V. M., & Hyde, J. S. (1995). Functional connectivity in the motor cortex of resting human brain using echo-planar MRI. *Magnetic Resonance in Medicine : Official Journal of the Society of Magnetic Resonance infile:///home/researchers/Desktop/biswal_fluc_coherence1995.pdf Medicine / Society of Magnetic Resonance in Medicine*, *34*(4), 537–41.

Bluhm, R. L., Miller, J., Lanius, R. A., Osuch, E. A., Boksman, K., Neufeld, R. W. J., … Williamson, P. (2007). Spontaneous low-frequency fluctuations in the BOLD signal in schizophrenic patients: anomalies in the default network. *Schizophrenia Bulletin*, *33*(4), 1004–12. http://doi.org/10.1093/schbul/sbm052

Boly, M., Seth, A. K., Wilke, M., Ingmundson, P., Baars, B., Laureys, S., … Tsuchiya, N. (2013). Consciousness in humans and non-human animals: recent advances and future directions. *Frontiers in Psychology*, *4*, 625. http://doi.org/10.3389/fpsyg.2013.00625

Boubela, R. N., Kalcher, K., Huf, W., Kronnerwetter, C., Filzmoser, P., & Moser, E. (2013). Beyond Noise: Using Temporal ICA to Extract Meaningful Information from High-Frequency fMRI Signal Fluctuations during Rest. *Frontiers in Human Neuroscience*, *7*, 168. http://doi.org/10.3389/fnhum.2013.00168

Bouchard, K. E., Mesgarani, N., Johnson, K., & Chang, E. F. (2013). Functional organization of human sensorimotor cortex for speech articulation. *Nature*, *495*(7441), 327–32. http://doi.org/10.1038/nature11911

Bowers, M. B., & Freedman, D. X. (1966). "Psychedelic" experiences in acute psychoses. *Archives of General Psychiatry*, *15*(3), 240–8

Bragin, A., Jandó, G., Nádasdy, Z., Hetke, J., Wise, K., & Buzsáki, G. (1995). Gamma (40-100 Hz) oscillation in the hippocampus of the behaving rat. *The Journal of Neuroscience : The Official Journal of the Society for Neuroscience*, *15*(1 Pt 1), 47–60. Breakspear, M. (2006). The nonlinear theory of schizophrenia. *The Australian and New Zealand Journal of Psychiatry*, *40*(1), 20–35. http://doi.org/10.1111/j.1440-1614.2006.01737.x

Buckner, R. L., Andrews-Hanna, J. R., & Schacter, D. L. (2008). The brain's default network: anatomy, function, and relevance to disease. *Annals of the New York Academy of Sciences*, *1124*, 1–38. http://doi.org/10.1196/annals.1440.011

Bullmore, E., Long, C., Suckling, J., Fadili, J., Calvert, G., Zelaya, F., … Brammer, M. (2001). Colored noise and computational inference in neurophysiological (fMRI) time series analysis: resampling methods in time and wavelet domains. *Human Brain Mapping*, *12*(2), 61–78.

Buzsaki, G. (2006). *Rhythms of the Brain*. Oxford University Press.

Buzsáki, G., & Draguhn, A. (2004). Neuronal oscillations in cortical networks. *Science (New York, N.Y.)*, *304*(5679), 1926–9. http://doi.org/10.1126/science.1099745

Buzsáki, G., Logothetis, N., & Singer, W. (2013). Scaling brain size, keeping timing: evolutionary preservation of brain rhythms. *Neuron*, *80*(3), 751–64. http://doi.org/10.1016/j.neuron.2013.10.002

Cabral, J., Kringelbach, M. L., & Deco, G. (2014). Exploring the network dynamics underlying brain activity during rest. *Progress in Neurobiology*, *114*, 102–31. http://doi.org/10.1016/j.pneurobio.2013.12.005

Caldirola, D., Bellodi, L., Caumo, A., Migliarese, G., & Perna, G. (2004). Approximate entropy of respiratory patterns in panic disorder. *The American Journal of Psychiatry*, *161*(1), 79–87.

Canolty, R. T., Edwards, E., Dalal, S. S., Soltani, M., Nagarajan, S. S., Kirsch, H. E., … Knight, R. T. (2006). High gamma power is phase-locked to theta oscillations in human neocortex. *Science (New York, N.Y.)*, *313*(5793), 1626–8. http://doi.org/10.1126/science.1128115

Canolty, R. T., & Knight, R. T. (2010). The functional role of cross-frequency coupling. *Trends in Cognitive Sciences*, *14*(11), 506–15. http://doi.org/10.1016/j.tics.2010.09.001

Carhart-Harris, R. L., Leech, R., Erritzoe, D., Williams, T. M., Stone, J. M., Evans, J., … Nutt, D. J. (2013). Functional connectivity measures after psilocybin inform a novel hypothesis of early psychosis. *Schizophrenia Bulletin*, *39*(6), 1343–51. http://doi.org/10.1093/schbul/sbs117

Catarino, A., Churches, O., Baron-Cohen, S., Andrade, A., & Ring, H. (2011). Atypical EEG complexity in autism spectrum conditions: A multiscale entropy analysis. *Clinical Neurophysiology*, *122*(12), 2375–2383. http://doi.org/10.1016/j.clinph.2011.05.004

Chai, X. J., Castañón, A. N., Ongür, D., & Whitfield-Gabrieli, S. (2012). Anticorrelations in resting state networks without global signal regression. *NeuroImage*, *59*(2), 1420–8. http://doi.org/10.1016/j.neuroimage.2011.08.048

Chai, X. J., Whitfield-Gabrieli, S., Shinn, A. K., Gabrieli, J. D. E., Nieto Castañón, A., McCarthy, J. M., … Ongür, D. (2011). Abnormal medial prefrontal cortex resting-state connectivity in bipolar disorder and schizophrenia. *Neuropsychopharmacology : Official Publication of the American College of Neuropsychopharmacology*, *36*(10), 2009–17. http://doi.org/10.1038/npp.2011.88

Cheng, D., Tsai, S.-J., Hong, C.-J., & Yang, A. C. (2009). Reduced Physiological Complexity in Robust Elderly Adults with the APOE ε4 Allele. *PLoS ONE*, *4*(11), e7733. http://doi.org/10.1371/journal.pone.0007733

Christoff, K., Gordon, A. M., Smallwood, J., Smith, R., & Schooler, J. W. (2009). Experience sampling during fMRI reveals default network and executive system contributions to mind wandering. *Proceedings of the National Academy of Sciences of the United States of America*, *106*(21), 8719–24. http://doi.org/10.1073/pnas.0900234106

Churchland, P. S. (2002). *Brain-wise: Studies in Neurophilosophy.* Cambridge, MA: MIT Press.

Ciuciu, P., Varoquaux, G., Abry, P., Sadaghiani, S., & Kleinschmidt, A. (2012). Scale-Free and Multifractal Time Dynamics of fMRI Signals during Rest and Task. *Frontiers in Physiology*, *3*, 186. http://doi.org/10.3389/fphys.2012.00186

Clarke, D., & Sokoloff, L. (1999). Circulation and energy metabolism of the brain. In B. W. Agranoff & G. J. Siegel (Eds.), *Basic neurochemistry. Molecular, cellular and medical aspects* (Ed 6, pp. 637–670). Philadelphia: Lippincott-Raven.

Cohen, A. L., Fair, D. A., Dosenbach, N. U. F., Miezin, F. M., Dierker, D., Van Essen, D. C., … Petersen, S. E. (2008). Defining functional areas in individual human brains using resting functional connectivity MRI. *NeuroImage*, *41*(1), 45–57. http://doi.org/10.1016/j.neuroimage.2008.01.066

Cohen, M. S. (1997). Parametric analysis of fMRI data using linear systems methods. *NeuroImage*, *6*(2), 93–103. http://doi.org/10.1006/nimg.1997.0278

Cordes, D., Haughton, V. M., Arfanakis, K., Wendt, G. J., Turski, P. A., Moritz, C. H., … Meyerand, M. E. (2000). Mapping functionally related regions of brain with functional connectivity MR imaging. *AJNR. American Journal of Neuroradiology*, *21*(9), 1636–44.

Costa, M., Goldberger, A. L., & Peng, C.-K. (2005). Multiscale entropy analysis of biological signals. *Physical Review. E, Statistical, Nonlinear, and Soft Matter Physics*, *71*(2 Pt 1), 021906.

Costa, M., Priplata, A. A., Lipsitz, L. A., Wu, Z., Huang, N. E., Goldberger, A. L., & Peng, C.-K. (2007). Noise and poise: Enhancement of postural complexity in the elderly with a stochastic-resonance-based therapy. *Europhysics Letters*, *77*, 68008. http://doi.org/10.1209/0295-5075/77/68008

Cremer, R., & Zeef, E. J. (1987). What kind of noise increases with age? *Journal of Gerontology*, *42*(5), 515–8.

D'Argembeau, A., Collette, F., Van der Linden, M., Laureys, S., Del Fiore, G., Degueldre, C., … Salmon, E. (2005). Self-referential reflective activity and its relationship with rest: a PET study. *NeuroImage*, *25*(2), 616–24. http://doi.org/10.1016/j.neuroimage.2004.11.048

D'Souza, D. C., Perry, E., MacDougall, L., Ammerman, Y., Cooper, T., Wu, Y., … Krystal, J. H. (2004). The Psychotomimetic Effects of Intravenous Delta-9-Tetrahydrocannabinol in Healthy Individuals: Implications for Psychosis. *Neuropsychopharmacology*, *29*(8), 1558–1572. http://doi.org/10.1038/sj.npp.1300496

Dale, A. M. (1999). Optimal experimental design for event-related fMRI. *Human Brain Mapping*, *8*(2-3), 109–14.

Darabi, H. (2015). *Radio Frequency Integrated Circuits and Systems*. Cambridge University Press.

Dastjerdi, M., Foster, B. L., Nasrullah, S., Rauschecker, A. M., Dougherty, R. F., Townsend, J. D., … Parvizi, J. (2011). Differential electrophysiological response during rest, self-referential, and non-self-referential tasks in human posteromedial cortex. *Proceedings of the National Academy of Sciences of the United States of America*, *108*(7), 3023–8. http://doi.org/10.1073/pnas.1017098108

Davidson, R. J. (2000). Affective style, psychopathology, and resilience: brain mechanisms and plasticity. *The American Psychologist*, *55*(11), 1196–214.

Dawson, N., Morris, B. J., & Pratt, J. A. (2011). Subanaesthetic Ketamine Treatment Alters Prefrontal Cortex Connectivity With Thalamus and Ascending Subcortical Systems. *Schizophrenia Bulletin*, *39*(2), 366–377. http://doi.org/10.1093/schbul/sbr144

De Pasquale, F., Della Penna, S., Snyder, A. Z., Marzetti, L., Pizzella, V., Romani, G. L., & Corbetta, M. (2012). A cortical core for dynamic integration of functional networks in the resting human brain. *Neuron*, *74*(4), 753–64. http://doi.org/10.1016/j.neuron.2012.03.031

Deco, G., Jirsa, V. K., & McIntosh, A. R. (2011). Emerging concepts for the dynamical organization of resting-state activity in the brain. *Nature Reviews. Neuroscience*, *12*(1), 43–56. http://doi.org/10.1038/nrn2961

Deco, G., Jirsa, V. K., & McIntosh, A. R. (2013). Resting brains never rest: computational insights into potential cognitive architectures. *Trends in Neurosciences*, *36*(5), 268–274. http://doi.org/10.1016/j.tins.2013.03.001

Deco, G., Jirsa, V., McIntosh, A. R., Sporns, O., & Kötter, R. (2009). Key role of coupling, delay, and noise in resting brain fluctuations. *Proceedings of the National Academy of Sciences of the United States of America*, *106*(25), 10302–7. http://doi.org/10.1073/pnas.0901831106

Destexhe, A., Rudolph, M., & Paré, D. (2003). The high-conductance state of neocortical neurons in vivo. *Nature Reviews. Neuroscience*, *4*(9), 739–51. http://doi.org/10.1038/nrn1198

Devlin, J. T., & Poldrack, R. A. (2007). In praise of tedious anatomy. *NeuroImage*, *37*(4), 1033–41; discussion 1050–8. http://doi.org/10.1016/j.neuroimage.2006.09.055

Dosenbach, N. U. F., Visscher, K. M., Palmer, E. D., Miezin, F. M., Wenger, K. K., Kang, H. C., … Petersen, S. E. (2006). A core system for the implementation of task sets. *Neuron*, *50*(5), 799–812. http://doi.org/10.1016/j.neuron.2006.04.031

Driesen, N. R., McCarthy, G., Bhagwagar, Z., Bloch, M., Calhoun, V., D'Souza, D. C., … Krystal, J. H. (2013). Relationship of resting brain hyperconnectivity and schizophrenia-like symptoms produced by the NMDA receptor antagonist ketamine in humans. *Molecular Psychiatry*. http://doi.org/10.1038/mp.2012.194

Eckblad, M., & Chapman, L. J. (1983). Magical ideation as an indicator of schizotypy. *Journal of Consulting and Clinical Psychology*, *51*(2), 215–25.

Ecker, C., Rocha-Rego, V., Johnston, P., Mourao-Miranda, J., Marquand, A., Daly, E. M., … Murphy, D. G. (2010). Investigating the predictive value of whole-brain structural MR scans in autism: a pattern classification approach. *NeuroImage*, *49*(1), 44–56. http://doi.org/10.1016/j.neuroimage.2009.08.024

Ehlers, C. L. (1995). Chaos and complexity. Can it help us to understand mood and behavior? *Archives of General Psychiatry*, *52*(11), 960–4.

Eke, A., Hermán, P., & Hajnal, M. (2006). Fractal and noisy CBV dynamics in humans: influence of age and gender. *Journal of Cerebral Blood Flow and Metabolism : Official Journal of the International Society of Cerebral Blood Flow and Metabolism*, *26*(7), 891–8. http://doi.org/10.1038/sj.jcbfm.9600243

Eke, A., Herman, P., Kocsis, L., & Kozak, L. R. (2002). Fractal characterization of complexity in temporal physiological signals. *Physiological Measurement*, *23*(1), R1–38.

El Boustani, S., Marre, O., Béhuret, S., Baudot, P., Yger, P., Bal, T., … Frégnac, Y. (2009). Network-state modulation of power-law frequency-scaling in visual cortical neurons. *PLoS Computational Biology*, *5*(9), e1000519. http://doi.org/10.1371/journal.pcbi.1000519

Engel, A. K., Fries, P., & Singer, W. (2001). Dynamic predictions: oscillations and synchrony in top-down processing. *Nature Reviews. Neuroscience*, *2*(10), 704–16. http://doi.org/10.1038/35094565

Evans, A., Collins, D., Millst, S., Brown, E., Kelly, R., & Peters, T. (1993). 3D statistical neuroanatomical models from 305 MRI volumes, 1813 – 1817.

Fair, D. A., Cohen, A. L., Power, J. D., Dosenbach, N. U. F., Church, J. A., Miezin, F. M., … Petersen, S. E. (2009). Functional brain networks develop from a "local to distributed" organization. *PLoS Computational Biology*, *5*(5), e1000381. http://doi.org/10.1371/journal.pcbi.1000381

Faisal, A. A., Selen, L. P. J., & Wolpert, D. M. (2008). Noise in the nervous system. *Nature Reviews. Neuroscience*, *9*(4), 292–303. http://doi.org/10.1038/nrn2258

Fan, Y., Duncan, N. W., de Greck, M., & Northoff, G. (2011). Is there a core neural network in empathy? An fMRI based quantitative meta-analysis. *Neuroscience and Biobehavioral Reviews*, *35*(3), 903–11. http://doi.org/10.1016/j.neubiorev.2010.10.009

Fernández, A., Andreina, M. M., Hornero, R., Ortiz, T., & López-Ibor, J. J. [Analysis of brain complexity and mental disorders]. *Actas Españolas de Psiquiatría*, *38*(4), 229–38.

Fernández, A., López-Ibor, M.-I., Turrero, A., Santos, J.-M., Morón, M.-D., Hornero, R., … López-Ibor, J. J. (2011). Lempel–Ziv complexity in schizophrenia: A MEG study. *Clinical Neurophysiology*, *122*(11), 2227–2235. http://doi.org/10.1016/j.clinph.2011.04.011

Fingelkurts, A. A., Fingelkurts, A. A., & Kähkönen, S. (2005). Functional connectivity in the brain--is it an elusive concept? *Neuroscience and Biobehavioral Reviews*, *28*(8), 827–36. http://doi.org/10.1016/j.neubiorev.2004.10.009

First, M., Spitzer, R., Gibbon, M., & Williams, J. (2002). Structured Clinical Interview for DSL-IV Axis I Disorders, Patient Version (SCID-CV). Washingon DC: America Psychiatric Press.

Fiser, J., Chiu, C., & Weliky, M. (2004). Small modulation of ongoing cortical dynamics by sensory input during natural vision. *Nature*, *431*(7008), 573–8. http://doi.org/10.1038/nature02907

Fourier, J. B. J. baron. (1878). *The Analytical Theory of Heat*. The University Press.

Fox, M. D., & Raichle, M. E. (2007). Spontaneous fluctuations in brain activity observed with functional magnetic resonance imaging. *Nature Reviews. Neuroscience*, *8*(9), 700–11. http://doi.org/10.1038/nrn2201

Fox, M. D., Snyder, A. Z., Vincent, J. L., & Raichle, M. E. (2007). Intrinsic fluctuations within cortical systems account for intertrial variability in human behavior. *Neuron*, *56*(1), 171–84. http://doi.org/10.1016/j.neuron.2007.08.023

Fox, M. D., Snyder, A. Z., Zacks, J. M., & Raichle, M. E. (2006). Coherent spontaneous activity accounts for trial-to-trial variability in human evoked brain responses. *Nature Neuroscience*, *9*(1), 23–5. http://doi.org/10.1038/nn1616

Fransson, P. (2005). Spontaneous low-frequency BOLD signal fluctuations: an fMRI investigation of the resting-state default mode of brain function hypothesis. *Human Brain Mapping*, *26*(1), 15–29. http://doi.org/10.1002/hbm.20113

Fransson, P., Metsäranta, M., Blennow, M., Åden, U., Lagercrantz, H., & Vanhatalo, S. (2013). Early development of spatial patterns of power-law frequency scaling in FMRI resting-state and EEG data in the newborn brain. *Cerebral Cortex (New York, N.Y. : 1991)*, *23*(3), 638–46. http://doi.org/10.1093/cercor/bhs047

FREEMAN, W. J. (2003). THE WAVE PACKET: AN ACTION POTENTIAL FOR THE 21st CENTURY. *Journal of Integrative Neuroscience*, *02*(01), 3–30. http://doi.org/10.1142/S0219635203000214

Freeman, W. J., & Zhai, J. (2008). Simulated power spectral density (PSD) of background electrocorticogram (ECoG). *Cognitive Neurodynamics*, *3*(1), 97–103. http://doi.org/10.1007/s11571-008-9064-y

Frith, C. D. (2007). *Making up the Mind: How the Brain Creates our Mental World.* Malden, MA.: Blackwell Pub.

Fukunaga, M., Horovitz, S. G., van Gelderen, P., de Zwart, J. A., Jansma, J. M., Ikonomidou, V. N., … Duyn, J. H. (2006). Large-amplitude, spatially correlated fluctuations in BOLD fMRI signals during extended rest and early sleep stages. *Magnetic Resonance Imaging*, *24*(8), 979–92. http://doi.org/10.1016/j.mri.2006.04.018

Gallagher, S. (2005). *How the Body Shapes the Mind.* Oxford/New York: Clarendon Press.

Ganzetti, M., & Mantini, D. (2013). Functional connectivity and oscillatory neuronal activity in the resting human brain. *Neuroscience*, *240*, 297–309. http://doi.org/10.1016/j.neuroscience.2013.02.032

Garrett, D. D., Kovacevic, N., McIntosh, A. R., & Grady, C. L. (2011). The importance of being variable. *The Journal of Neuroscience : The Official Journal of the Society for Neuroscience*, *31*(12), 4496–503. http://doi.org/10.1523/JNEUROSCI.5641-10.2011

Garrett, D. D., Kovacevic, N., McIntosh, A. R., & Grady, C. L. (2012). The Modulation of BOLD Variability between Cognitive States Varies by Age and Processing Speed. *Cerebral Cortex*, *23*(3), 684–693. http://doi.org/10.1093/cercor/bhs055

Garrity, A. G., Pearlson, G. D., McKiernan, K., Lloyd, D., Kiehl, K. A., & Calhoun, V. D. (2007). Aberrant "default mode" functional connectivity in schizophrenia. *The American Journal of Psychiatry*, *164*(3), 450–7. http://doi.org/10.1176/ajp.2007.164.3.450

Ghosh, A., Rho, Y., McIntosh, A. R., Kötter, R., & Jirsa, V. K. (2008). Noise during rest enables the exploration of the brain's dynamic repertoire. *PLoS Computational Biology*, *4*(10), e1000196. http://doi.org/10.1371/journal.pcbi.1000196

Glass, L., & Mackey, M. C. (1988). *From Clocks to Chaos: The Rhythms of Life*. Princeton University Press.

Goldberger, A. L., Amaral, L. A. N., Hausdorff, J. M., Ivanov, P. C., Peng, C.-K., & Stanley, H. E. (2002). Fractal dynamics in physiology: Alterations with disease and aging. *Proceedings of the National Academy of Sciences*, *99*(Supplement 1), 2466–2472. http://doi.org/10.1073/pnas.012579499

Gottschalk, A., Bauer, M. S., & Whybrow, P. C. (1995). Evidence of chaotic mood variation in bipolar disorder. *Archives of General Psychiatry*, *52*(11), 947–59.

Goulden, N., Khusnulina, A., Davis, N. J., Bracewell, R. M., Bokde, A. L., McNulty, J. P., & Mullins, P. G. (2014). The salience network is responsible for switching between the default mode network and the central executive network: replication from DCM. *NeuroImage*, *99*, 180–90. http://doi.org/10.1016/j.neuroimage.2014.05.052

Greicius, M. D., Krasnow, B., Reiss, A. L., & Menon, V. (2003). Functional connectivity in the resting brain: a network analysis of the default mode hypothesis. *Proceedings of the National Academy of Sciences of the United States of America*, *100*(1), 253–8. http://doi.org/10.1073/pnas.0135058100

Greicius, M. D., & Menon, V. (2004). Default-mode activity during a passive sensory task: uncoupled from deactivation but impacting activation. *Journal of Cognitive Neuroscience*, *16*(9), 1484–92. http://doi.org/10.1162/0898929042568532

Han, Y., Wang, J., Zhao, Z., Min, B., Lu, J., Li, K., … Jia, J. (2011). Frequency-dependent changes in the amplitude of low-frequency fluctuations in amnestic mild cognitive impairment: a resting-state fMRI study. *NeuroImage*, *55*(1), 287–95. http://doi.org/10.1016/j.neuroimage.2010.11.059

He, B. J. (2011). Scale-free properties of the functional magnetic resonance imaging signal during rest and task. *The Journal of Neuroscience : The Official Journal of the Society for Neuroscience*, *31*(39), 13786–95. http://doi.org/10.1523/JNEUROSCI.2111-11.2011

He, B. J. (2014). Scale-free brain activity: past, present, and future. *Trends in Cognitive Sciences*, *18*(9), 480–487. http://doi.org/10.1016/j.tics.2014.04.003

He, B. J., & Raichle, M. E. (2009). The fMRI signal, slow cortical potential and consciousness. *Trends in Cognitive Sciences*, *13*(7), 302–9. http://doi.org/10.1016/j.tics.2009.04.004

He, B. J., Zempel, J. M., Snyder, A. Z., & Raichle, M. E. (2010). The temporal structures and functional significance of scale-free brain activity. *Neuron*, *66*(3), 353–369. http://doi.org/10.1016/j.neuron.2010.04.020

Ho, K. K., Moody, G. B., Peng, C. K., Mietus, J. E., Larson, M. G., Levy, D., & Goldberger, A. L. (1997). Predicting survival in heart failure case and control subjects by use of fully automated methods for deriving nonlinear and conventional indices of heart rate dynamics. *Circulation*, *96*(3), 842–8.

Hoffmann, R. E., Buchsbaum, M. S., Jensen, R. V, Guich, S. M., Tsai, K., & Nuechterlein, K. H. (1996). Dimensional complexity of EEG waveforms in neuroleptic-free schizophrenic patients and normal control subjects. *The Journal of Neuropsychiatry and Clinical Neurosciences*, *8*(4), 436–41.

Honey, C. J., Thesen, T., Donner, T. H., Silbert, L. J., Carlson, C. E., Devinsky, O., … Hasson, U. (2012). Slow cortical dynamics and the accumulation of information over long timescales. *Neuron*, *76*(2), 423–34. http://doi.org/10.1016/j.neuron.2012.08.011

Honey, G. D., Corlett, P. R., Absalom, A. R., Lee, M., Pomarol-Clotet, E., Murray, G. K., … Fletcher, P. C. (2008). Individual differences in psychotic effects of ketamine are predicted by brain function measured under placebo. *The Journal of Neuroscience : The Official Journal of the Society for Neuroscience*, *28*(25), 6295–303. http://doi.org/10.1523/JNEUROSCI.0910-08.2008

Hoptman, M. J., Zuo, X.-N., Butler, P. D., Javitt, D. C., D'Angelo, D., Mauro, C. J., & Milham, M. P. (2010). Amplitude of low-frequency oscillations in schizophrenia: a resting state fMRI study. *Schizophrenia Research*, *117*(1), 13–20. http://doi.org/10.1016/j.schres.2009.09.030

Howes, O. D., & Kapur, S. (2009). The dopamine hypothesis of schizophrenia: version III--the final common pathway. *Schizophrenia Bulletin*, *35*(3), 549–62. http://doi.org/10.1093/schbul/sbp006

Hsü, K. J., & Hsü, A. (1991). Self-similarity of the "1/f noise" called music. *Proceedings of the National Academy of Sciences of the United States of America*, *88*(8), 3507–9.

Huang, Z., Dai, R., Wu, X., Yang, Z., Liu, D., Hu, J., … Northoff, G. (2014a). The self and its resting state in consciousness: An investigation of the vegetative state. *Human Brain Mapping*, *35*(5), 1997–2008. http://doi.org/10.1002/hbm.22308

Huang, Z., Wang, Z., Zhang, J., Dai, R., Wu, J., Li, Y., … Northoff, G. (2014b). Altered temporal variance and neural synchronization of spontaneous brain activity in anesthesia. *Human Brain Mapping*, *5378*(November 2013), 5368–5378. http://doi.org/10.1002/hbm.22556

Huettel, S. A., Song, A. W., & McCarthy, G. (2004). *Functional Magnetic Resonance Imaging*. Freeman.

Huettel, S. A., Song, A. W., & McCarthy, G. (2009). *Functional Magnetic Resonance Imaging*. Freeman.

Hunter, M. D., Eickhoff, S. B., Miller, T. W. R., Farrow, T. F. D., Wilkinson, I. D., & Woodruff, P. W. R. (2006). Neural activity in speech-sensitive auditory cortex during silence. *Proceedings of the National Academy of Sciences of the United States of America*, *103*(1), 189–94. http://doi.org/10.1073/pnas.0506268103

HURST, H. E. (1956). METHODS OF USING LONG-TERM STORAGE IN RESERVOIRS. *ICE Proceedings*, *5*(5), 519–543. http://doi.org/10.1680/iicep.1956.11503

Jafri, M. J., Pearlson, G. D., Stevens, M., & Calhoun, V. D. (2008). A method for functional network connectivity among spatially independent resting-state components in schizophrenia. *NeuroImage*, *39*(4), 1666–81. http://doi.org/10.1016/j.neuroimage.2007.11.001

Javitt, D. C., Zukin, S. R., Heresco-Levy, U., & Umbricht, D. (2012). Has an angel shown the way? Etiological and therapeutic implications of the PCP/NMDA model of schizophrenia. *Schizophrenia Bulletin*, *38*(5), 958–66. http://doi.org/10.1093/schbul/sbs069

Jenkinson, M., Beckmann, C. F., Behrens, T. E. J., Woolrich, M. W., & Smith, S. M. (2012). FSL. *NeuroImage*, *62*(2), 782–90. http://doi.org/10.1016/j.neuroimage.2011.09.015

Jones, T. B., Bandettini, P. A., & Birn, R. M. (2008). Integration of motion correction and physiological noise regression in fMRI. *NeuroImage*, *42*(2), 582–90. http://doi.org/10.1016/j.neuroimage.2008.05.019

Kahn, I., Knoblich, U., Desai, M., Bernstein, J., Graybiel, A. M., Boyden, E. S., … Moore, C. I. (2013). Optogenetic drive of neocortical pyramidal neurons generates fMRI signals that are correlated with spiking activity. *Brain Research*, *1511*, 33–45. http://doi.org/10.1016/j.brainres.2013.03.011

Kalcher, K., Huf, W., Boubela, R. N., Filzmoser, P., Pezawas, L., Biswal, B., … Windischberger, C. (2012). Fully exploratory network independent component analysis of the 1000 functional connectomes database. *Frontiers in Human Neuroscience*, *6*, 301. http://doi.org/10.3389/fnhum.2012.00301

Karbasforoushan, H., & Woodward, N. D. (2012). Resting-state networks in schizophrenia. *Current Topics in Medicinal Chemistry*, *12*(21), 2404–14.

Karlsgodt, K. H., Robleto, K., Trantham-Davidson, H., Jairl, C., Cannon, T. D., Lavin, A., & Jentsch, J. D. (2011). Reduced dysbindin expression mediates N-methyl-D-aspartate receptor hypofunction and impaired working memory performance. *Biological Psychiatry*, *69*(1), 28–34. http://doi.org/10.1016/j.biopsych.2010.09.012

Kay, S. R., Flszbein, A., & Opfer, L. A. (n.d.). The Positive and Negative Syndrome Scale (PANSS) for Schizophrenia.

Kehrer, C., Maziashvili, N., Dugladze, T., & Gloveli, T. (2008). Altered Excitatory-Inhibitory Balance in the NMDA-Hypofunction Model of Schizophrenia. *Frontiers in Molecular Neuroscience*, *1*, 6. http://doi.org/10.3389/neuro.02.006.2008

Kello, C. T., Brown, G. D. A., Ferrer-I-Cancho, R., Holden, J. G., Linkenkaer-Hansen, K., Rhodes, T., & Van Orden, G. C. (2010). Scaling laws in cognitive sciences. *Trends in Cognitive Sciences*, *14*(5), 223–32. http://doi.org/10.1016/j.tics.2010.02.005

Khader, P., Schicke, T., Röder, B., & Rösler, F. (2008). On the relationship between slow cortical potentials and BOLD signal changes in humans. *International Journal of Psychophysiology : Official Journal of the International Organization of Psychophysiology*, *67*(3), 252–61. http://doi.org/10.1016/j.ijpsycho.2007.05.018

Kim, S.-Y., Lee, H., Kim, H.-J., Bang, E., Lee, S.-H., Lee, D.-W., … Choe, B.-Y. (2011). In vivo and ex vivo evidence for ketamine-induced hyperglutamatergic activity in the cerebral cortex of the rat: Potential relevance to schizophrenia. *NMR in Biomedicine*, *24*(10), 1235–42. http://doi.org/10.1002/nbm.1681

KLEE, G. D. (1963). Lysergic acid diethylamide (LSD-25) and ego functions. *Archives of General Psychiatry*, *8*, 461–74.

Knill, D. C., & Pouget, A. (2004). The Bayesian brain: the role of uncertainty in neural coding and computation. *Trends in Neurosciences*, *27*(12), 712–9. http://doi.org/10.1016/j.tins.2004.10.007

Koch, C. (2004). *The Quest for Consciousness: A Neurobiological Approach.* Denver, CO: Roberts and Co.

Konishi, K., Kumashiro, M., Izumi, H., Higuchi, Y., & Awa, Y. (2009). Effects of the menstrual cycle on language and visual working memory: a pilot study. Industrial Health, 47(5), 560–8

Koukkou, M., Lehmann, D., Wackermann, J., Dvorak, I., & Henggeler, B. (1993). Dimensional complexity of EEG brain mechanisms in untreated schizophrenia. *Biological Psychiatry*, *33*(6), 397–407.

Koutsoukos, E., Angelopoulos, E., Maillis, A., Papadimitriou, G. N., & Stefanis, C. (2013). Indication of increased phase coupling between theta and gamma EEG rhythms associated with the experience of auditory verbal hallucinations. *Neuroscience Letters*, *534*, 242–5. http://doi.org/10.1016/j.neulet.2012.12.005

Krystal, J. H., Karper, L. P., Seibyl, J. P., Freeman, G. K., Delaney, R., Bremner, J. D., … Charney, D. S. (1994). Subanesthetic effects of the noncompetitive NMDA antagonist, ketamine, in humans. Psychotomimetic, perceptual, cognitive, and neuroendocrine responses. *Archives of General Psychiatry*, *51*(3), 199–214.

Lai, M.-C., Lombardo, M. V., Chakrabarti, B., Sadek, S. A., Pasco, G., Wheelwright, S. J., … Suckling, J. (2010). A Shift to Randomness of Brain Oscillations in People with Autism. *Biological Psychiatry*, *68*(12), 1092–1099. http://doi.org/10.1016/j.biopsych.2010.06.027

Lakatos, P., Karmos, G., Mehta, A. D., Ulbert, I., & Schroeder, C. E. (2008). Entrainment of neuronal oscillations as a mechanism of attentional selection. *Science (New York, N.Y.)*, *320*(5872), 110–3. http://doi.org/10.1126/science.1154735

Lau, C.-I., Wang, H.-C., Hsu, J.-L., & Liu, M.-E. (2013). Does the dopamine hypothesis explain schizophrenia? *Reviews in the Neurosciences*, *24*(4), 389–400. http://doi.org/10.1515/revneuro-2013-0011

Lei, X., Wang, Y., Yuan, H., & Chen, A. (2015a). Brain scale-free properties in awake rest and NREM sleep: a simultaneous EEG/fMRI study. *Brain Topography*, *28*(2), 292–304. http://doi.org/10.1007/s10548-014-0399-x

Lei, X., Wang, Y., Yuan, H., & Chen, A. (2015b). Brain scale-free properties in awake rest and NREM sleep: a simultaneous EEG/fMRI study. *Brain Topography*, *28*(2), 292–304. http://doi.org/10.1007/s10548-014-0399-x

Leniger-Follert, E., & Lübbers, D. W. (1976). Behavior of microflow and localP O 2 of the brain cortex during and after direct electrical stimulation. *Pflügers Archiv European Journal of Physiology*, *366*(1), 39–44. http://doi.org/10.1007/BF02486558

Lennie, P. (2003). The cost of cortical computation. *Current Biology : CB*, *13*(6), 493–7.

Linkenkaer-Hansen, K., Nikouline, V. V, Palva, J. M., & Ilmoniemi, R. J. (2001). Long-range temporal correlations and scaling behavior in human brain oscillations. *The Journal of Neuroscience : The Official Journal of the Society for Neuroscience*, *21*(4), 1370–7

Lipsitz, L. A., & Goldberger, A. L. (1992). Loss of "complexity" and aging. Potential applications of fractals and chaos theory to senescence. *JAMA*, *267*(13), 1806–9.

Logothetis, N. K. (2002). The neural basis of the blood-oxygen-level-dependent functional magnetic resonance imaging signal. *Philosophical Transactions of the Royal Society of London. Series B, Biological Sciences*, *357*(1424), 1003–37. http://doi.org/10.1098/rstb.2002.1114

Logothetis, N. K., Murayama, Y., Augath, M., Steffen, T., Werner, J., & Oeltermann, A. (2009). How not to study spontaneous activity. *NeuroImage*, *45*(4), 1080–9. http://doi.org/10.1016/j.neuroimage.2009.01.010

Logothetis, N. K., & Wandell, B. A. (2004). Interpreting the BOLD signal. *Annual Review of Physiology*, *66*, 735–69. http://doi.org/10.1146/annurev.physiol.66.082602.092845

Lowen, S. B., Cash, S. S., Poo, M., & Teich, M. C. (1997). Quantal neurotransmitter secretion rate exhibits fractal behavior. *The Journal of Neuroscience : The Official Journal of the Society for Neuroscience*, *17*(15), 5666–77.

Ma, W. J., Beck, J. M., Latham, P. E., & Pouget, A. (2006). Bayesian inference with probabilistic population codes. *Nature Neuroscience*, *9*(11), 1432–8. http://doi.org/10.1038/nn1790

Maandag, N. J. G., Coman, D., Sanganahalli, B. G., Herman, P., Smith, A. J., Blumenfeld, H., … Hyder, F. (2007). Energetics of neuronal signaling and fMRI activity. *Proceedings of the National Academy of*

Sciences of the United States of America, *104*(51), 20546–51. http://doi.org/10.1073/pnas.0709515104

Magioncalda, P., Martino, M., Conio, B., Escelsior, A., Piaggio, N., Presta, A., … Amore, M. (2015). Functional connectivity and neuronal variability of resting state activity in bipolar disorder-reduction and decoupling in anterior cortical midline structures. *Human Brain Mapping*, *36*(2), 666–682. http://doi.org/10.1002/hbm.22655

Mäkikallio, T. H., Seppänen, T., Airaksinen, K. E., Koistinen, J., Tulppo, M. P., Peng, C. K., … Huikuri, H. V. (1997). Dynamic analysis of heart rate may predict subsequent ventricular tachycardia after myocardial infarction. *The American Journal of Cardiology*, *80*(6), 779–83.

Mandelbrot, B. B. (2013). *Multifractals and 1/f Noise: Wild Self-Affinity in Physics (1963–1976)*. Springer.

Manning, J. R., Jacobs, J., Fried, I., & Kahana, M. J. (2009). Broadband shifts in local field potential power spectra are correlated with single-neuron spiking in humans. *The Journal of Neuroscience : The Official Journal of the Society for Neuroscience*, *29*(43), 13613–20. http://doi.org/10.1523/JNEUROSCI.2041-09.2009

Margulies, D. S., Böttger, J., Long, X., Lv, Y., Kelly, C., Schäfer, A., … Villringer, A. (2010). Resting developments: a review of fMRI post-processing methodologies for spontaneous brain activity. *Magma (New York, N.Y.)*, *23*(5-6), 289–307. http://doi.org/10.1007/s10334-010-0228-5

Maxim, V., Sendur, L., Fadili, J., Suckling, J., Gould, R., Howard, R., & Bullmore, E. (2005). Fractional Gaussian noise, functional MRI and Alzheimer's disease. *NeuroImage*, *25*(1), 141–58. http://doi.org/10.1016/j.neuroimage.2004.10.044

McIntosh, A. R., Kovacevic, N., Lippe, S., Garrett, D., Grady, C., & Jirsa, V. (2010). The development of a noisy brain. *Archives Italiennes de Biologie*, *148*(3), 323–37.

Méndez, M. A., Zuluaga, P., Hornero, R., Gómez, C., Escudero, J., Rodríguez-Palancas, A., … Fernández, A. (2012). Complexity analysis of spontaneous brain activity: effects of depression and antidepressant treatment. *Journal of Psychopharmacology (Oxford, England)*, *26*(5), 636–43. http://doi.org/10.1177/0269881111408966

Menon, V. (2011). Large-scale brain networks and psychopathology: a unifying triple network model. *Trends in Cognitive Sciences*, *15*(10), 483–506. http://doi.org/10.1016/j.tics.2011.08.003

Meunier, D., Achard, S., Morcom, A., & Bullmore, E. (2009). Age-related changes in modular organization of human brain functional networks. *NeuroImage*, *44*(3), 715–23. http://doi.org/10.1016/j.neuroimage.2008.09.062

Miller, K. J., Sorensen, L. B., Ojemann, J. G., & den Nijs, M. (2009). Power-law scaling in the brain surface electric potential. *PLoS Computational Biology*, *5*(12), e1000609. http://doi.org/10.1371/journal.pcbi.1000609

Milstein, J., Mormann, F., Fried, I., & Koch, C. (2009). Neuronal shot noise and Brownian 1/f2 behavior in the local field potential. *PloS One*, *4*(2), e4338. http://doi.org/10.1371/journal.pone.0004338

Morris, B. J., Cochran, S. M., & Pratt, J. A. (2005). PCP: from pharmacology to modelling schizophrenia. *Current Opinion in Pharmacology*, *5*(1), 101–6. http://doi.org/10.1016/j.coph.2004.08.008

Mujica-Parodi, L. R., Yeragani, V., & Malaspina, D. (2005). Nonlinear complexity and spectral analyses of heart rate variability in medicated and unmedicated patients with schizophrenia. *Neuropsychobiology*, *51*(1), 10–5. http://doi.org/10.1159/000082850

Narr, K. L., Bilder, R. M., Kim, S., Thompson, P. M., Szeszko, P., Robinson, D., … Toga, A. W. (2004). Abnormal gyral complexity in first-episode schizophrenia. *Biological Psychiatry*, *55*(8), 859–67. http://doi.org/10.1016/j.biopsych.2003.12.027

Newcomer, J. W., Farber, N. B., Jevtovic-Todorovic, V., Selke, G., Melson, A. K., Hershey, T., … Olney, J. W. (1999). Ketamine-induced NMDA receptor hypofunction as a model of memory impairment and psychosis. *Neuropsychopharmacology : Official Publication of the American College of Neuropsychopharmacology*, *20*(2), 106–18. http://doi.org/10.1016/S0893-133X(98)00067-0

Niesters, M., Khalili-Mahani, N., Martini, C., Aarts, L., van Gerven, J., van Buchem, M. A., … Rombouts, S. (2012). Effect of subanesthetic ketamine on intrinsic functional brain connectivity: a placebo-controlled functional magnetic resonance imaging study in healthy male volunteers. *Anesthesiology*, *117*(4), 868–77. http://doi.org/10.1097/ALN.0b013e31826a0db3

Nikulin, V. V, & Brismar, T. (2004). Comment on "Multiscale entropy analysis of complex physiologic time series". *Physical Review Letters*, *92*(8), 089803; author reply 089804.

Nørretranders, T. (1998). *The User Illusion: Cutting Consciousness Down to Size*. A. Lane.

Northoff, G. (2004). *Philosophy of the Brain: The Brain Problem.* Netherlands: John Benjamins Pub.

Northoff, G. (2014a). Do cortical midline variability and low frequency fluctuations mediate William James' "Stream of Consciousness"? "Neurophenomenal Balance Hypothesis" of "Inner Time Consciousness". *Consciousness and Cognition*, *30*, 184–200. http://doi.org/10.1016/j.concog.2014.09.004

Northoff, G. (2014b). Unlocking the Brain: Volume 1: Coding

Northoff, G. (2014c). Unlocking the Brain: Volume 2: Consciousness.

Northoff, G. (2015a). Is schizophrenia a spatiotemporal disorder of the brain's resting state? *World Psychiatry : Official Journal of the World Psychiatric Association (WPA)*, *14*(1), 34–5. http://doi.org/10.1002/wps.20177

Northoff, G. (2015b). Spatiotemporal psychopathology I: No rest for the brain's resting state activity in depression? spatiotemporal psychopathology of depressive symptoms. *Journal of Affective Disorders*. http://doi.org/10.1016/j.jad.2015.05.007

Northoff, G., Heinzel, A., de Greck, M., Bermpohl, F., Dobrowolny, H., & Panksepp, J. (2006). Self-referential processing in our brain--a meta-analysis of imaging studies on the self. *NeuroImage*, *31*(1), 440–57. http://doi.org/10.1016/j.neuroimage.2005.12.002

Northoff, G., & Qin, P. (2011). How can the brain's resting state activity generate hallucinations? A "resting state hypothesis" of auditory verbal hallucinations. *Schizophrenia Research*, *127*(1-3), 202–14. http://doi.org/10.1016/j.schres.2010.11.009

Northoff, G., Qin, P., & Nakao, T. (2010). Rest-stimulus interaction in the brain: a review. *Trends in Neurosciences*, *33*(6), 277–84. http://doi.org/10.1016/j.tins.2010.02.006

Ogawa, S., Lee, T. M., Kay, A. R., & Tank, D. W. (1990). Brain magnetic resonance imaging with contrast dependent on blood oxygenation. *Proceedings of the National Academy of Sciences of the United States of America*, *87*(24), 9868–72.

Olney, J. W., & Farber, N. B. (1995). Glutamate receptor dysfunction and schizophrenia. *Archives of General Psychiatry*, *52*(12), 998–1007.

Olney, J. W., Newcomer, J. W., & Farber, N. B. NMDA receptor hypofunction model of schizophrenia. *Journal of Psychiatric Research*, *33*(6), 523–33.

Palva, J. M., Zhigalov, A., Hirvonen, J., Korhonen, O., Linkenkaer-Hansen, K., & Palva, S. (2013). Neuronal long-range temporal correlations and avalanche dynamics are correlated with behavioral scaling laws. *Proceedings of the National Academy of Sciences of the United States of America*, *110*(9), 3585–90. http://doi.org/10.1073/pnas.1216855110

Pan, W.-J., Thompson, G. J., Magnuson, M. E., Jaeger, D., & Keilholz, S. (2013). Infraslow LFP correlates to resting-state fMRI BOLD signals. *NeuroImage*, *74*, 288–97. http://doi.org/10.1016/j.neuroimage.2013.02.035

Park, C., Lazar, N. A., Ahn, J., & Sornborger, A. (2010). A multiscale analysis of the temporal characteristics of resting-state fMRI data. *Journal of Neuroscience Methods*, *193*(2), 334–42. http://doi.org/10.1016/j.jneumeth.2010.08.021

Patriat, R., Molloy, E. K., Meier, T. B., Kirk, G. R., Nair, V. A., Meyerand, M. E., … Birn, R. M. (2013). The effect of resting condition on resting-state fMRI reliability and consistency: a comparison between resting with eyes open, closed, and fixated. *NeuroImage*, *78*, 463–73. http://doi.org/10.1016/j.neuroimage.2013.04.013

Paulus, M. P., & Braff, D. L. (2003). Chaos and schizophrenia: does the method fit the madness? *Biological Psychiatry*, *53*(1), 3–11.

Paulus, M. P., Geyer, M. A., & Braff, D. L. (1996). Use of methods from chaos theory to quantify a fundamental dysfunction in the behavioral organization of schizophrenic patients. *The American Journal of Psychiatry*, *153*(5), 714–7.

Peng, C. K., Buldyrev, S. V, Havlin, S., Simons, M., Stanley, H. E., & Goldberger, A. L. (1994). Mosaic organization of DNA nucleotides. *Physical Review. E, Statistical Physics, Plasmas, Fluids, and Related Interdisciplinary Topics*, *49*(2), 1685–9

Peng, C.-K., Costa, M., & Goldberger, A. L. (2009). ADAPTIVE DATA ANALYSIS OF COMPLEX FLUCTUATIONS IN PHYSIOLOGIC TIME SERIES. *Advances in Adaptive Data Analysis*, *1*(1), 61–70. http://doi.org/10.1142/S1793536909000035

Penhune, V. B., Zatorre, R. J., MacDonald, J. D., & Evans, A. C. Interhemispheric anatomical differences in human primary auditory cortex: probabilistic mapping and volume measurement from magnetic resonance scans. *Cerebral Cortex (New York, N.Y. : 1991)*, *6*(5), 661–72.

Penttonen, M., & Buzsáki, G. (2006). Natural logarithmic relationship between brain oscillators. *Thalamus and Related Systems*, *2*(02), 145. http://doi.org/10.1017/S1472928803000074

Pettersson-Yeo, W., Allen, P., Benetti, S., McGuire, P., & Mechelli, A. (2011). Dysconnectivity in schizophrenia: where are we now? *Neuroscience and Biobehavioral Reviews*, *35*(5), 1110–24. http://doi.org/10.1016/j.neubiorev.2010.11.004

Pilowsky, L. S., Bressan, R. A., Stone, J. M., Erlandsson, K., Mulligan, R. S., Krystal, J. H., & Ell, P. J. (2006). First in vivo evidence of an NMDA receptor deficit in medication-free schizophrenic patients. *Molecular Psychiatry*, *11*(2), 118–9. http://doi.org/10.1038/sj.mp.4001751

Poldrack, R. (2011). *Handbook of functional MRI data analysis*. New York: Cambridge University Press.

Power, J. D., Cohen, A. L., Nelson, S. M., Wig, G. S., Barnes, K. A., Church, J. A., … Petersen, S. E. (2011). Functional network organization of the human brain. *Neuron*, *72*(4), 665–78. http://doi.org/10.1016/j.neuron.2011.09.006

Qin, P., & Northoff, G. (2011). How is our self related to midline regions and the default-mode network? *NeuroImage*, *57*(3), 1221–33. http://doi.org/10.1016/j.neuroimage.2011.05.028

Rademacher, J., Morosan, P., Schormann, T., Schleicher, A., Werner, C., Freund, H. J., & Zilles, K. (2001). Probabilistic mapping and volume measurement of human primary auditory cortex. *NeuroImage*, *13*(4), 669–83. http://doi.org/10.1006/nimg.2000.0714

Raghavendra, B. S., Dutt, D. N., Halahalli, H. N., & John, J. P. (2009). Complexity analysis of EEG in patients with schizophrenia using fractal dimension. *Physiological Measurement*, *30*(8), 795–808. http://doi.org/10.1088/0967-3334/30/8/005

Raichle, M. E. (2009). A paradigm shift in functional brain imaging. *The Journal of Neuroscience : The Official Journal of the Society for Neuroscience*, *29*(41), 12729–34. http://doi.org/10.1523/JNEUROSCI.4366-09.2009

Raichle, M. E. (2010). Two views of brain function. *Trends in Cognitive Sciences*, *14*(4), 180–90. http://doi.org/10.1016/j.tics.2010.01.008

Raichle, M. E., MacLeod, A. M., Snyder, A. Z., Powers, W. J., Gusnard, D. A., & Shulman, G. L. (2001). A default mode of brain function. *Proceedings of the National Academy of Sciences of the United States of America*, *98*(2), 676–82. http://doi.org/10.1073/pnas.98.2.676

Raja Beharelle, A., Kovačević, N., McIntosh, A. R., & Levine, B. (2012). Brain signal variability relates to stability of behavior after recovery from diffuse brain injury. *NeuroImage*, *60*(2), 1528–37. http://doi.org/10.1016/j.neuroimage.2012.01.037

Ray, S., & Maunsell, J. H. R. (2011). Different origins of gamma rhythm and high-gamma activity in macaque visual cortex. *PLoS Biology*, *9*(4), e1000610. http://doi.org/10.1371/journal.pbio.1000610

Rees, G., Friston, K., & Koch, C. (2000). A direct quantitative relationship between the functional properties of human and macaque V5. *Nature Neuroscience*, *3*(7), 716–23. http://doi.org/10.1038/76673

Reich, D. L., & Silvay, G. (1989). Ketamine: an update on the first twenty-five years of clinical experience. *Canadian Journal of Anaesthesia = Journal Canadien D'anesthésie*, *36*(2), 186–97. http://doi.org/10.1007/BF03011442

Richman, J. S., & Moorman, J. R. (2000). Physiological time-series analysis using approximate entropy and sample entropy. *American Journal of Physiology. Heart and Circulatory Physiology*, *278*(6), H2039–49.

Rilling, J. K., Barks, S. K., Parr, L. A., Preuss, T. M., Faber, T. L., Pagnoni, G., … Votaw, J. R. (2007). A comparison of resting-state brain activity in humans and chimpanzees. *Proceedings of the National*

Academy of Sciences of the United States of America, *104*(43), 17146–51. http://doi.org/10.1073/pnas.0705132104

Roberts, B. M., Seymour, P. A., Schmidt, C. J., Williams, G. V, & Castner, S. A. (2010). Amelioration of ketamine-induced working memory deficits by dopamine D1 receptor agonists. *Psychopharmacology*, *210*(3), 407–18. http://doi.org/10.1007/s00213-010-1840-9

Rosenfeld, A., & Kak, A. C. (1982). Digital Picture Processing.

Rowland, L. M., Bustillo, J. R., Mullins, P. G., Jung, R. E., Lenroot, R., Landgraf, E., … Brooks, W. M. (2005). Effects of ketamine on anterior cingulate glutamate metabolism in healthy humans: a 4-T proton MRS study. *The American Journal of Psychiatry*, *162*(2), 394–6. http://doi.org/10.1176/appi.ajp.162.2.394

Salthouse, T. A., & Lichty, W. (1985). Tests of the neural noise hypothesis of age-related cognitive change. *Journal of Gerontology*, *40*(4), 443–50.

Salvador, R., Sarró, S., Gomar, J. J., Ortiz-Gil, J., Vila, F., Capdevila, A., … Pomarol-Clotet, E. (2010). Overall brain connectivity maps show cortico-subcortical abnormalities in schizophrenia. *Human Brain Mapping*, *31*(12), 2003–14. http://doi.org/10.1002/hbm.20993

Searle, J. R. (2004). *Mind: A Brief Introduction.* Oxford/New York: Oxford University Press.

Seeley, W. W., Menon, V., Schatzberg, A. F., Keller, J., Glover, G. H., Kenna, H., … Greicius, M. D. (2007). Dissociable intrinsic connectivity networks for salience processing and executive control. *The Journal of Neuroscience : The Official Journal of the Society for Neuroscience*, *27*(9), 2349–56. http://doi.org/10.1523/JNEUROSCI.5587-06.2007

Shim, G., Oh, J. S., Jung, W., Jang, J., Choi, C.-H., Kim, E., … Kwon, J. (2010). Altered resting-state connectivity in subjects at ultra-high risk for psychosis: an fMRI study. *Behavioral and Brain Functions*, *6*(1), 58. http://doi.org/10.1186/1744-9081-6-58

Shulman, G. L., Astafiev, S. V, Franke, D., Pope, D. L. W., Snyder, A. Z., McAvoy, M. P., & Corbetta, M. (2009). Interaction of stimulus-driven reorienting and expectation in ventral and dorsal frontoparietal and basal ganglia-cortical networks. *The Journal of Neuroscience : The Official Journal of the Society for Neuroscience*, *29*(14), 4392–407. http://doi.org/10.1523/JNEUROSCI.5609-08.2009

Shulman, R. G., Hyder, F., & Rothman, D. L. (2009). Baseline brain energy supports the state of consciousness. *Proceedings of the National Academy of Sciences of the United States of America*, *106*(27), 11096–101. http://doi.org/10.1073/pnas.0903941106

Shulman, R. G., Hyder, F., & Rothman, D. L. (2014). Insights from neuroenergetics into the interpretation of functional neuroimaging: an alternative empirical model for studying the brain's support of behavior. *Journal of Cerebral Blood Flow and Metabolism : Official Journal of the International Society of Cerebral Blood Flow and Metabolism*, *34*(11), 1721–35. http://doi.org/10.1038/jcbfm.2014.145

Shulman, R. G., Rothman, D. L., Behar, K. L., & Hyder, F. (2004). Energetic basis of brain activity: implications for neuroimaging. *Trends in Neurosciences*, *27*(8), 489–95. http://doi.org/10.1016/j.tins.2004.06.005

Sibson, N. R., Dhankhar, A., Mason, G. F., Rothman, D. L., Behar, K. L., & Shulman, R. G. (1998). Stoichiometric coupling of brain glucose metabolism and glutamatergic neuronal activity. *Proceedings of the National Academy of Sciences of the United States of America*, *95*(1), 316–21.

Sladky, R., Friston, K. J., Tröstl, J., Cunnington, R., Moser, E., & Windischberger, C. (2011). Slice-timing effects and their correction in functional MRI. *NeuroImage*, *58*(2), 588–94. http://doi.org/10.1016/j.neuroimage.2011.06.078

Smit, D. J. A., de Geus, E. J. C., van de Nieuwenhuijzen, M. E., van Beijsterveldt, C. E. M., van Baal, G. C. M., Mansvelder, H. D., … Linkenkaer-Hansen, K. (2011). Scale-free modulation of resting-state neuronal oscillations reflects prolonged brain maturation in humans. *The Journal of Neuroscience : The Official Journal of the Society for Neuroscience*, *31*(37), 13128–36. http://doi.org/10.1523/JNEUROSCI.1678-11.2011

Smit, D. J. A., Linkenkaer-Hansen, K., & de Geus, E. J. C. (2013). Long-range temporal correlations in resting-state α oscillations predict human timing-error dynamics. *The Journal of Neuroscience : The Official Journal of the Society for Neuroscience*, *33*(27), 11212–20. http://doi.org/10.1523/JNEUROSCI.2816-12.2013

Smith, D. J., Whitham, E. A., & Ghaemi, S. N. (2012). Bipolar disorder. *Handbook of Clinical Neurology*, *106*, 251–63. http://doi.org/10.1016/B978-0-444-52002-9.00015-2

Smith, R. X., Yan, L., & Wang, D. J. J. (2014). Multiple time scale complexity analysis of resting state FMRI. *Brain Imaging and Behavior*, *8*(2), 284–91. http://doi.org/10.1007/s11682-013-9276-6

Smith, S. M. (2002). Fast robust automated brain extraction. *Human Brain Mapping*, *17*(3), 143–55. http://doi.org/10.1002/hbm.10062

Smith, S. M., Fox, P. T., Miller, K. L., Glahn, D. C., Fox, P. M., Mackay, C. E., … Beckmann, C. F. (2009). Correspondence of the brain's functional architecture during activation and rest. *Proceedings of the National Academy of Sciences of the United States of America*, *106*(31), 13040–5. http://doi.org/10.1073/pnas.0905267106

Smythies, J. (2002). The adrenochrome hypothesis of schizophrenia revisited. *Neurotoxicity Research*, *4*(2), 147–50. http://doi.org/10.1080/10298420290015827

SOKOLOFF, L., MANGOLD, R., WECHSLER, R. L., KENNEY, C., & KETY, S. S. (1955). The effect of mental arithmetic on cerebral circulation and metabolism. *The Journal of Clinical Investigation*, *34*(7, Part 1), 1101–8. http://doi.org/10.1172/JCI103159

Sokunbi, M. O., Fung, W., Sawlani, V., Choppin, S., Linden, D. E. J., & Thome, J. (2013). Resting state fMRI entropy probes complexity of brain activity in adults with ADHD. *Psychiatry Research*, *214*(3), 341–8. http://doi.org/10.1016/j.pscychresns.2013.10.001

Sokunbi, M. O., Gradin, V. B., Waiter, G. D., Cameron, G. G., Ahearn, T. S., Murray, A. D., … Staff, R. T. (2014). Nonlinear complexity analysis of brain FMRI signals in schizophrenia. PloS One, 9(5), e95146. http://doi.org/10.1371/journal.pone.0095146

Sommer, I. E., Clos, M., Meijering, A. L., Diederen, K. M. J., & Eickhoff, S. B. (2012). Resting state functional connectivity in patients with chronic hallucinations. *PloS One*, *7*(9), e43516. http://doi.org/10.1371/journal.pone.0043516

Sporns, O. (2011). Networks of the brain. Cambridge, Mass. : MIT Press,.

Stehling, M. K., Turner, R., & Mansfield, P. (1991). Echo-planar imaging: magnetic resonance imaging in a fraction of a second. *Science (New York, N.Y.)*, *254*(5028), 43–50.

Stein, R. B., Gossen, E. R., & Jones, K. E. (2005). Neuronal variability: noise or part of the signal? *Nature Reviews. Neuroscience*, *6*(5), 389–97. http://doi.org/10.1038/nrn1668

Stone, J. M., Dietrich, C., Edden, R., Mehta, M. A., De Simoni, S., Reed, L. J., … Barker, G. J. (2012). Ketamine effects on brain GABA and glutamate levels with 1H-MRS: relationship to ketamine-induced psychopathology. *Molecular Psychiatry*, *17*(7), 664–5. http://doi.org/10.1038/mp.2011.171

Strakowski, S. M., Delbello, M. P., & Adler, C. M. (2005). The functional neuroanatomy of bipolar disorder: a review of neuroimaging findings. *Molecular Psychiatry*, *10*(1), 105–16. http://doi.org/10.1038/sj.mp.4001585

Tagliazucchi, E., von Wegner, F., Morzelewski, A., Brodbeck, V., Jahnke, K., & Laufs, H. (2013). Breakdown of long-range temporal dependence in default mode and attention networks during deep sleep. *Proceedings of the National Academy of Sciences of the United States of America*, *110*(38), 15419–24. http://doi.org/10.1073/pnas.1312848110

Takahashi, T., Cho, R. Y., Mizuno, T., Kikuchi, M., Murata, T., Takahashi, K., & Wada, Y. (2010). Antipsychotics reverse abnormal EEG complexity in drug-naive schizophrenia: a multiscale entropy analysis. *NeuroImage*, *51*(1), 173–82. http://doi.org/10.1016/j.neuroimage.2010.02.009

Talairach, J. (1967). *Atlas d'anatomie stéréotaxique du télencéphale: études anatomo-radiologiques*. Masson et Cie.

Talairach, J. (1988). Co-planar stereotaxic atlas of the human brain : 3-dimensional proportional system an approach to cerebral imaging. Stuttgart : Georg Thieme Verlag,.

Talbot, K., Eidem, W. L., Tinsley, C. L., Benson, M. A., Thompson, E. W., Smith, R. J., … Arnold, S. E. (2004). Dysbindin-1 is reduced in intrinsic, glutamatergic terminals of the hippocampal formation in schizophrenia. *The Journal of Clinical Investigation*, *113*(9), 1353–63. http://doi.org/10.1172/JCI20425

Thatcher, R. W., North, D. M., & Biver, C. J. (2008). Development of cortical connections as measured by EEG coherence and phase delays. *Human Brain Mapping*, *29*(12), 1400–15. http://doi.org/10.1002/hbm.20474

Thornberg, S. A., & Saklad, S. R. A review of NMDA receptors and the phencyclidine model of schizophrenia. *Pharmacotherapy*, *16*(1), 82–93.

Tort, A. B. L., Kramer, M. A., Thorn, C., Gibson, D. J., Kubota, Y., Graybiel, A. M., & Kopell, N. J. (2008). Dynamic cross-frequency couplings of local field potential oscillations in rat striatum and hippocampus during performance of a T-maze task. *Proceedings of the National Academy of Sciences*, *105*(51), 20517–20522. http://doi.org/10.1073/pnas.0810524105

Turner, R., Howseman, A., Rees, G. E., Josephs, O., & Friston, K. (1998). Functional magnetic resonance imaging of the human brain: data acquisition and analysis. *Experimental Brain Research*, *123*(1-2), 5–12.

Uddin, L. Q., Kelly, A. M., Biswal, B. B., Castellanos, F. X., & Milham, M. P. (2009). Functional connectivity of default mode network components: correlation, anticorrelation, and causality. *Human Brain Mapping*, *30*(2), 625–37. http://doi.org/10.1002/hbm.20531

Vaillancourt, D. E., & Newell, K. M. Changing complexity in human behavior and physiology through aging and disease. *Neurobiology of Aging*, *23*(1), 1–11

Vakorin, V. A., Lippé, S., & McIntosh, A. R. (2011). Variability of brain signals processed locally transforms into higher connectivity with brain development. *The Journal of Neuroscience : The Official Journal of the Society for Neuroscience*, *31*(17), 6405–13. http://doi.org/10.1523/JNEUROSCI.3153-10.2011

Vanhatalo, S., Palva, J. M., Holmes, M. D., Miller, J. W., Voipio, J., & Kaila, K. (2004). Infraslow oscillations modulate excitability and interictal epileptic activity in the human cortex during sleep. *Proceedings of the National Academy of Sciences of the United States of America*, *101*(14), 5053–7. http://doi.org/10.1073/pnas.0305375101

Vanhaudenhuyse, A., Demertzi, A., Schabus, M., Noirhomme, Q., Bredart, S., Boly, M., … Laureys, S. (2011). Two distinct neuronal networks mediate the awareness of environment and of self. *Journal of Cognitive Neuroscience*, *23*(3), 570–8. http://doi.org/10.1162/jocn.2010.21488

Vanhaudenhuyse, A., Noirhomme, Q., Tshibanda, L. J.-F., Bruno, M.-A., Boveroux, P., Schnakers, C., … Boly, M. (2010). Default network connectivity reflects the level of consciousness in non-communicative brain-damaged patients. *Brain : A Journal of Neurology*, *133*(Pt 1), 161–71. http://doi.org/10.1093/brain/awp313

Vargas, C., López-Jaramillo, C., & Vieta, E. (2013). A systematic literature review of resting state network--functional MRI in bipolar disorder. *Journal of Affective Disorders*, *150*(3), 727–35. http://doi.org/10.1016/j.jad.2013.05.083

Vincent, J. L., Patel, G. H., Fox, M. D., Snyder, A. Z., Baker, J. T., Van Essen, D. C., … Raichle, M. E. (2007). Intrinsic functional architecture in the anaesthetized monkey brain. *Nature*, *447*(7140), 83–86. http://doi.org/10.1038/nature05758

Voss, L. J., Baas, C. H., Hansson, L., Steyn-Ross, D. A., Steyn-Ross, M., & Sleigh, J. W. (2012). Investigation into the effect of the general anaesthetics etomidate and ketamine on long-range coupling of population activity in the mouse neocortical slice. *European Journal of Pharmacology*, *689*(1-3), 111–7. http://doi.org/10.1016/j.ejphar.2012.06.003

Wei, M., Qin, J., Yan, R., Li, H., Yao, Z., & Lu, Q. (2013). Identifying major depressive disorder using Hurst exponent of resting-state brain networks. *Psychiatry Research - Neuroimaging*, *214*(3), 306–312. http://doi.org/10.1016/j.pscychresns.2013.09.008

Weickert, C. S., Straub, R. E., McClintock, B. W., Matsumoto, M., Hashimoto, R., Hyde, T. M., … Kleinman, J. E. (2004). Human dysbindin (DTNBP1) gene expression in normal brain and in schizophrenic prefrontal cortex and midbrain. *Archives of General Psychiatry*, *61*(6), 544–55. http://doi.org/10.1001/archpsyc.61.6.544

Wernicke, C. (1906). *Grundrisse der Psychiatrie*. Leipzig, Germany.

Whitfield-Gabrieli, S., Moran, J. M., Nieto-Castañón, A., Triantafyllou, C., Saxe, R., & Gabrieli, J. D. E. (2011). Associations and dissociations between default and self-reference networks in the human brain. *NeuroImage*, *55*(1), 225–32. http://doi.org/10.1016/j.neuroimage.2010.11.048

Whitfield-Gabrieli, S., Thermenos, H. W., Milanovic, S., Tsuang, M. T., Faraone, S. V, McCarley, R. W., … Seidman, L. J. (2009). Hyperactivity and hyperconnectivity of the default network in schizophrenia and in first-degree relatives of persons with schizophrenia. *Proceedings of the National*

Academy of Sciences of the United States of America, *106*(4), 1279–84. http://doi.org/10.1073/pnas.0809141106

Wiebking, C., de Greck, M., Duncan, N. W., Heinzel, A., Tempelmann, C., & Northoff, G. (2011). Are emotions associated with activity during rest or interoception? An exploratory fMRI study in healthy subjects. *Neuroscience Letters*, *491*(1), 87–92. http://doi.org/10.1016/j.neulet.2011.01.012

Wiebking, C., Duncan, N. W., Tiret, B., Hayes, D. J., Marjańska, M., Doyon, J., … Northoff, G. (2014). GABA in the insula - a predictor of the neural response to interoceptive awareness. *NeuroImage*, *86*, 10–8. http://doi.org/10.1016/j.neuroimage.2013.04.042

Wong, K.-F., & Wang, X.-J. (2006). A recurrent network mechanism of time integration in perceptual decisions. *The Journal of Neuroscience : The Official Journal of the Society for Neuroscience*, *26*(4), 1314–28. http://doi.org/10.1523/JNEUROSCI.3733-05.2006

Woodward, N. D., Rogers, B., & Heckers, S. (2011). Functional resting-state networks are differentially affected in schizophrenia. *Schizophrenia Research*, *130*(1-3), 86–93. http://doi.org/10.1016/j.schres.2011.03.010

Yang, A. C., Hong, C.-J., Liou, Y.-J., Huang, K.-L., Huang, C.-C., Liu, M.-E., … Tsai, S.-J. (2015). Decreased resting-state brain activity complexity in schizophrenia characterized by both increased regularity and randomness. *Human Brain Mapping*, *2186*(201), n/a–n/a. http://doi.org/10.1002/hbm.22763

Yang, A. C., & Tsai, S.-J. (2012). Is mental illness complex? From behavior to brain. *Progress in Neuro-Psychopharmacology and Biological Psychiatry*, *45*, 253–257. http://doi.org/10.1016/j.pnpbp.2012.09.015

Yang, G. J., Murray, J. D., Repovs, G., Cole, M. W., Savic, A., Glasser, M. F., … Anticevic, A. (2014). Altered global brain signal in schizophrenia. *Proceedings of the National Academy of Sciences of the United States of America*, *111*(20), 7438–43. http://doi.org/10.1073/pnas.1405289111

Yu, Q., Allen, E. A., Sui, J., Arbabshirani, M. R., Pearlson, G., & Calhoun, V. D. (2012). Brain connectivity networks in schizophrenia underlying resting state functional magnetic resonance imaging. *Current Topics in Medicinal Chemistry*, *12*(21), 2415–25.

Yue, Y., Loh, J. M., & Lindquist, M. (2010). Adaptive spatial smoothing of fMRI images. *Statistics and Its Interface*, *3*, 3–13.

Yu-Feng, Z., Yong, H., Chao-Zhe, Z., Qing-Jiu, C., Man-Qiu, S., Meng, L., … Yu-Feng, W. (2007). Altered baseline brain activity in children with ADHD revealed by resting-state functional MRI. *Brain and Development*, *29*(2), 83–91. http://doi.org/10.1016/j.braindev.2006.07.002

Zang, Y., Jiang, T., Lu, Y., He, Y., & Tian, L. (2004). Regional homogeneity approach to fMRI data analysis. *NeuroImage*, *22*(1), 394–400. http://doi.org/10.1016/j.neuroimage.2003.12.030

Zhang, D., Snyder, A. Z., Shimony, J. S., Fox, M. D., & Raichle, M. E. (2010). Noninvasive functional and structural connectivity mapping of the human thalamocortical system. *Cerebral Cortex (New York, N.Y. : 1991)*, *20*(5), 1187–94. http://doi.org/10.1093/cercor/bhp182

Zuo, X.-N., Kelly, C., Adelstein, J. S., Klein, D. F., Castellanos, F. X., & Milham, M. P. (2010). Reliable intrinsic connectivity networks: test-retest evaluation using ICA and dual regression approach. *NeuroImage*, *49*(3), 2163–77. http://doi.org/10.1016/j.neuroimage.2009.10.080

Zuo, X.-N., Xu, T., Jiang, L., Yang, Z., Cao, X.-Y., He, Y., … Milham, M. P. (2013). Toward reliable characterization of functional homogeneity in the human brain: preprocessing, scan duration, imaging resolution and computational space. *NeuroImage*, *65*, 374–86. http://doi.org/10.1016/j.neuroimage.2012.10.017

6. Appendices.

6.1. Whole brain template regions: (Power et al., 2011)

			Coordinates in MNI space		
ROI#	**AREA (focus point)**	**BA**	**X**	**Y**	**Z**
1	Lingual Gyrus L	18	-25	-98	-12
2	Lingual Gyrus R	18	27	-97	-13
3	Middle Frontal Gyrus R		24	32	-18
4	Inferior Temporal Gyrus L	37	-56	-45	-24
5	Orbital Gyrus R		8	41	-24
6	Parahippocampal Gyrus L	35	-21	-22	-20
7	Culmen R		17	-28	-17
8	Parahippocampal Gyrus L		-37	-29	-26
9	Inferior Temporal Gyrus R	20	65	-24	-19
10	Fusiform Gyrus		52	-34	-27
11	Middle Temporal Gyrus R		55	-31	-17
12	Middle Frontal Gyrus R	11	34	38	-12
13	Precuneus L	7	-7	-52	61
14	Cingulate Gyrus L	24	-14	-18	40
15	Paracentral Lobule L		0	-15	47
16	Cingulate Gyrus R		10	-2	45
17	Medial Frontal Gyrus L		-7	-21	65
18	Paracentral Lobule L		-7	-33	72
19	Precentral Gyrus R		13	-33	75
20	Postcentral Gyrus L		-54	-23	43
21	Precentral Gyrus R		29	-17	71
22	Postcentral Gyrus R		10	-46	73
23	Precentral Gyrus L		-23	-30	72
24	Precentral Gyrus L		-40	-19	54
25	Postcentral Gyrus R		29	-39	59
26	Postcentral Gyrus R	3	50	-20	42
27	Precentral Gyrus L		-38	-27	69
28	Precentral Gyrus L	4	20	-29	60
29	Precentral Gyrus R	6	44	-8	57
30	Postcentral Gyrus L	5	-29	-43	61
31	Medial Frontal Gyrus R		10	-17	74
32	Postcentral Gyrus R		22	-42	69
33	Postcentral Gyrus L	40	-45	-32	47

34	Postcentral Gyrus L	3	-21	-31	61
35	Superior Frontal Gyrus L		-13	-17	75
36	Postcentral Gyrus R	3	42	-20	55
37	Precentral Gyrus L		-38	-15	69
38	Postcentral Gyrus L		-16	-46	73
39	Medial Frontal Gyrus R	6	2	-28	60
40	Medial Frontal Gyrus R	6	3	-17	58
41	Precentral Gyrus L		38	-17	45
42	Precentral Gyrus L		-49	-11	35
43	Insula R		36	-9	14
44	Precentral Gyrus R	6	51	-6	32
45	Precentral Gyrus L		-53	-10	24
46	Precentral Gyrus R		66	-8	25
47	Medial Frontal Gyrus L		-3	2	53
48	Inferior Parietal Lobule R	2	54	-28	34
49	Middle Frontal Gyrus R	6	19	-8	64
50	Superior Frontal Gyrus L		-16	-5	71
51	Cingulate Gyrus L		-10	-2	42
52	Insula R		37	1	-4
53	Superior Frontal Gyrus R		13	-1	70
54	Medial Frontal Gyrus R	32	7	8	51
55	Precentral Gyrus L	44	-45	0	9
56	Superior Temporal Gyrus R		49	8	-1
57	Clustrum L		-34	3	4
58	Superior Temporal Gyrus L	22	-51	8	-2
59	Cingulate Gyrus L		-5	18	34
60	Insula R		36	10	1
61	Insula R	13	32	-26	13
62	Superior Temporal Gyrus R	42	65	-33	20
63	Superior Temporal Gyrus R		58	-16	7
64	Superior Temporal Gyrus L	41	-38	-33	17
65	Postcentral Gyrus L	40	-60	-25	14
66	Superior Temporal Gyrus L	41	-49	-26	5
67	insula R		43	-23	20
68	Inferior Parietal Lobule L		-50	-34	26
69	Postcentral Gyrus L		-53	-22	23
70	Precentral Gyrus L		-55	-9	12
71	Precentral Gyrus R		56	-5	13
72	Postcentral Gyrus R	3	59	-17	29
73	Insula L		-30	-27	12

74	Middle Temporal Gyrus L		-41	-75	26
75	Superior Frontal Gyrus R		6	67	-4
76	Medial Frontal Gyrus R		8	48	-15
77	Parahippocampal Gyrus L	30	-13	-40	1
78	Superior Frontal Gyrus L	11	-18	63	-9
79	Middle Temporal Gyrus L	39	-46	-61	21
80	Middle Temporal Gyrus R		43	-72	28
81	Superior Temporal Gyrus L	38	-44	12	-34
82	Superior Temporal Gyrus R	38	46	16	-30
83	Middle Temporal Gyrus L		-68	-23	-16
84	Middle Temporal Gyrus L	21	-58	-26	-15
85	Inferior Frontal Gyrus R		27	16	-17
86	Angular Gyrus L		-44	-65	35
87	Superior Parietal Lobule L		-39	-75	44
88	Cingulate Gyrus		-7	-55	27
89	Precuneus R		6	-59	35
90	Posterior Cingulate L		-11	-56	16
91	Poaterior Cingulate L	30	-3	-49	13
92	Cingulate Gyrus R	31	8	-48	31
93	Precuneus R	31	15	-63	26
94	Cingulate Gyrus L	31	-2	-37	44
95	Posterior Cingulate R		11	-54	17
96	Angular Gyrus R		52	-59	36
97	Superior Frontal Gyrus R	8	23	33	48
98	Superior Frontal Gyrus L		-10	39	52
99	Superior Frontal Gyrus L		-16	29	53
100	Middle Frontal Gyrus L	8	-35	20	51
101	Superior Frontal Gyrus R	9	22	39	39
102	Superior Frontal Gyrus R		13	55	38
103	Superior Frontal Gyrus L	9	-10	55	39
104	Superior Frontal Gyrus L	9	-20	45	39
105	Medial Frontal Gyrus L		6	54	16
106	Medial Frontal Gyrus R	10	6	64	22
107	Medial Frontal Gyrus L	10	-7	51	-1
108	Medial Frontal Gyrus R	10	9	54	3
109	Medial Frontal Gyrus L	11	-3	44	-9
110	Anterior Cingulate R	10	8	42	-5
111	Anterior Cingulate L		-11	45	8
112	Medial Frontal Gyrus L	9	-2	38	36
113	Anterior Cingulate L	32	-3	42	16

114	Superior Frontal Gyrus L	10	-20	64	19
115	Medial Frontal Gyrus L		-8	48	23
116	Inferior Temporal Gyrus R	21	65	-12	-19
117	Middle Temporal Gyrus L		-56	-13	-10
118	Middle Temporal Gyrus L		-58	-30	-4
119	Middle Temporal Gyrus R		65	-31	-9
120	Middle Temporal Gyrus L		-68	-41	-5
121	Superior Frontal Gyrus R	6	13	30	59
122	Anterior Cingulate R	32	12	36	20
123	Middle Temporal Gyrus R		52	-2	-16
124	Parahippocampal Gyrus L		-26	-40	-8
125	Parahippocampal Gyrus R		27	-37	-13
126	Fusiform Gyrus L	37	-34	-38	-16
127	Uvula R		28	-77	-32
128	Middle Temporal Gyrus R	21	52	7	-30
129	Middle Temporal Gyrus L		-53	3	-27
130	Supramarginal Gyrus R		47	-50	29
131	Middle Temporal Gyrus L		-49	-42	1
132	Inferior Frontal Gyrus L		-31	19	-19
133	Cingulate Gyrus L	31	-2	-35	31
134	Precuneus L	7	-7	-71	42
135	Precuneus R	7	11	-66	42
136	Precuneus R	7	4	-48	51
137	Inferior Frontal Gyrus L		-46	31	-13
138	Superior Frontal Gyrus L		-10	11	67
139	Inferior Frontal Gyrus R		49	35	-12
140	Lingual Gyrus R		8	-91	-7
141	Inferior Occipital Gyrus R		17	-91	-14
142	Lingual Gyrus L	17	-12	-95	-13
143	Parahippocampal Gyrus R	19	18	-47	-10
144	Middle Temporal Gyrus R		40	-72	14
145	Cuneus R		8	-72	11
146	Cunues L		-8	-81	7
147	Middle Occipital Gyrus L		-28	-79	19
148	Lingual Gyrus R		20	-66	2
149	Cuneus L		-24	-91	19
150	Parahippocampal Gyrus R		27	-59	-9
151	Lingual Gyrus L		-15	-72	-8
152	Cuneus L		-18	-68	5
153	Inferior Occipital Gyrus R	19	43	-78	-12

154	Middle Occipital Gyrus L		-47	-76	-10
155	Cuneus L	19	-14	-91	31
156	Precuneus R	19	15	-87	37
157	Cuneus R		29	-77	25
158	Lingual Gyrus R	17	20	-86	-2
159	Cuneus R	7	15	-77	31
160	Lingual Gyrus L		-16	-52	-1
161	Middle Occipital Gyrus R		42	-66	-8
162	Cuneus R		24	-87	24
163	Precuneus R		6	-72	24
164	Middle Occipital Gyrus L		-42	-74	0
165	Right Lingual Gyrus	18	26	-79	-16
166	Precuneus L		-16	-77	34
167	Cuneus L	18	-3	-81	21
168	Inferior Occipital Gyrus L		-40	-88	-6
169	Middle Occipital Gyrus R		37	-84	13
170	Cuneus R		6	-81	6
171	Middle Occipital Gyrus L	19	-26	-90	3
172	Middle Occipital Gyrus L		-33	-79	-13
173	Middle Occipital Gyrus R		37	-81	1
174	Middle Frontal Gyrus L		-44	2	46
175	Middle Frontal Gyrus R		48	25	27
176	Inferior Frontal Gyrus L		-47	11	23
177	Inferior Parietal Lobule L		-53	-49	43
178	Middle Frontal Gyrus L		-23	11	64
179	Middle Temporal Gyrus R	37	58	-53	-14
180	Superior Frontal Gyrus R	11	24	45	-15
181	Middle Frontal Gyrus R		34	54	-13
182	Superior Frontal Gyrus L	11	-21	41	-20
183	Declive L		-18	-76	-24
184	Uvula R		17	-80	-34
185	Uvula R		35	-67	-34
186	Middle Frontal Gyrus R	9	47	10	33
187	Inferior Frontal Gyrus L		-41	6	33
188	Middle Frontal Gyrus L	46	-42	38	21
189	Middle Frontal Gyrus R		38	43	15
190	Inferior Parietal Lobule R		49	-42	45
191	Superior Parietal Lobule L		-28	-58	48
192	Inferior Parietal Lobule R	40	44	-53	47
193	Superior Frontal Gyrus R		32	14	56

194	Inferior Parietal Lobule R		37	-65	40
195	Inferior Parietal Lobule L	40	-42	-55	45
196	Precentral Gyrus R		40	18	40
197	Middle Frontal Gyrus L	10	-34	55	4
198	Middle Frontal Gyrus L		-42	45	-2
199	Inferior Parietal Lobule R		33	-53	44
200	Middle Frontal Gyrus R		43	49	-2
201	Middle Frontal Gyrus L		-42	25	30
202	Medial Frontal Gyrus L	8	-3	26	44
203	Paracentral Lobule R	5	11	-39	50
204	Supramarginal Gyrus R		55	-45	37
205	Middle Frontal Gyrus R	6	42	0	47
206	Middle Frontal Gyrus R		31	33	26
207	Inferior Frontal Gyrus R	45	48	22	10
208	Insula L	47	-35	20	0
209	Insula R	13	36	22	3
210	Inferior Frontal Gyrus R		37	32	-2
211	Inferior Frontal Gyrus R		34	16	-8
212	Antrior Cingulate L		-11	26	25
213	Cingulate Gyrus L		-1	15	44
214	Superior Frontal Gyrus L		-28	52	21
215	Anterior Cinguate L		0	30	27
216	Cingulate Gyrus R	32	5	23	37
217	Antrior Cingulate R		10	22	27
218	Middle Frontal Gyrus R		31	56	14
219	Superior Frontal Gyrus R	10	26	50	27
220	Middle Frontal Gyrus L	10	-39	51	17
221	Cingulate Gyrus R		2	-24	30
222	Thalamus R		6	-24	0
223	Thalamus L		-2	-13	12
224	Thalamus L/Medial Dorsal Nuclus L		-10	-18	7
225	Thalamus R		12	-17	8
226	Thalamus L		-5	-28	-4
227	Lentiform Nucleus L/Putamen L		-22	7	-5
228	Lentiform Nucleus L/Putamen L		-15	4	8
229	Lentiform Nucleus R/Putamen R		31	-14	2
230	Lentiform Nucleus R/Putamen R		23	10	1
231	Lentiform Nucleus R/Putamen R		29	1	4
232	Lentiform Nucleus L/Putamen L		-31	-11	0
233	Lentiform Nucleus R/Putamen R		15	5	7

234	Thalamus R/Ventral Anterior Nuclues R		9	-4	6
235	Inferior Parietal Lobule R	13	54	-43	22
236	Superior Temporal Gyrus L		-56	-50	10
237	Superior Temporal Gyrus L		-55	-40	14
238	Superior Temporal Gyrus R		52	-33	8
239	Middle Temporal Gyrus R	21	51	-29	-4
240	Superior Temporal Gyrus R		56	-46	11
241	Inferior Frontal Gyrus R		53	33	1
242	Inferior Frontal Gyrus L	47	-49	25	-1
243	Declive L		-16	-65	-20
244	Declive L		-32	-55	-25
245	Declive R		22	-58	-23
246	Declive R		1	-62	-18
247	Uncus R		33	-12	-34
248	Uncus L	20	-31	-10	-36
249	Inferior Temporal Gyrus R	20	49	-3	-38
250	Inferior Temporal Gyrus L		-50	-7	-39
251	Precuneus R	7	10	-62	61
252	Middle Temporal Gyrus L		-52	-63	5
253	Fusiform Gyrus L		-47	-51	-21
254	Fusiform Gyrus R		46	-47	-17
255	Postcentral Gyrus R		47	-30	49
256	Precuneus R		22	-65	48
257	Middle Temporal Gyrus R		46	-59	4
258	Superior Parietal Lobule R	7	25	-58	60
259	Inferior Parietal Lobule L		-33	-46	47
260	Precuneus L		-27	-71	37
261	Middle Frontal Gyrus L	6	-32	-1	54
262	Middle Occipiatal Ggyrus L		-42	-60	-9
263	Superior Parietal Lobule L	7	-17	-59	64
264	Middle Frontal Gyrus R		29	-5	54

6.2 Network specific brain template: (De Pasquale et al., 2012):

Network	Name	NODE	Abbreviation	MNI Coordinates mm		
Dorsal Attention	Left posterior Intra Parietal sulcus	NODE1	lpIPS	-25	-67	48
Dorsal Attention	Right posterior Intra Parietal Sulcus	NODE2	RpIPS	23	-69	49
Dorsal Attention	Left Fronta Eye Field	NODE3	LFEF	-26	-12	53
Dorsal Attention	Right frontal eye field	NODE4	RFEF	30	-13	53
Dorsal Attention	Left Middle Temporal	NODE5	LMT	-43	-72	-8
Dorsal Attention	Right Middle temporal	NODE6	RMT	42	-70	-11
Ventral Attention	Right middle Frontal Gyrus	NODE7	RMFG	41	17	31
Ventral Attention	Right Pre-central sulcus	NODE8	RPCS	41	2	50
Ventral Attention	Right supramarginal Gyrus	NODE9	RSMG	52	-48	28
Ventral Attention	Right superior Temporal Gyrus	NODE10	RSTG	58	-48	10
Ventral Attention	Right Ventral Frontal Cortex	NODE11	RVFC	40	21	-4
Default Mode Network	Left Angular Gyrus	NODE12	LAG	-43	-76	35
Default Mode Network	Right Angular Gyrus	NODE13	RAG	51	-64	32
Default Mode Network	Posterior Cingulate/Precuneus	NODE14	PCC	-3	-54	31
Default Mode Network	Ventral Medial Prefrontal Cortex	NODE15	vMPFC	-2	51	2
Default Mode Network	Dorsal Medial Prefrontal Cortex	NODE16	dMPFC	-13	52	23
Default Mode Network	Right medial Prefrontal Cortex	NODE17	RMPFC	2	53	24
Default Mode Network	Left Inferior Temporal Gyrus	NODE18	LITG	-57	-25	-17
Visual Network	Right Area V1	NODE19	RV1	11	-88	-4
Visual Network	Left Area V2 Dorsal	NODE20	LV2d	-8	-99	7
Visual Network	Right Area V2 Dorsal	NODE21	RV2d	14	-96	13
Visual Network	Left Area V4	NODE22	LV4	-31	-77	-17
Visual Network	Right Area V4	NODE23	RV4	27	-71	-14
Visual Network	Left Area V7	NODE24	LV7	-23	-78	26
Visual Network	Right Area V7	NODE25	RV7	32	-78	25
Motor Network	left second somatosensory	NODE26	LSII	-60	-28	24
Motor Network	Right Central Sulcus	NODE27	RCS	35	-26	55
Motor Network	Left Central Sulcus	NODE28	LCS	-37	-19	53
Motor Network	Right Second Somatosensory	NODE29	RSII	57	-28	23
Motor Network	Left Supplementary Motor Area	NODE30	LSMA	-1	-17	55
Motor Network	Left Putamen	NODE31	LPUT	-30	-18	10
Motor Network	Right Putamen	NODE32	RPUT	30	-17	9
Language Network	Superior Temporal Sulcus	NODE33	STS	-50	-54	22
Language Network	Anterior Superior Temporal Gyrus	NODE34	T1a	-56	-12	-3
Language Network	Upper part of the Pars Opercularis of IFG	NODE35	F3OPD	-44	21	24
Language Network	Pars triangularis opercularis of the IFG	NODE36	F3TV	-43	20	4
Salience Network	SACC	NODE37	SACC	-1	20	28
Salience Network	Left Anterior Insula	NODE38	LAI	-42	14	0
Salience Network	Right Anterior Insula	NODE39	RAI	40	12	0
Salience Network	Left Thalamus	NODE40	LT	-12	-16	4
Salience Network	Right Thalamus	NODE41	RT	14	-20	8